C/ORNL 92-0076

ornl

OAK RIDGE NATIONAL LABORATORY

LOCKHEED MARTIN

CRADA Final Report
for
CRADA Number C/ORNL 92-0076

In-Service Testing of Ni_3Al Coupons and Trays in Carburizing Furnaces at Delphi Saginaw

V. K. Sikka, M. L. Santella, S. Viswanathan, and R. W. Swindeman
Oak Ridge National Laboratory

Madhu Chatterjee
General Motors Corporation, Saginaw Division

Date Published: August 1998

Prepared by the
Oak Ridge National Laboratory
Oak Ridge, Tennessee 37831
managed by
Lockheed Martin Energy Research Corporation
for the
U.S. Department of Energy
under contract DE-AC05-96OR22464

APPROVED FOR PUBLIC RELEASE

UNLIMITED DISTRIBUTION

MANAGED AND OPERATED BY
LOCKHEED MARTIN ENERGY RESEARCH CORPORATION
FOR THE UNITED STATES
DEPARTMENT OF ENERGY

ORNL-27 (3-96)

CONTENTS

Abstract

This Cooperative Research and Development Agreement (CRADA) report deals with the development of nickel aluminide alloy for improved longer life heat-resistant fixture assemblies for batch and continuous pusher carburizing furnaces. The nickel aluminide development was compared in both coupon and component testing with the currently used Fe-Ni-Cr heat-resisting alloy known as HU. The specific goals of the CRADA were: (1) casting process development, (2) characterization and possible modification of the alloy composition to optimize its manufacturing ability and performance under typical furnace operating conditions, and (3) testing and evaluation of specimens and prototype fixtures.

In support of the CRADA objectives, coupons of nickel aluminide and the HU alloy were installed in both batch and pusher furnaces. The coupons were taken from two silicon levels and contained welds made with two different filler compositions (IC-221LA and IC-221W).

Both nickel-aluminide and HU coupons were removed from the batch and pusher carburizing furnace at time intervals ranging from one month to one year. The exposed coupons were cut and mounted for metallographic, hardness, and microprobe analysis. The results of the microstructural analysis have been transmitted to General Motors Corporation, Saginaw Division (Delphi Saginaw) through reports that were presented at periodic CRADA review meetings. The following are the major observations from the coupons:

1. The Ni_3Al-based alloy coupons remained nonmagnetic even after one-year exposure in a carburizing furnace, whereas the HU coupons became increasingly magnetic with exposure time. The increasing magnetic behavior of HU implies increasing amounts of carburization.

2. The microhardness of the HU samples increased with exposure time, whereas it remained constant for the Ni_3Al-based alloy. This again implied that the HU alloy was carburizing and the Ni_3Al alloy was not.

3. The Ni_3Al coupons showed some microstructural change with exposure. However, it did not exceed 5 mil from the surface. It appears that zirconium and chromium in the IC-221M alloy do form carbides. It is recommended that chromium-free and low-zirconium alloy IC-50 instead of IC-221M may be even a better candidate for fixtures in carburizing furnaces. Preoxidation at 1100°C for 3 h of the IC-221M produces predominantly a Al_2O_3 film on the castings. Since Al_2O_3 is the primary reason for resisting the carbon diffusion, it is believed that preoxidation of the casting is a way to improve the carburization resistance of IC-221M type of nickel-aluminide alloy.

4. The results of the coupon testing were verified on an actual tray, where an HU tray failed because of extensive carburization as opposed to essentially no observable change for the IC-221M tray.

Research sponsored by the U.S. Department of Energy, Assistant Secretary for Energy Efficiency and Renewable Energy, Office of Industrial Technologies, Advanced Industrial Materials Program, under contract DE-AC05-96OR22464 with Lockheed Martin Energy Research Corp.

Based on coupon testing and verification of the coupon results with the testing of trays, Delphi Saginaw moved forward with the use of six additional trays in a batch furnace and two assemblies in a pusher furnace. Fifty percent of the trays and fixtures are in the as-cast condition and the remaining trays and fixtures are in the preoxidized condition.

The successful operating experience of two assemblies in the pusher furnace for nearly a year formed the basis for a production run of 63 more assemblies. The production run required melting of 94 heats weighing 500 lb each. Twenty-six of the 94 heats were from virgin stock, and 68 were from the revert that used 50% virgin and 50% revert. Detailed chemical analysis of the 94 heats reflected that the nickel aluminide can be cast into heat-treat fixtures under production conditions. In addition to the chemical analysis, the castings showed excellent dimensional reproducibility.

A total of six batch furnace trays and 65 pusher furnace assemblies of nickel aluminide alloy IC-221M are currently operating in production furnaces at Delphi Saginaw. Two of the pusher furnace assemblies have completed two years of service without any failure.

The CRADA has accomplished the goal of demonstrating that the nickel aluminide can be produced under commercial production conditions and it has superior performance over the currently used HU alloy in both batch and pusher furnaces. Longer test duration in the production furnaces is required to predict the factors of improvement in life over the HU components.

CRADA Objective

The objective of the subject CRADA was to develop longer life, heat-resistant fixture assemblies for heat-treating furnaces in a carburizing atmosphere. The assemblies are used to hold the parts to be heat treated and consist of trays, lower grids, upper grids, and posts. Work was to focus on Ni_3Al-based cast alloys. The specific goals of the CRADA were to achieve the following:

1. Casting process development.

2. Characterization and possible modification of the alloy composition to optimize its manufacturing ability and performance under typical furnace operating conditions.

3. Testing and evaluation of specimens and prototype parts.

Completion of Objective

The objective of the CRADA was met within the constraints of the modified duration and funding. This included:

1. Identification of the alloy composition for heat-treating fixtures — The composition is known as IC-221M.

2. Development of the alloy melting process — This melting process is known as Exo-Melt™ and is being commercially used.

3. Computer simulations to improve the mold filling design to minimize casting defects — This was accomplished by using commercial software known as ProCast.

4. Microstructural and mechanical property characterization of coupons and test bars — A large number of test coupons were exposed in the batch and pusher furnaces. The coupons were periodically removed and characterized for microstructural changes. Mechanical properties were the tensile tests at room temperature and 950°C for the test bars cast from the IC-221M composition. Selective creep tests were done on the test bars.

5. A small batch and a commercial-size batch of trays and fixtures were cast under controlled and production conditions. The results showed that the experience on the small batch under controlled conditions can be scaled up to production conditions. A batch of 94 heats made for the production run showed good chemistry control for both the virgin and revert stock melted heats.

6. Weld wire compositions and application were developed to carry out any weld repair needed to fix any casting defects in the trays and fixtures.

7. The evaluation of the trays and fixtures was accomplished by installing six batch furnace and 65 pusher furnace assemblies. As of January 1998, all of the trays and fixtures are operating under production conditions without any indication of failure. The duration of tests is not sufficiently long enough to determine the exact multiplier for life improvement over the currently used HU alloy trays and fixtures.

CRADA Benefits to DOE

The Department of Energy (DOE) benefited significantly from this CRADA. It benefited in using the coupon and actual furnace test results to introduce the nickel aluminide alloy IC-221M to a large number of heat-treating applications. It gave Alloy Engineering & Casting Company the confidence with the alloy casting process and market development to the extent that they signed a license to commercially produce the alloy trays, fixtures, and radiant burner tubes. The implementation of nickel aluminide into the heat-treating furnace has a large potential for energy savings through the enhanced component life, which is consistent with the mission of DOE-supported research. The DOE also benefited in developing working relations with a large company like Delphi Saginaw and a small company like Alloy Engineering & Casting Company. The commercialization of nickel aluminide for heat-treating trays and fixtures has clearly given the United States a lead position in the world with advanced materials for these applications. Furthermore, it has created a strong potential for exporting DOE-developed technology-based components.

Technical Discussion

Introduction

The carburization of steel components is a widely used process for enhancing specific properties such as hardness and wear resistance. Typical carburization processing consists of exposing the components to a gaseous environment of known carbon potential for a specific time at a selected temperature. The process is carried out either in a batch or a continuous furnace. In a batch furnace, the components to be carburized are loaded in boxes that are supported on trays. In the continuous furnace, the components are loaded in an assembly that consists of a base tray, a bottom fixture, and a top fixture. The top fixture is supported by four posts. In both the batch and continuous furnaces, the trays and assemblies are quenched in oil along with carburized components. After a cycle is complete, the trays and fixtures are washed, dried, and reused. A typical cycle time for a batch furnace is 8 h, and the cycle time for a pusher or continuous furnace is 24 h.

The most common industry practice is to use cast trays and assembly components made from an Fe-Ni-Cr alloy known as HU (see Table 1 for composition). Some slight variations of HU steels are also used. During the carburization process, the HU trays and fixtures are carburized under production conditions, along with the parts. The carburization process causes: (1) growth of trays and assemblies from carbon pickup, (2) makes them very brittle, and (3) makes them highly magnetic from only slightly magnetic in virgin condition. The brittleness from the carbon pickup causes cracking of the trays and assemblies from thermal cycle resulting from quenching from the carburization temperature to the oil temperature. Typical life of an HU tray may approach 12 to 15 months.

Table 1. Compositions of Ni_3Al-based alloys and commercially available competing alloys

Element	Weight percent			
	IC-396M[a]	IC-221M[b]	HU[c]	Alloy 800[d]
Al	7.98	8.0	--	0.4
Cr	7.72	7.7	18.0	21.0
Mo	3.02	1.43	--	--
Zr	0.85	1.7	--	--
B	0.005	0.008	--	--
C	--	--	0.55	0.05
Fe	--	--	42.45	45.5
Ti	--	--	--	0.4
Ni	80.42	81.1	39.0	32.5
Si	--	--	--	--
Y	--	--	--	--

[a]Castable alloy for static applications (some microporosity).

[b]Castable alloy for dynamic applications (minimum microporosity).

[c]Cast alloy.

[d]Wrought alloy.

The unpredictable failure of a fixture in a pusher furnace can result in a component being dropped off the fixture onto the furnace rail. This can result in furnace shutdown with several consequences including: (1) lost inventory because the furnace load is generally discarded because of interruption in the standard carburization cycle, (2) lost furnace time because the furnace has to be cooled down for the operators to go in and remove the obstruction, (3) missed schedule because the components discarded from the furnaces need to be remanufactured, and (4) loss of energy from shutting down the furnace.

The above factors can have a substantial effect on the manufacturing cost. The CRADA between Delphi Saginaw and ORNL was to evaluate the use of cast components of Ni_3Al-based alloys for trays and fixtures for batch and pusher furnaces. The Ni_3Al-based alloys

developed at ORNL were considered for this application because of their superior carburization and oxidation resistances and higher strength over the HU material. The resistance to change in mass of the Ni_3Al-based alloys (see Table 1 for composition) in carburization environments is significantly better than Alloy 800, which is similar in composition to HU (see Fig. 1). The oxidation resistance of the Ni_3Al-based alloys is also significantly better than Alloy 800 (see Fig. 2). The oxidation resistance is important because the carburization furnaces are periodically oxidized at higher temperatures to burn off excess carbon deposit. The cast Ni_3Al-based alloys (IC-396M and IC-221M) have significantly higher tensile strength (see Fig. 3) and creep strength (see Fig. 4) as opposed to the HU material. Based on the data shown in Figs. 1 through 4, Ni_3Al-based alloys appear suitable for trays and fixtures in carburizing furnaces. However, Delphi Saginaw would only consider using these materials if the following could be demonstrated:

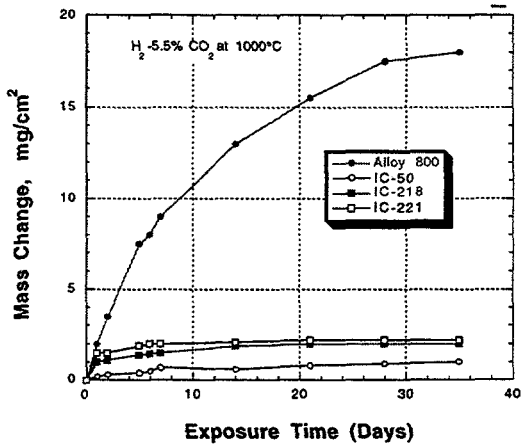

(*a*)

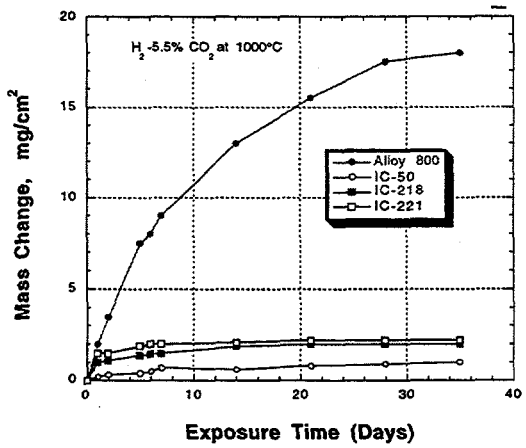

(*b*)

Fig. 1. Comparison of carburization resistance of Ni_3Al-based alloys with Alloy 800: (*a*) oxidizing carburizing environment and (*b*) reducing carburizing environment. [Data were developed at The International Nickel Company, New York, NY (15).]

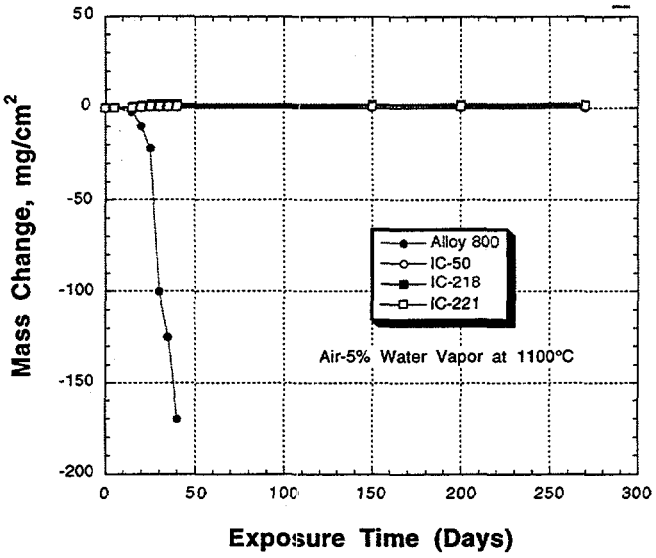

Fig. 2. Comparison of oxidation resistance of Ni_3Al-based alloys with Alloy 800 in air with 5% water vapor at 1100°C. [Data were developed at The International Nickel Company, New York, NY (15).]

1. Ni_3Al-based alloys can be melted and sand cast into trays, fixtures, and posts of current designs made from the HU alloy.

2. Demonstrate weld repair capability of casting defects.

3. Coupons of Ni_3Al-based alloy and HU to be exposed in the carburization furnaces at Delphi Saginaw and evaluated for changes at periodic intervals.

4. Test trays and tray and fixture assemblies in actual batch and pusher carburizing furnaces at Delphi Saginaw.

The purpose of this report is to chart the progress made in all of the above mentioned areas during the course of this CRADA.

Melting and Casting of Trays and Fixtures

A new process known as Exo-Melt™ was developed for melting Ni_3Al-based alloys. The process is based on loading techniques of component elements so that the heat of formation of Ni_3Al from its elements nickel and aluminum is used most effectively. The Exo-Melt™ process was developed using a 15-lb capacity air-induction-melting furnace at ORNL. The process has also been successfully demonstrated for several 600-lb heats at Alloy Engineering & Casting Company (AEC) [Champaign, Illinois]. AEC is the foundry used by Delphi Saginaw for the manufacture of their heat-treating fixtures from HU alloys. The Exo-Melt™ process has many advantages for melting Ni_3Al-based alloys: (1) it uses 50% less energy than the conventional process, (2) it uses 50% less time than the conventional process, (3) it prevents overheating of the melt, (4) it minimizes the excessive reaction with the furnace crucible, (5) chemical analyses are more reproducible, and (6) inclusions are minimized because of less time at temperature and no overheating.

The Exo-Melt™ process has been used for melting virgin heats and remelt stock. The furnace-loading sequence for Ni_3Al-based alloy IC-221M is shown in Fig. 5.

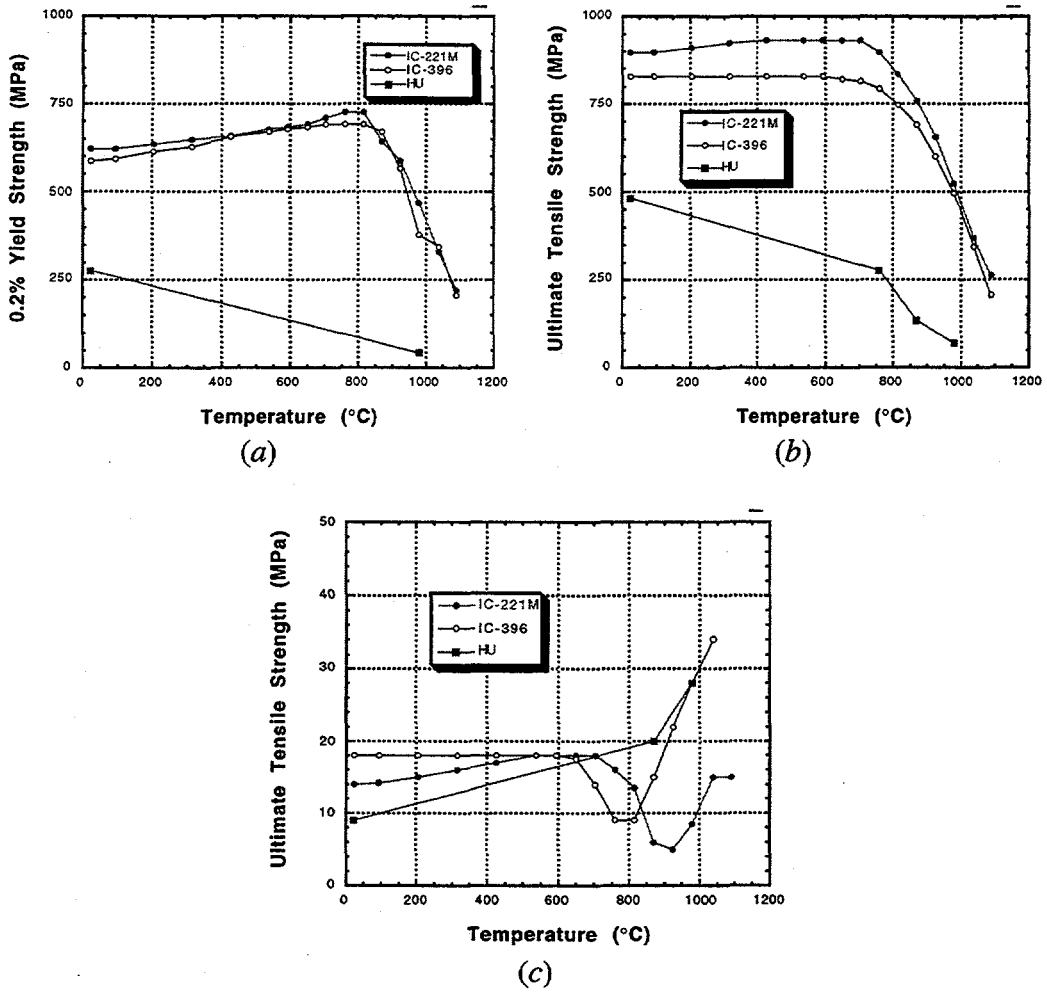

Fig. 3. Comparison of tensile properties of cast Ni_3Al-based alloys with cast HU alloy: (*a*) 0.2% yield strength, (*b*) ultimate tensile strength, and (*c*) total elongation.

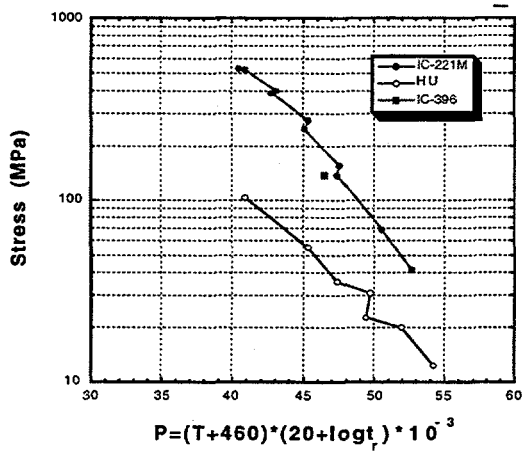

Fig. 4. Comparison of creep-rupture strength of cast Ni_3Al-based alloys with cast HU alloy.

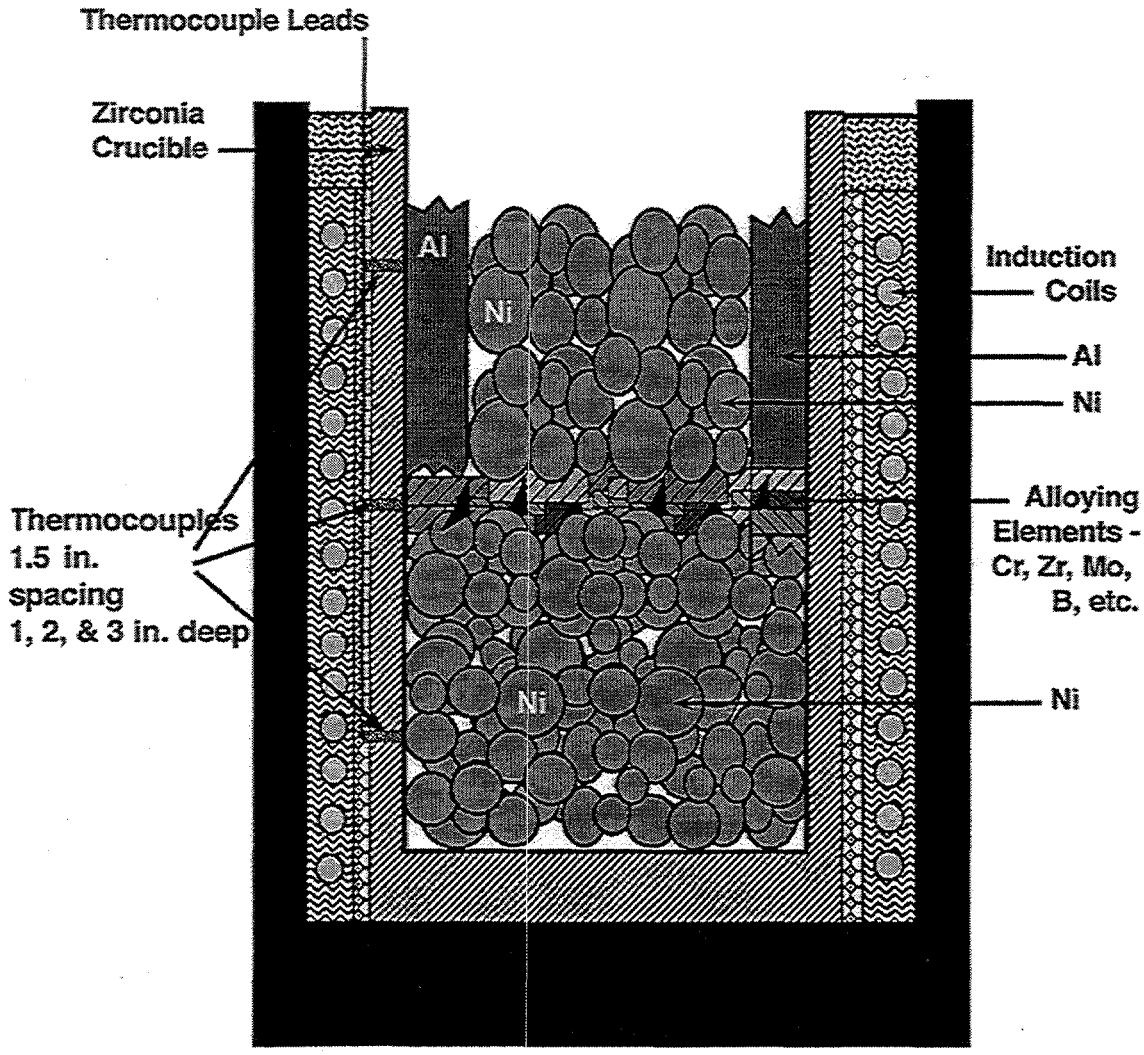

Fig. 5. Schematic of furnace-loading sequence employed for the Exo-Melt™ process to melt nickel aluminides.

For casting of trays and fixtures, the initial patterns, sands, and pouring techniques used at AEC were identical to that used for HU steels. However, during casting trials, it was recognized that the casting of Ni_3Al-based alloy would require different patterns to modify the mold filling and, thereby, improve casting quality. A comprehensive solidification modeling for the Ni_3Al-based alloy IC-221M was carried out to develop modified patterns and mold filling technique. The tray and fixture castings of IC-221M, prepared using the new patterns and modified pouring technique, were of consistent high quality. The new casting technique produced better surface finish, minimum intenal porosity, minimum slag entrapments, and folds. Photographs of recent castings of batch and pusher furnace trays and fixtures are shown in Figs. 6 and 7. From the quality of the castings shown in these figures, it is concluded that the melting and casting of Ni_3Al-based alloy IC-221M are no longer an issue.

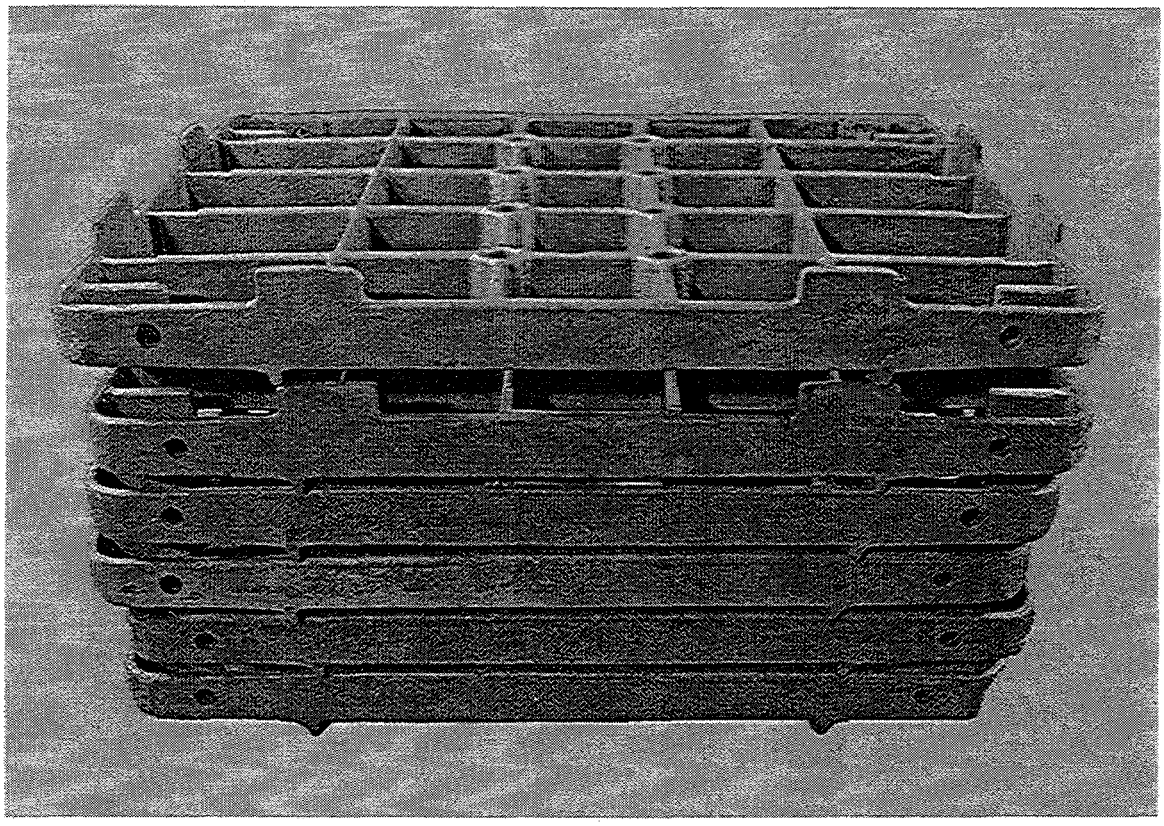

Fig. 6. Stack of six cast batch furnace trays of IC-221M.

Demonstration of the Weld Repair of Castings for Any Casting Defects

The castings for Figs. 6 and 7 were inspected for casting defects. The areas with defects were gauged by grinding and were weld repaired. The weld repair was carried out using IC-221LA (see Table 2 for composition) weld wire and gas tungsten arc process. The number of repair welds and their locations are summarized in Table 3. No problems were encountered during these weld repairs and, thus, it is concluded that the cast parts of Ni_3Al-based alloy IC-221M can be weld repaired.

Testing of IC-221M and HU Coupons in Carburizing Furnaces at Delphi Saginaw

Test coupons of geometry shown in Fig. 8 were cut from trays of Ni_3Al-based alloy IC-221M and HU. The IC-221M coupons were cut from trays of slightly different silicon concentration and, thereby, are labeled as low- and high-silicon tray coupons. The nickel-aluminide coupons also contained one weld bead each of heat 15101 (IC-221LA) and IC-221W. The compositions of IC-221LA and IC-221W weld wires are shown in Table 2. Welds were made on the machined surface of the coupons. The IC-221M and HU coupons were loaded in both the batch (aluminum case) and the pusher (continuous) furnace. The coupon number, installation date, and the removal schedule are summarized in Table 4. In addition to coupons, one tray each of IC-221M and HU was also set in the batch furnace for testing under real operating conditions. The IC-221M and HU coupons were attached to both the trays, and the actual attachment scheme for the coupons is shown in Fig. 9.

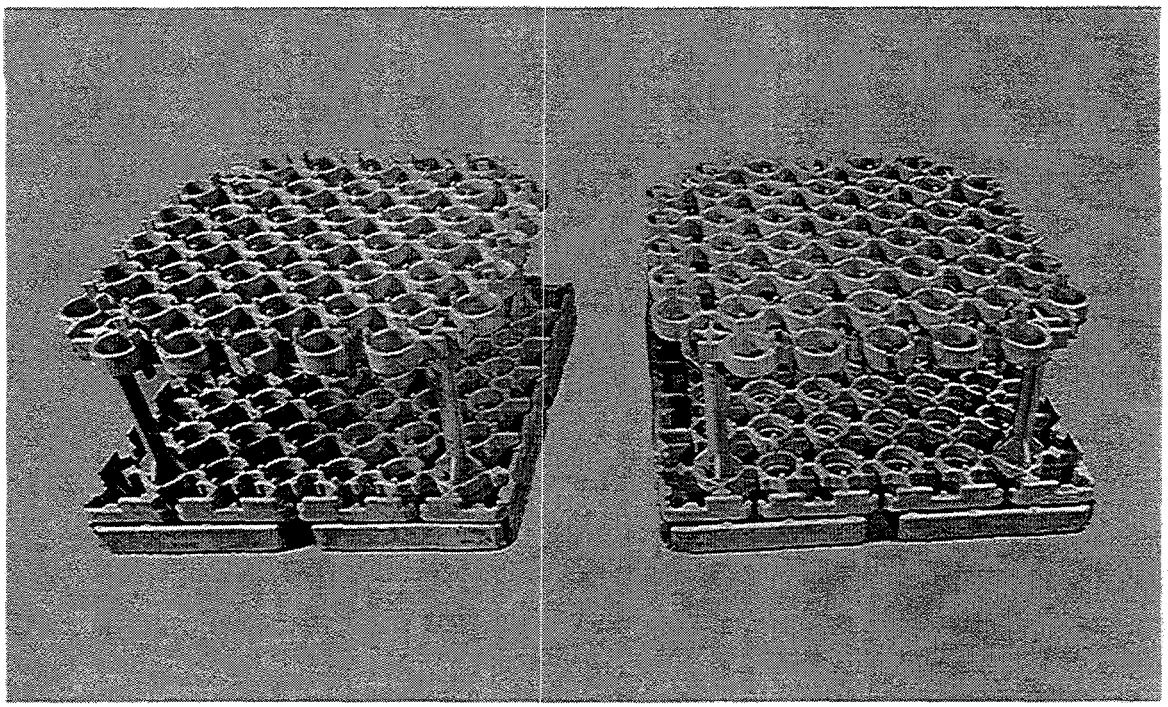

Fig. 7. Two cast tray and fixture assemblies of IC-221M for pusher carburizing furnace.

Table 2. Nominal chemical analysis of IC-221LA and IC-221W filler wires for use with Ni_3Al-based alloy IC-221M

Element	Weight percent	
	IC-221LA	IC-221W
Cr	16.0	7.70
Ni	78.50	79.80
Mo	--	1.50
Al	4.00	8.00
B	0.003	0.003
Zr	1.50	3.00

Table 3. Summary of weld repairs carried out on the batch and pusher furnace components cast from IC-221M alloy

No.	Component verification	Furnace	Number of weld repairs			
			Bottom	Top	Sides	Total
1	Tray No. 1	Batch[a]	1	5	0	6
2	Tray No. 2	Batch[a]	2	4	0	6
3	Tray No. 3	Batch[a]	0	1	0	1
4	Top fixture No. 1	Pusher[a]	0	1	0	1
5	Bottom fixture No. 2	Pusher[a]	0	0	0	0
6	Tray No. 1	Pusher[a]	9	0	1	10
7	Four posts	Pusher[a]	0	0	0	0
8	Tray No. 4	Batch[b]	0	5	0	5
9	Tray No. 5	Batch[b]	0	5	0	5
10	Tray No. 6	Batch[b]	4	3	1	8
11	Top fixture No. 3	Pusher[b]	0	0	0	0
12	Bottom fixture No. 4	Pusher[b]	0	0	0	0
13	Tray No. 2	Pusher[b]	8	0	4	12
14	Four posts	Pusher[b]	0	0	0	0

[a]As cast.

[b]Cast, welded, and preoxidized for 3 h at 1100°C in air.

The coupons and trays in both the batch furnace and in the pusher furnace were exposed to carburization and oil-quenching cycle. Each cycle in the batch furnace lasted 8 h, and the duration cycle in the pusher furnace was 24 h. Thus, the batch furnace trays and coupons underwent three cycles per day, whereas, coupons in the pusher furnace cycled only once a day.

In addition to coupon testing at Delphi Saginaw, simulated coupon testing was also carried out at ORNL. The simulated testing consisted of exposing the coupons in an air furnace at 900°C for 30 min followed by oil quenching. The same quenching oil was used by Delphi Saginaw for production heat treat. The effect of simulated cycles or actual cycles in the batch and pusher furnaces was analyzed by hardness change and microstructural analysis.

The hardness data for the IC-221M and HU coupons removed from the batch and pusher furnaces are presented in Table 5. The hardness data of the coupons exposed in the carburizing furnaces and those subjected to the simulated cycles are compared in

Low-Silicon Tray Coupon

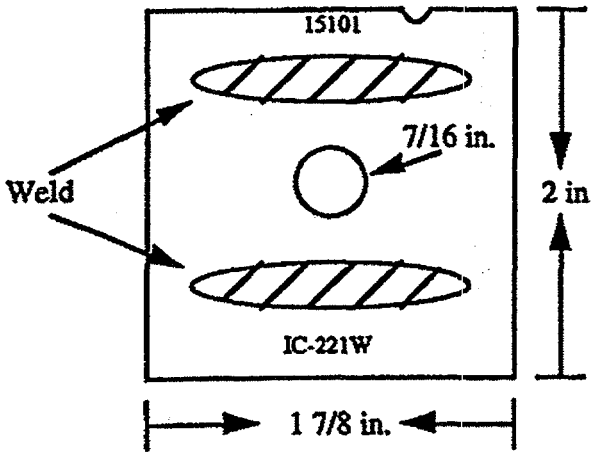

- o Welds on machined surface.
- o All other surfaces are in the as-cast condition.

High-Silicon Tray Coupon

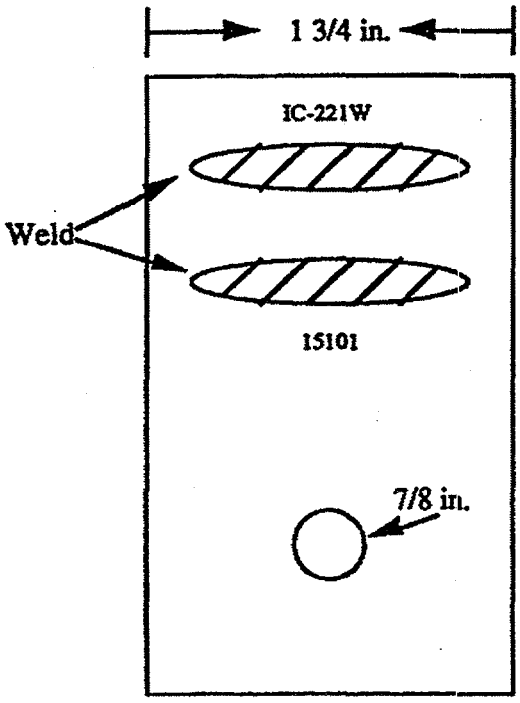

- o Welds on machined surface.
- o All other surfaces are in the as-cast condition.

Fig. 8. Geometry of low- and high-silicon tray test coupons.

Table 4. Coupon removal schedule[a]

Schedules removal (months)	Ni-Al Allcase test coupons			Ni-Al Plant 5 pusher test coupons		
	Sample		Days	Sample		Days
1.4	#20S, 20L	20-Aug-93	31	#76	01-Mar-94	31
	#1HU	20-Aug-93	31	HU		
2.6	#6HU	24-Sep-93	56	#77	08-Apr-94	57
	$65	19-Apr-94	68	HU		
3.7	#5HU	28-Oct-93	80	--		--
	#62	24-May-94	89	--		--
5.9	#2HU	14-Jan-94	128	#78	01-Sep-94	128
	#21L, 22S	28-Jan-94	125	HU		
9.6	#11HU	22-Dec-94	208	#79	23-Dec-94	206
	#63	10-Nov-94	208	HU		
11.8	#8HU	20-Jul-94	256	--		--
	#39L, 40S	22-Aug-94	256	#80	14-Mar-95	256
	#51PO	10-Nov-94	256	HU		
15.5	#12HU	06-Jul-95	336	--		--
	#64	24-May-95	336	--		--
	#61 Spare	24-May-95	336	--		--
17.5	#9HU	23-Jan-95	379	--		--
	#23S	23-Feb-95	379	--		--
	--		--	#81	12-Sep-95	379
	--		--	HU		
23.3	#10HU	24-Jul-95	504	--		--
	#24S, 25L	24-Aug-95	504	--		--
	--		--	#82	07-Mar-96	504
	--		--	HU		

[a]Nickel-aluminide test program, Oak Ridge National Laboratory.

Notes: 1. Samples 1-10 original HU test coupons on outside of allcase box (08-Jul-93); 2. HU samples 3, 4, 7, 8, 9, & 10 sheared off. Samples 8, 9, & 10 reinstalled on inside of box (24-Feb-94); 3. Replacement HU samples 11 & 12 attached to inside of allcase box (24-Feb-94); 4. Samples 21-30 original Ni-Al test coupons installed on outside of allcase box (08-Jul-93); 5. Samples 21-25 original allcase Ni-Al samples. Samples sheared off and reattached to inside of box. Lost service time from 10/18-10/28/93; 6. Samples 39 & 40 original Ni-Al samples removed and reattached. Lost service 9/24-10/28/93; 7. Preoxidized Ni-Al coupon 51 installed on inside of allcase box (28-Oct-93); 8. Replacement Ni-Al test coupons 61-65 installed on inside of allcase box (14-Jan-94); 9. Original Ni-Al coupons 76-82 installed on outside of spidercarburizer box (14-Jan-94); 10. Original HU coupons installed on outside of spider carburizer box (14-Jan-94); 11. Spider carb at Plant 5 down 4/8-5/24/94.

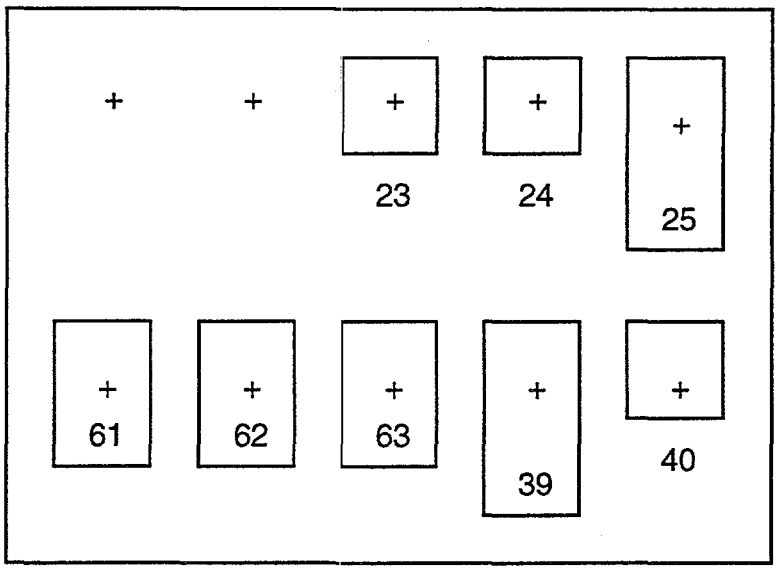

Inside of back pot (on nickel-aluminide tray)

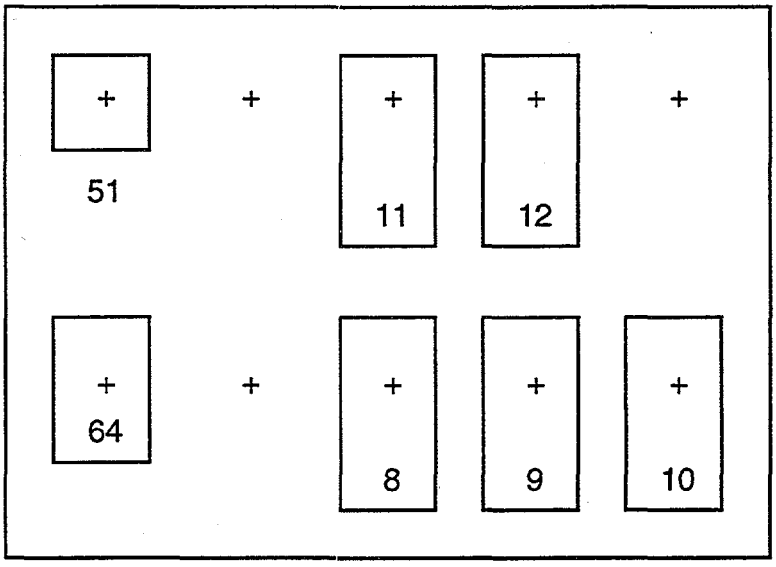

Outside of front pot (on HU-base tray)

Fig. 9. Attachment scheme for the IC-221M and HU coupons to the box setting on IC-221M and HU trays.

Figs. 10 through 12. In the as-cast condition, the HU coupons exhibited low hardness. The hardness increased with either the simulated cycles in the laboratory or actual cycles in the carburizing furnace. The IC-221M coupons either showed no change in hardness or it dropped in some cases. There was substantial scatter in the data for coupons removed from the carburizing furnaces. This scatter could result from the way the coupons were handled. For example, some coupons were sand blasted after removal and some were removed after a carbon burn-off cycle.

Table 5. Coupon surface hardness data

Material	Time (days)	Cycles	Furnace type	Surface condition	Hardness (R_C)
HU	57	57	Pusher	Cast	7.3
Ni_3Al (low silicon)	57	57	Pusher	Cast	27.2[a]
Ni_3Al (low silicon)	57	57	Pusher	Machined	18.4[a]
Ni_3Al (low silicon)	68	204	Batch	Cast	27.3
Ni_3Al (low silicon)	68	204	Batch	Machined	25.3
Ni_3Al (low silicon)	89	267	Batch	Cast	28.91
Ni_3Al (low silicon)	89	267	Batch	Machined	19.71
HU	258	774	Batch	Cast	*b*

[a]Coupon was accidentally sand blasted at General Motors-Saginaw prior to receipt at the Oak Ridge National Laboratory.

[b]Surface hardness was R_B86 (average of ten readings).

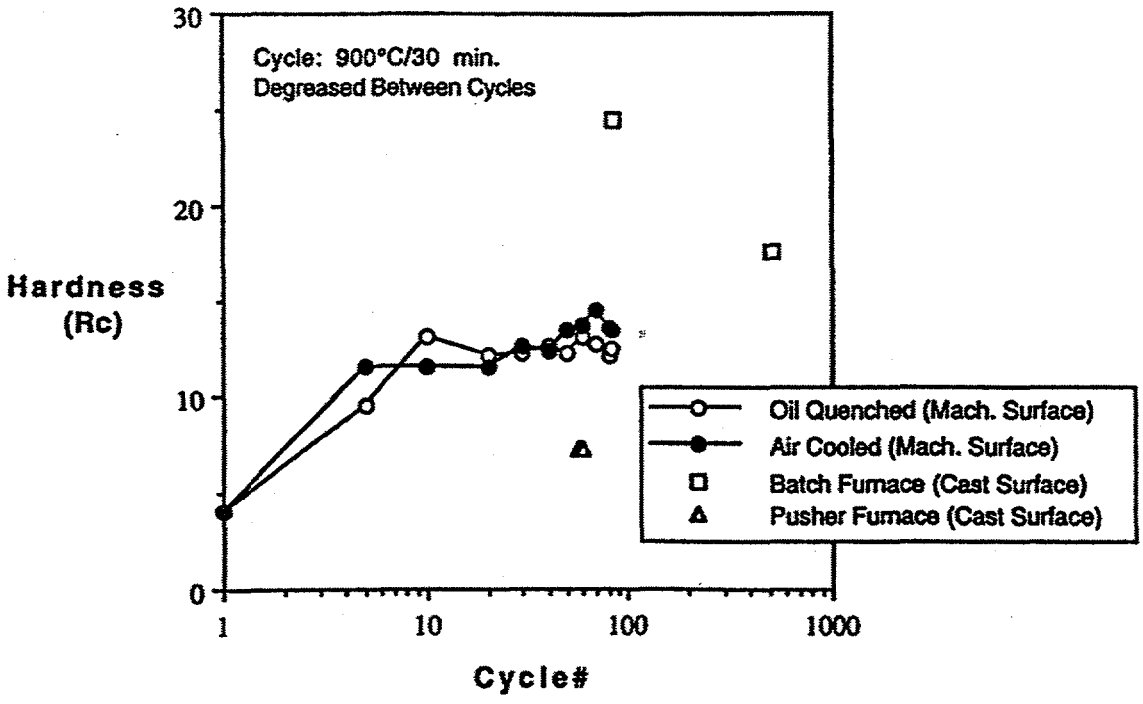

Fig. 10. Thermal cycle hardness data of HU.

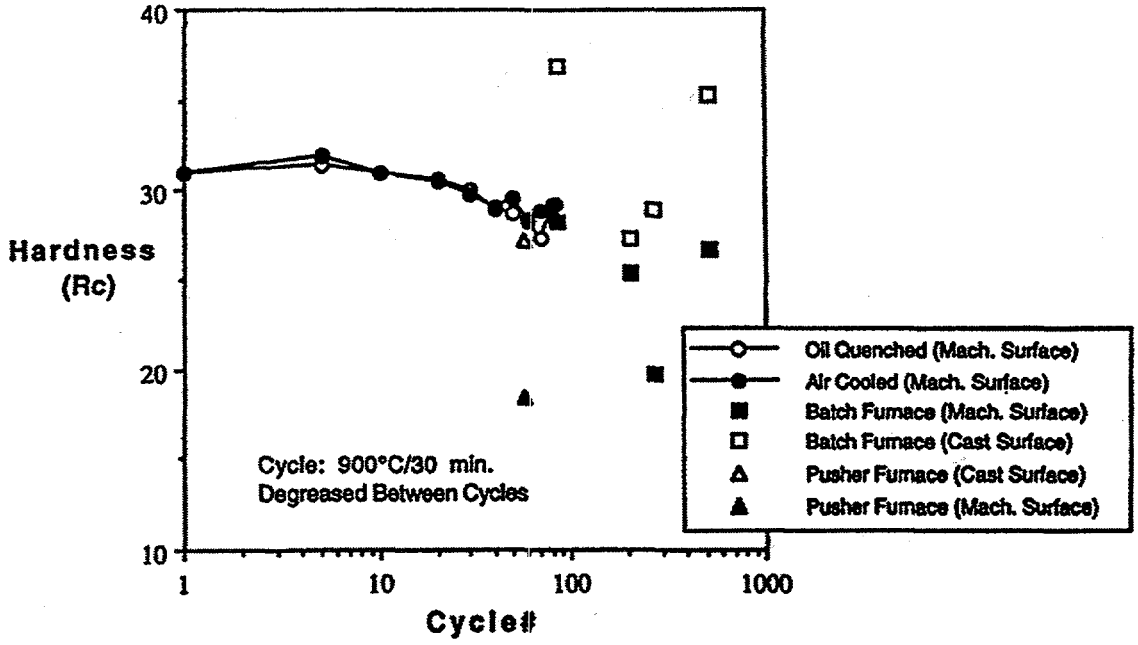

Fig. 11. Hardness data as a function of thermal cycles on coupons from tray sections of IC-221M alloy containing low silicon.

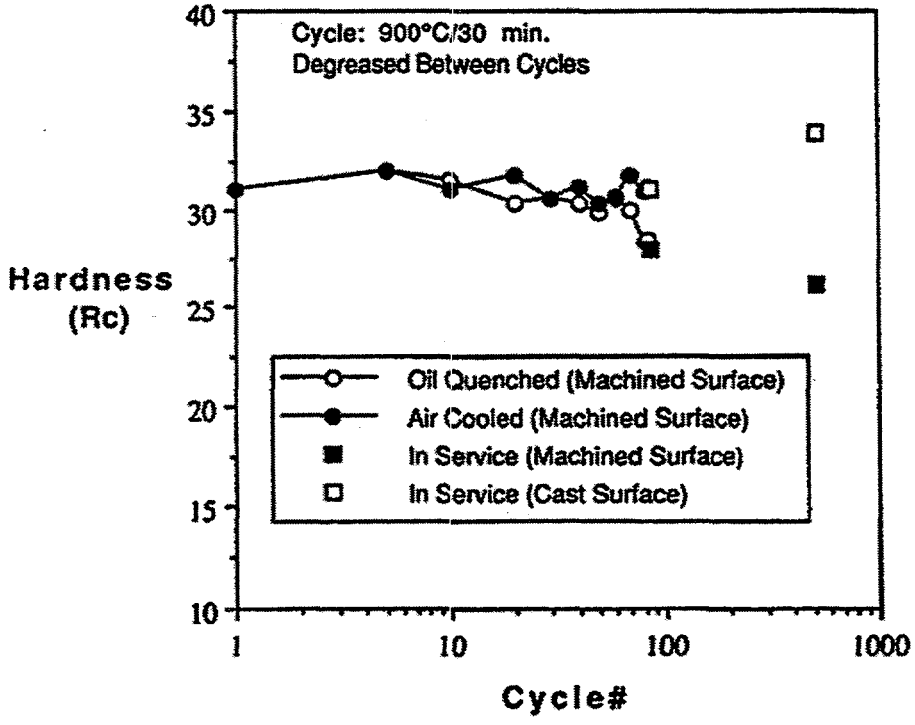

Fig. 12. Hardness data as a function of thermal cycles on coupons from tray sections of IC-221M alloy containing high silicon.

In order to investigate the depth of hardness change, microhardness measurements were made from the surface to near the center of the coupon thickness. Photomicrographs showing the actual indentations are shown in Fig. 13 for HU and IC-221M coupons after six months exposure in the batch carburizing furnace. The microhardness data are plotted as a function of distance in Fig. 14. The high hardness is indicative of hardening from the carburization products (carbides and increased matrix carbon). Data in Fig. 14 show that the carburization after a six-months exposure in a batch furnace has penetrated throughout the coupon thickness for the HU coupons, whereas, it only penetrated approximately 20 mil deep for the IC-221M coupons.

Photomicrographs of coupons of HU and IC-221M of low and high silicon after six months exposure in the batch carburization furnace at Delphi Saginaw are presented in Figs. 15 through 17. The photomicrographs show the variation of microstructure from the edge to the coupon center. The HU coupons show no surface scale, and the carburization product appears to have propagated through the coupon thickness. The IC-221M coupons show surface-scale and carburization-related changes only to a small distance beneath the scale. The scale thicknesses of IC-221M coupons after exposure in batch and pusher furnaces are summarized in Table 6. Data in this table include the measurements for the base- and weld-metal regions. The scale thickness for the exposed coupons of IC-221M is plotted as a function of the number of cycles in Fig. 18.

Scanning electron microscopy and microprobe analysis were carried out to determine the nature of the scale and microstructural changes in the matrix. A typical set of back-scattered electron images and the maps of Cr, Al, Ni, Zr, C, O, and Si are shown in Figs. 19 through 23. A similar set of micrographs for HU are shown in Figs. 24 through 27. The quantitative electron microprobe data showing the composition of various species observed in the exposed coupons of IC-221M and HU are summarized in Tables 7 and 8. The microstructural changes in the Ni_3Al-based alloy IC-221M consisted of four distinct areas: (1) the base metal appeared unaffected by the carburization treatment, (2) a zone between the corrosion layer and the matrix (more than 200 μm thick) showed a slight nickel enrichment with a corresponding decrease in chromium, (3) a 10-μm-thick band under the corrosion layer exhibited substantial nickel enrichment with a corresponding decrease in chromium and aluminum, and (4) the corrosion layer made up of a matrix that contained a high concentration of nickel with severe depletion of chromium and aluminum and low Z inclusions that ranged from chromium oxide to aluminum oxide.

For the HU material, the matrix grain boundaries were enriched with chromium and carbon; the outer corrosion layer was chromium oxide and the inner corrosion layer was primarily silicon oxide.

In addition to the detailed analysis of coupons at ORNL, Delphi Saginaw made several observations regarding the appearance of the coupons and trays and the dimensional changes for the trays (see Fig. 28). Note that the coupon observations are consistent with the observations made on the trays. For example, the HU tray started to show cracking and had grown from 30 to 30-5/16 in. as opposed to no observable changes in the IC-221M tray and the dimenstional change only to 30-3/16.

The latest IC-221M coupon (No. 51) removed after 336 days exposure from the batch furnace was installed in the preoxidized condition. The coupon (No. 61) removed at the same time had an exposure time of 208 days (624 cycles). This sample was installed in

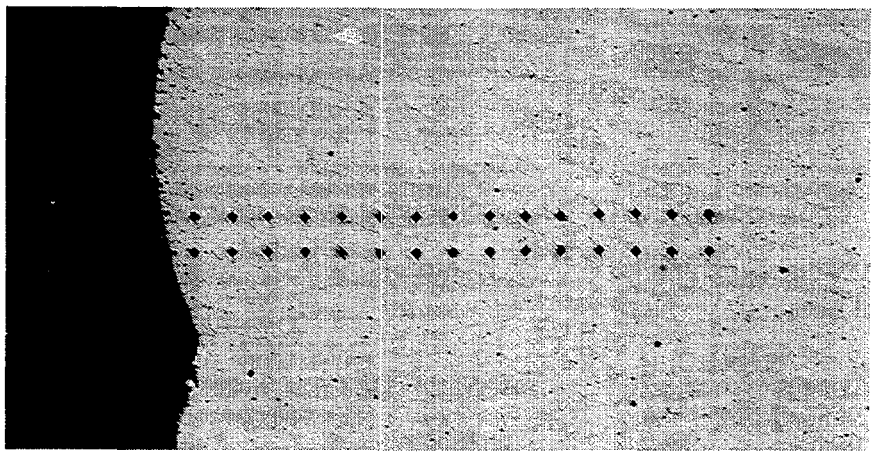

94-0296-006

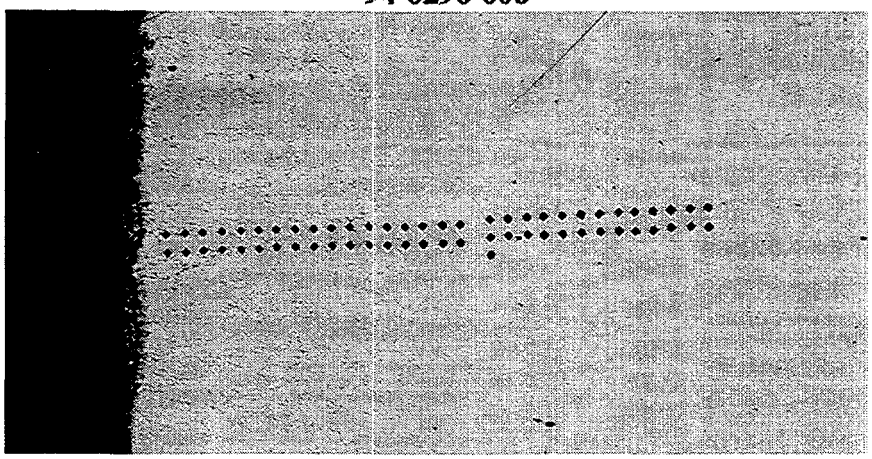

94-0301-007

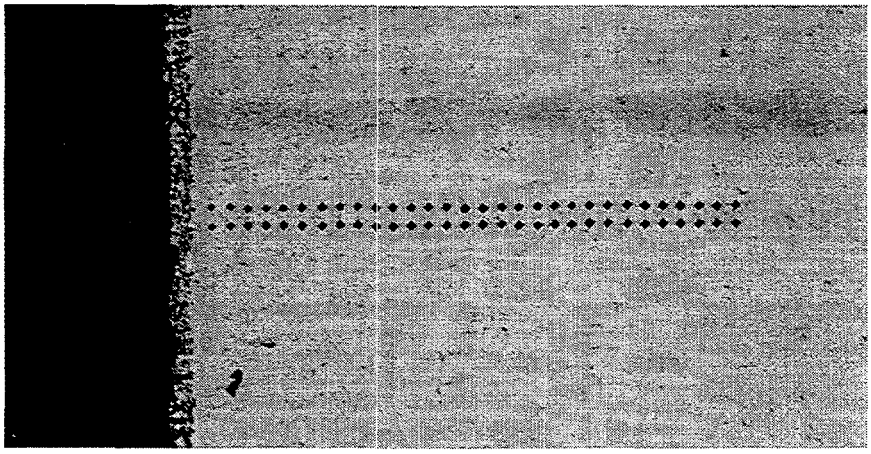

94-0299-007

Fig. 13. Optical micrographs showing diamond pyramid microhardness indentations made in HU and nickel-aluminide coupons exposed for six months in a carburizing batch furnace at Delphi Saginaw. The first micrograph is HU, the second is low-silicon nickel aluminide, and the third is high-silicon nickel aluminide.

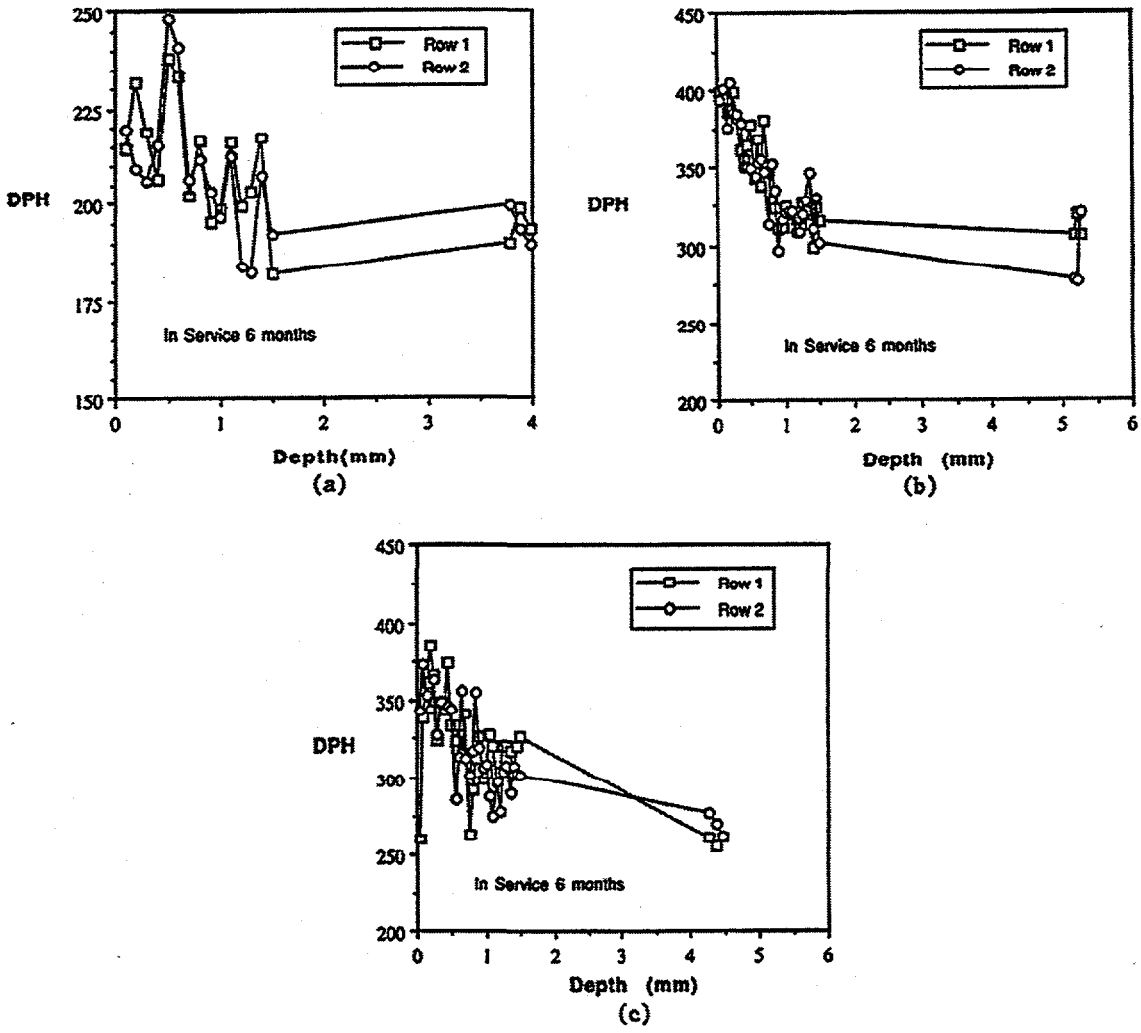

Fig. 14. Depth of carbon penetration after six-months exposure in a batch furnace throughout the coupon thickness for: (a) HU, (b) low-silicon nickel aluminide, and (c) high-silicon nickel aluminide.

furnace in the as-cast condition. The optical microstructures of the edge and center of coupons 51 and 61 are shown in Figs. 29 and 30. Photomicrographs comparing the weld crowns of IC-221LA and IC-221W on coupon No. 51 after 336 days exposure are shown in Fig. 31. These photomicrographs show the following:

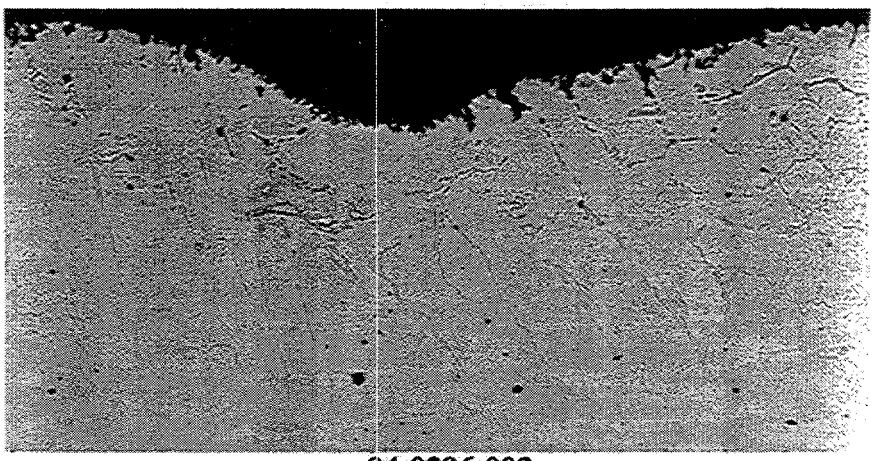

94-0296-003

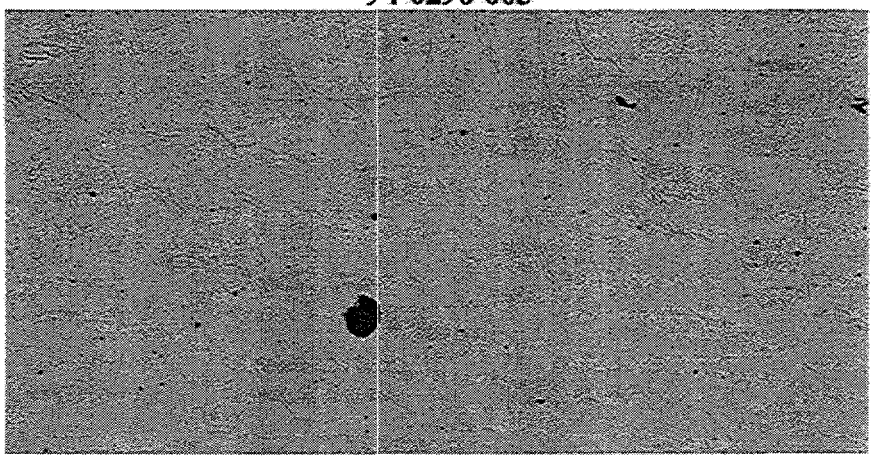

94-0296-004

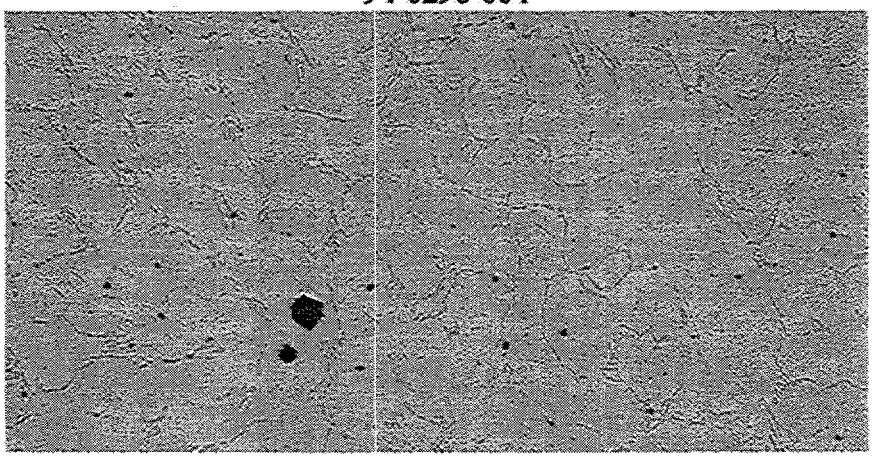

94-0296-005

Fig. 15. Optical micrographs showing the variation of microstructure from the edge to the center of the HU coupon exposed for six months in a carburizing batch furnace at Delphi Saginaw.

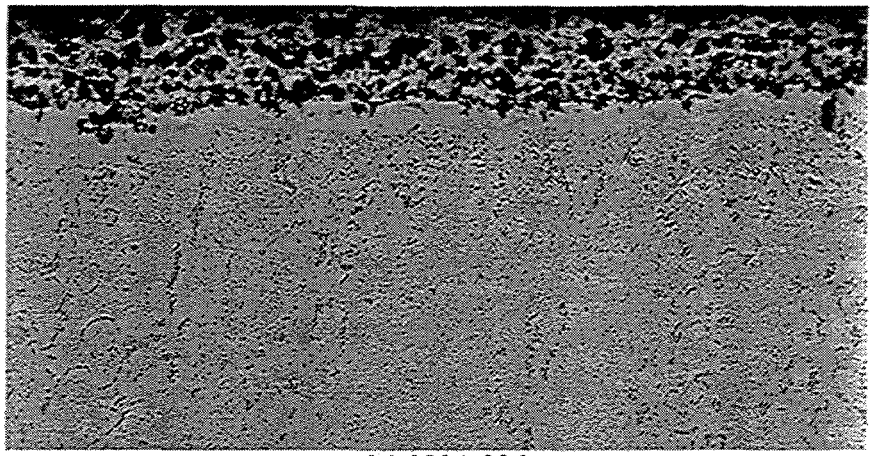

94-0301-004

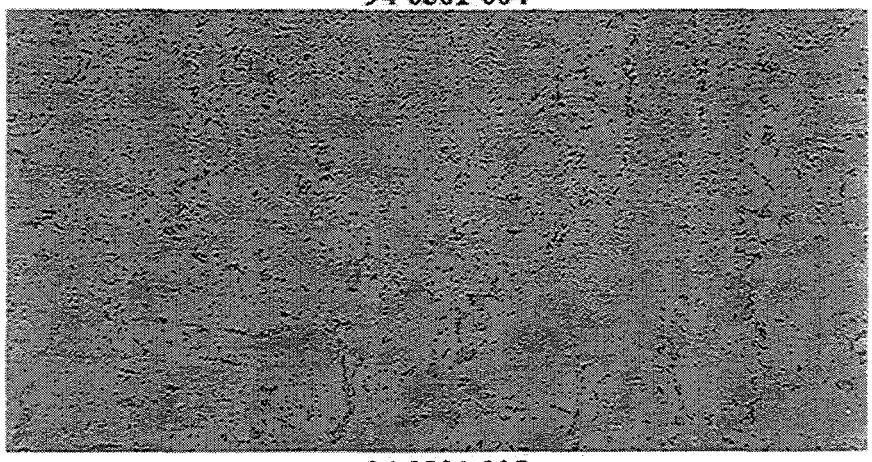

94-0301-005

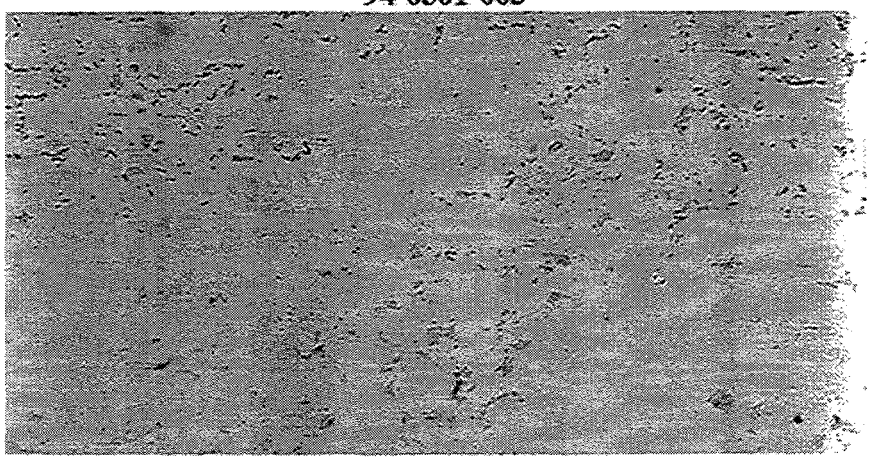

94-0301-006

Fig. 16. Optical micrographs showing the variation of microstructure from the edge to the center of the low-silicon nickel-aluminide coupon exposed for six months in a carburizing batch furnace at Delphi Saginaw.

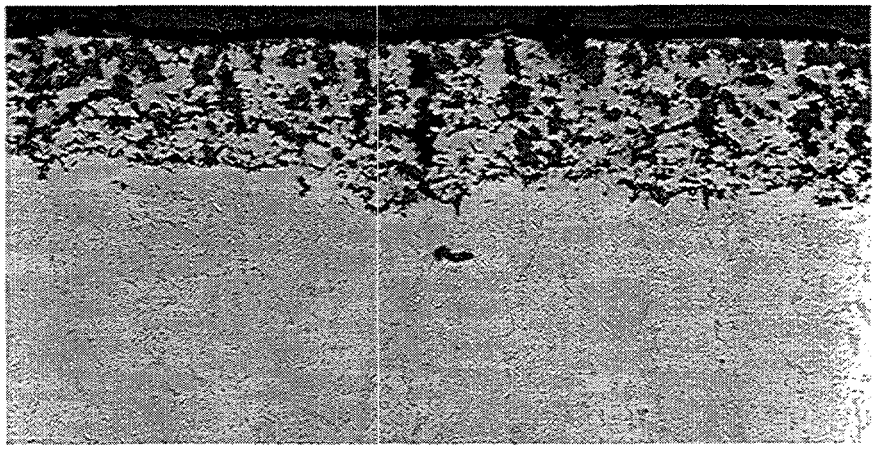

94-0299-004

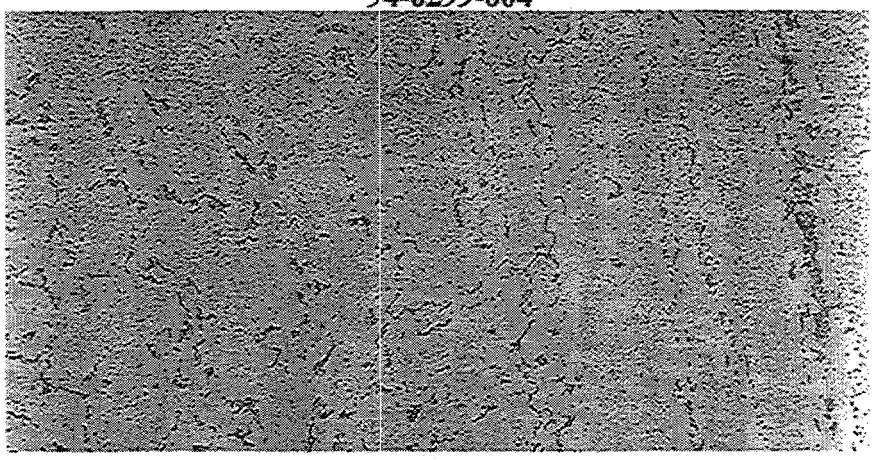

94-0299-005

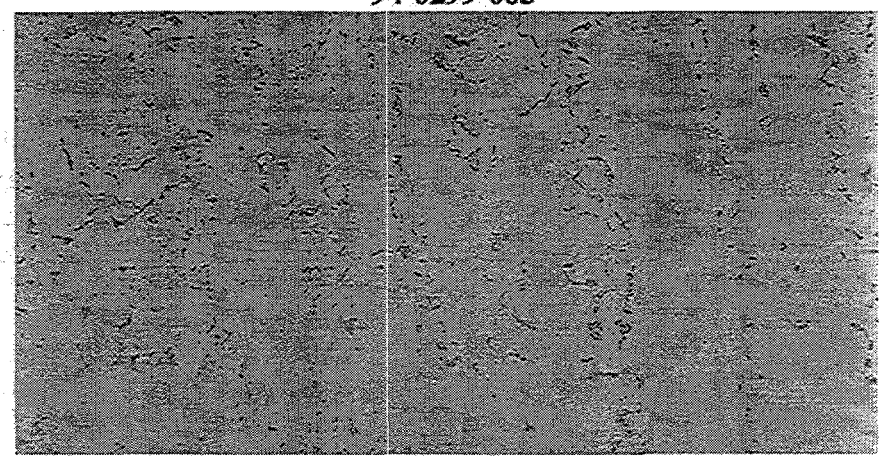

94-0299-006

Fig. 17. Optical micrographs showing the variation of microstructure from the edge to the center of the high-silicon nickel-aluminide coupon exposed for six months in a carburizing batch furnace at Delphi Saginaw.

Table 6. Scale thickness of nickel-aluminide coupons after exposure in batch and pusher furnaces

Coupon type	Time (months)	Actual time (days)	Furnace type	Scale thickness (mils)
Low silicon	2.6	57	Pusher	2.5
Low silicon	2.6	68	Batch	2.5 to 3.75
Low silicon (IC-221W weld)	2.6	57	Pusher	2.19
Low silicon (IC-221LA weld)	2.6	57	Pusher	2.5
Low silicon (IC-221LA weld)	2.6	68	Batch	2.5
Low silicon	3.7	89	Batch	2.5
Low silicon (IC-221LA weld)	3.7	89	Batch	2.19

1. The corrosion layer on IC-221M grows with exposure time. However, the growth is still near the surface unlike the deep penetration in HU coupons.

2. The preoxidized coupon with 336 days exposure showed less corrosion layer as opposed to the as-cast coupon after 208 days, indicating that preoxidation impedes the carburization process in IC-221M.

3. The welds of both IC-221LA and IC-221W show similar corrosion layer. However, the IC-221W shows a highly enriched nickel layer similar to that of the IC-221M base metal as opposed to no such layer in IC-221LA. This difference may be due to higher chromium and lower aluminum content of IC-221LA as opposed to IC-221W.

Testing of Trays and Tray and Assemblies in Batch and Pusher Carburizing Furnaces

An HU and IC-221M tray went into service in a batch carburizing furnace on July 8, 1993, at Plant 3 in Delphi Saginaw. A letter from Delphi Saginaw (see Fig. 28) indicated that the HU tray had cracked and showed significant dimensional growth as opposed to the IC-221M tray. Since that letter, the HU tray has broken at several places and has been removed from the furnace and is now being stored at ORNL. The broken HU tray is shown in Fig. 32. The IC-221M tray, showing no cracks, was also removed from the furnace along with the HU tray and is currently being stored at Delphi Saginaw. The IC-221M tray will go into service along with a new HU tray.

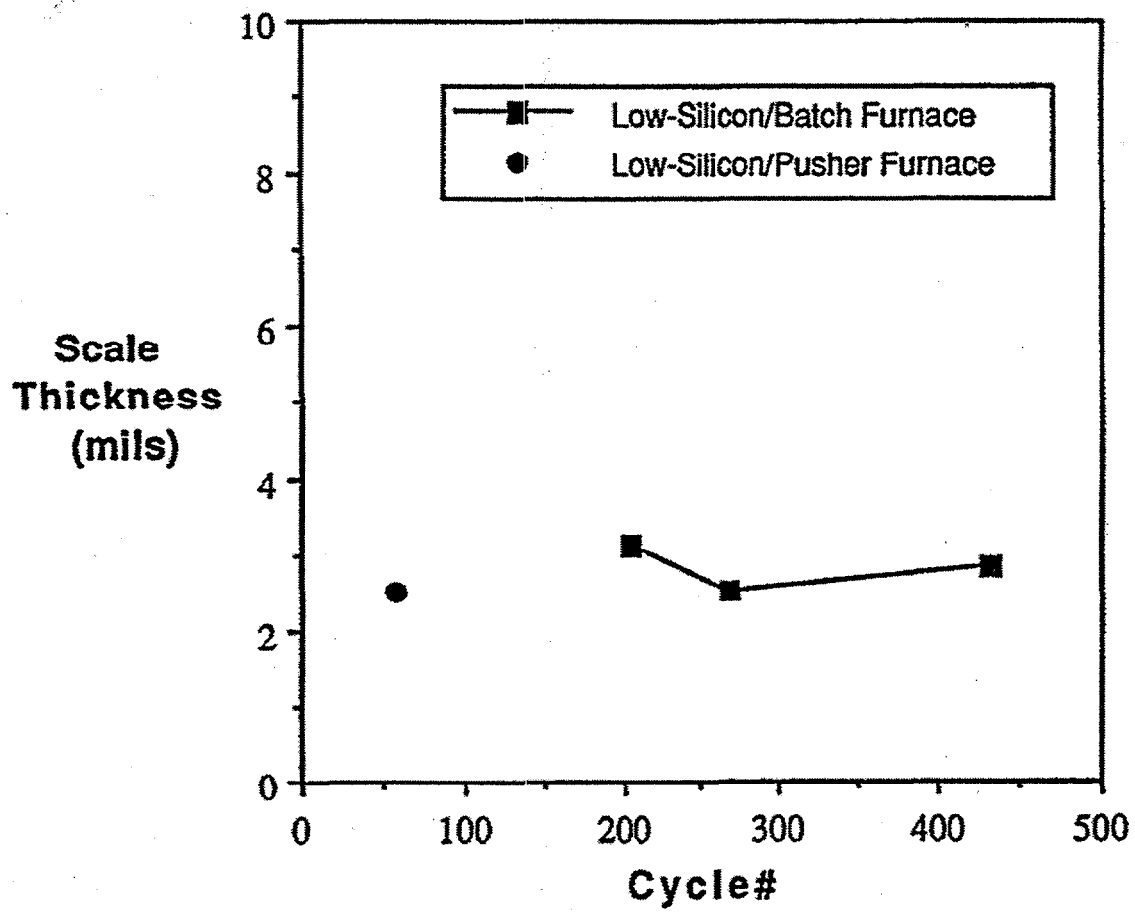

Fig. 18. Surface scale thickness of nickel-aluminide coupons versus exposure time in batch and pusher carburizing furnaces at Delphi Saginaw.

The coupon and tray results encouraged that Delphi Saginaw to install six additional trays in the batch furnaces and two assemblies in the pusher furnace. Also, based on the results of a preoxidized coupon, it was decided that three of the six batch furnace trays and one of the two pusher furnace assemblies will be preoxidized. The preoxidation treatment was selected to be 1100°C for 3 h in air. The as-cast and preoxidized trays and assemblies of IC-221M are shown in Figs. 33 and 34. These trays and assemblies are currently at Delphi Saginaw.

Commercial Production of a Large Number of Pusher Furnace Assemblies

One of the goals of the CRADA was to produce a large number of pusher assemblies. There were several reasons for using the large number of assemblies, including: (1) to demonstrate that nickel aluminide can be produced under production conditions, (2) it can be produced under production conditions using revert stock, (3) weld repair of the assemblies can be accomplished, (4) dimensional stability of the castings can be achieved, (5) metal feed system can be cut and ground under commercially used foundry conditions, and (6) finished components can be preoxidized at 1100°C for 1 h under commercial heat-treating conditions.

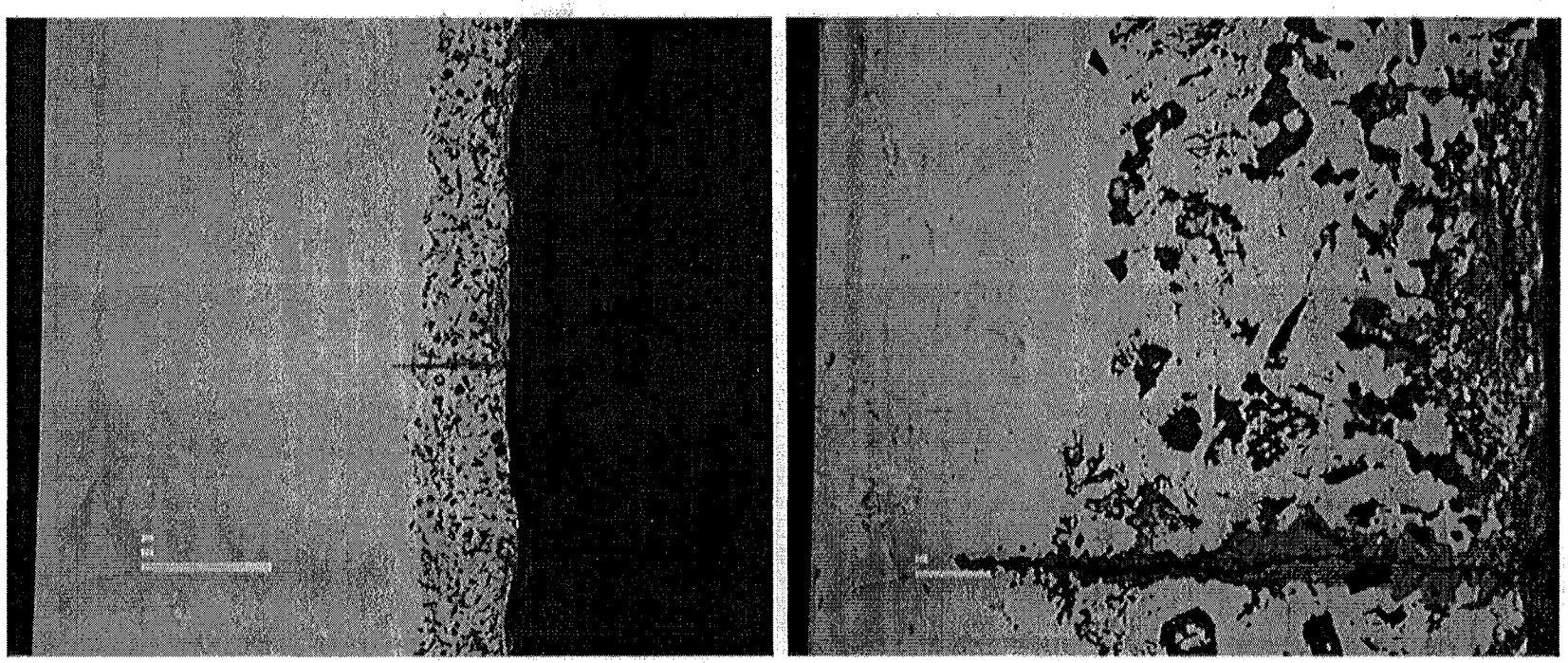

(a) *(b)*

Fig. 19. Backscattered electron image of low-silicon nickel-aluminide coupon exposed 18 days in a batch furnace at Delphi Saginaw: (*a*) low magnification of 200× and (*b*) high magnification of 100×.

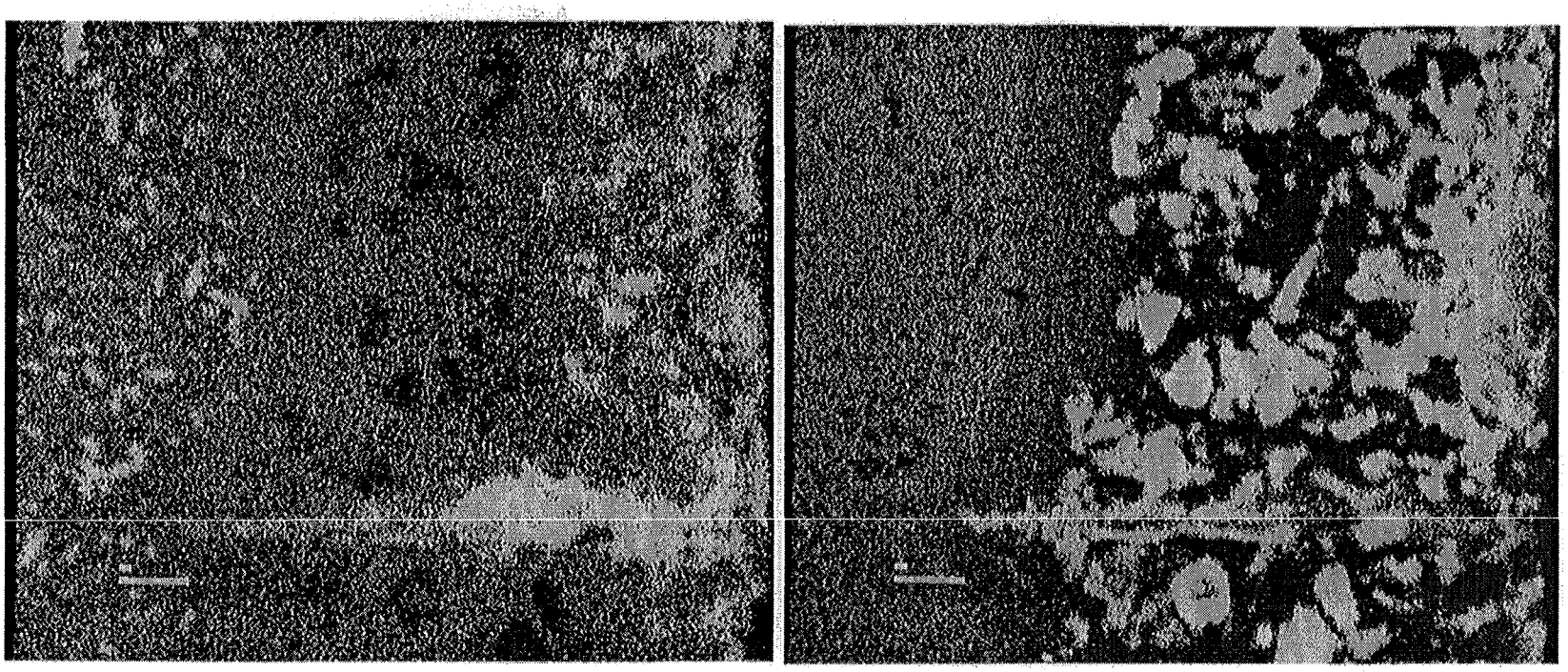

(c) *(d)*

Fig. 20. (*c*) and (*d*) are chromium and aluminum maps of the region shown in the backscattered electron image shown in (*b*) of Fig. 19 of the low-silicon nickel-aluminide coupon exposed for 68 days in a batch furnace at Delphi Saginaw.

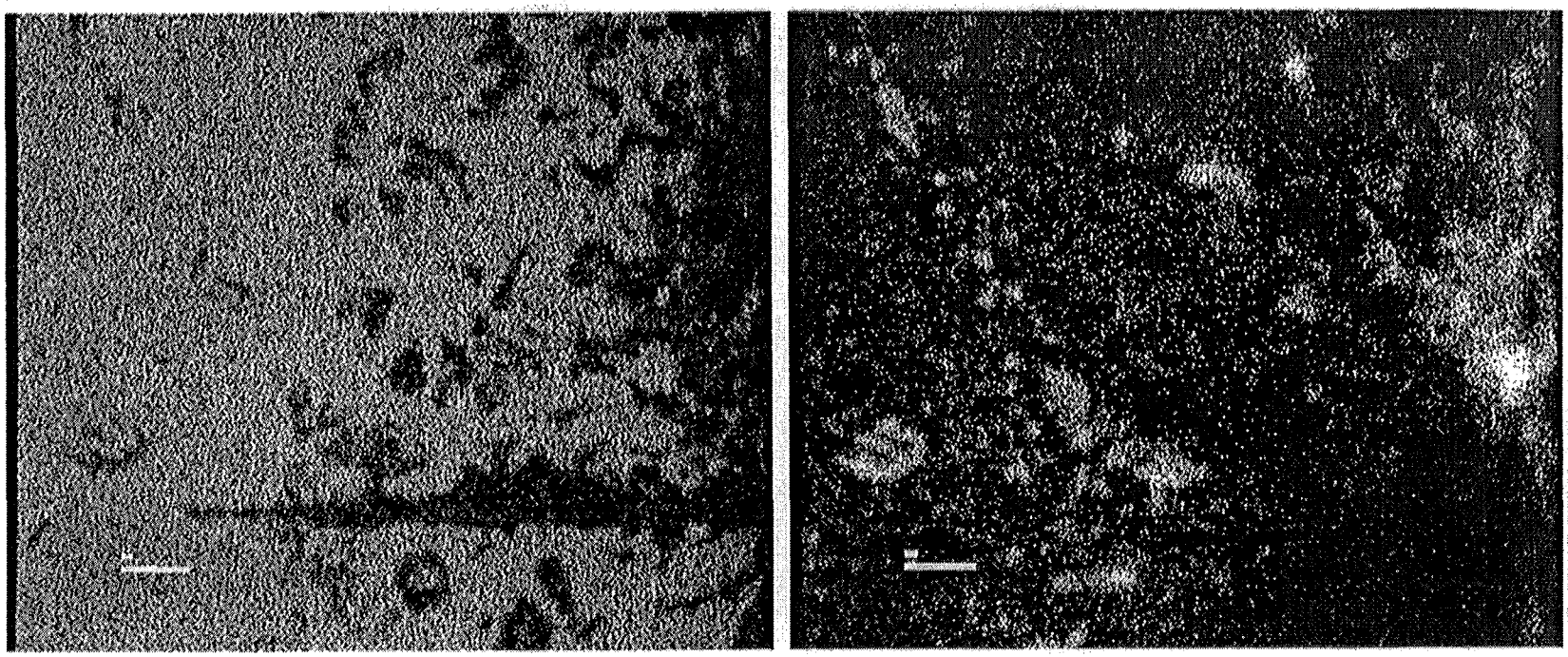

(e) (f)

Fig. 21. (*e*) and (f) are nickel and zirconium maps of the region shown in the backscattered electron image shown in (*b*) of Fig. 19 of the low-silicon nickel-aluminide coupon exposed for 68 days in a batch furnace at Delphi Saginaw.

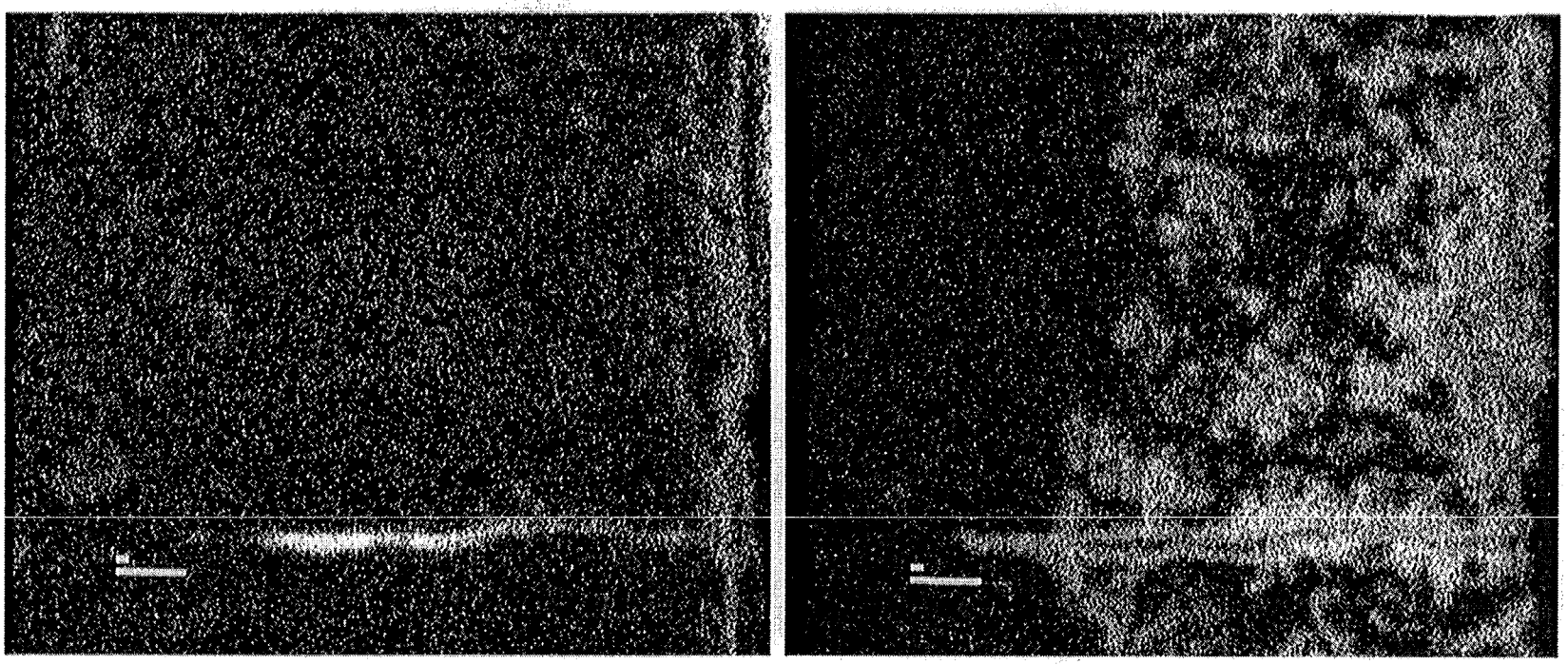

(g) *(h)*

Fig. 22. (*g*) and (*h*) are carbon and oxygen maps of the region shown in the backscattered electron image shown in (*b*) of Fig. 19 of the low-silicon nickel-aluminide coupon exposed for 68 days in a batch furnace at Delphi Saginaw.

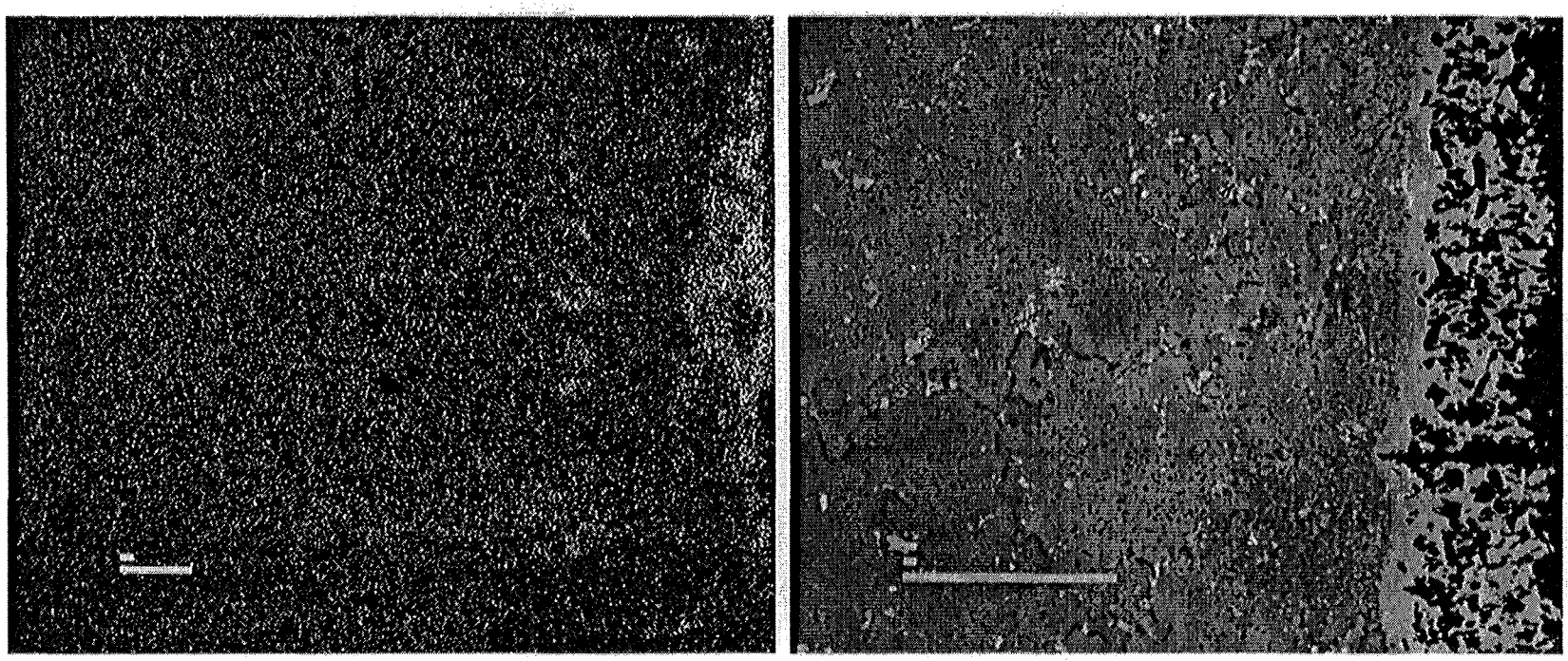

(i) *(j)*

Fig. 23. (*i*) is silicon map at 1000× and (*j*) is the backscattered electron image at 300× of the backscattered electron image shown in (*b*) of Fig. 19 of the low-silicon nickel-aluminide coupon exposed for 68 days in a batch furnace at Delphi Saginaw.

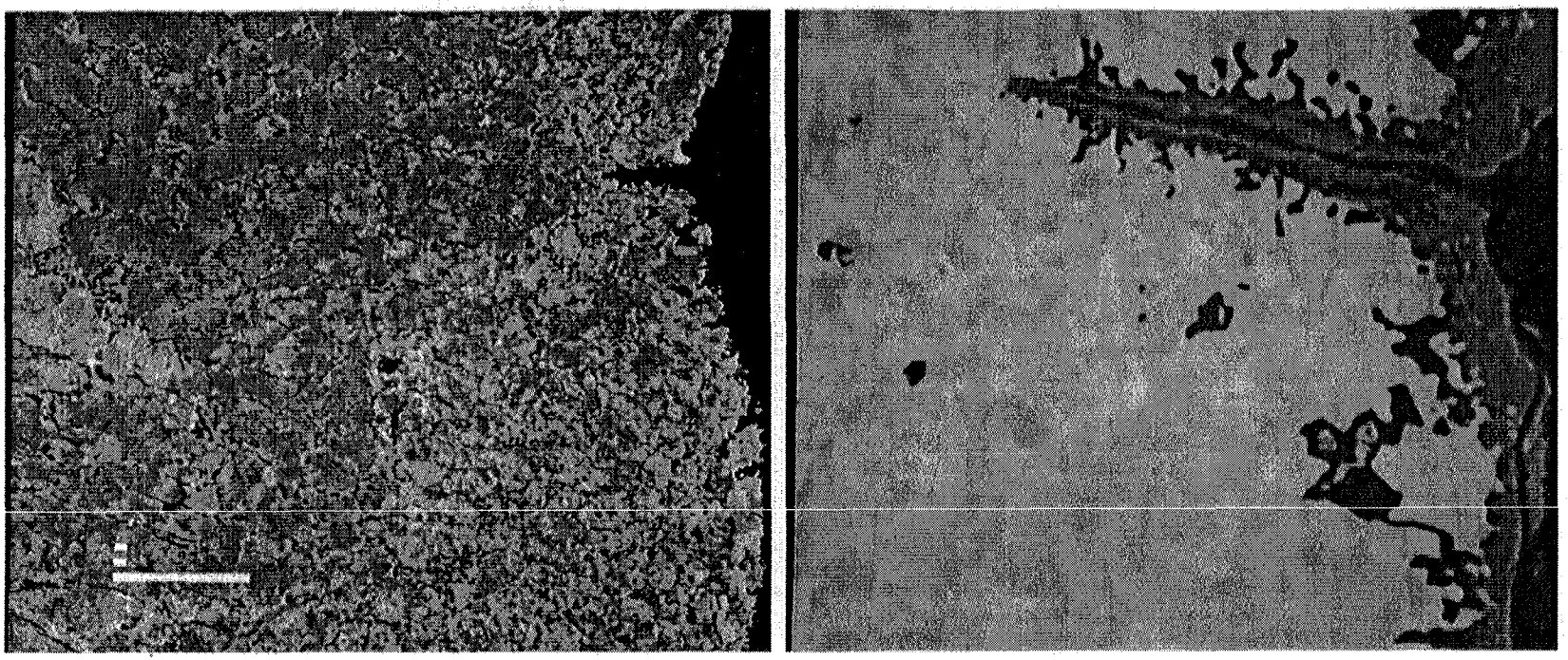

(a) *(b)*

Fig. 24. Backscattered electron image of HU coupon exposed for 258 days in a carburizing batch furnace at Delphi Saginaw: (*a*) low magnification is 200× and (*b*) high magnification is 1000×.

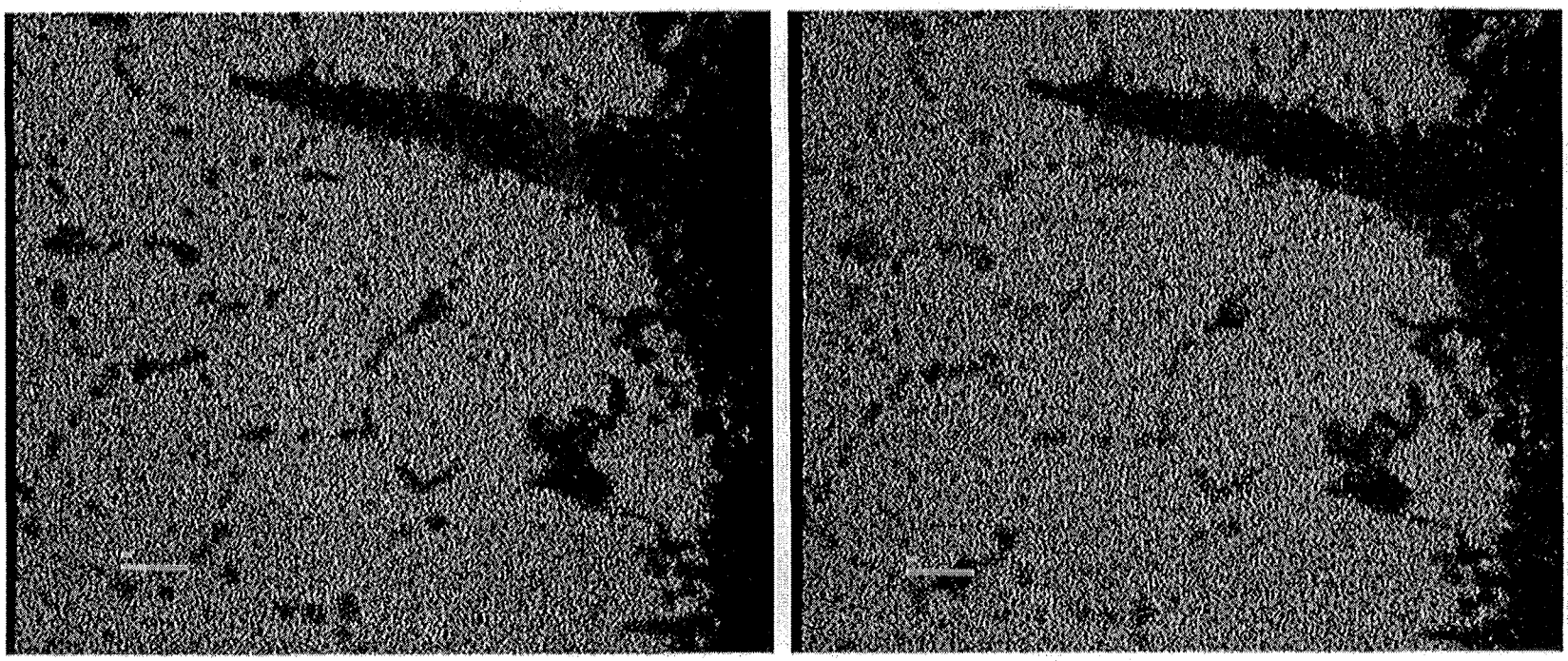

(c) *(d)*

Fig. 25. (*c*) and (*d*) are nickel and iron maps of the region shown in the backscattered electron image shown in (*b*) of Fig. 24 of HU coupon exposed for 258 days in a carburizing batch furnace at Delphi Saginaw.

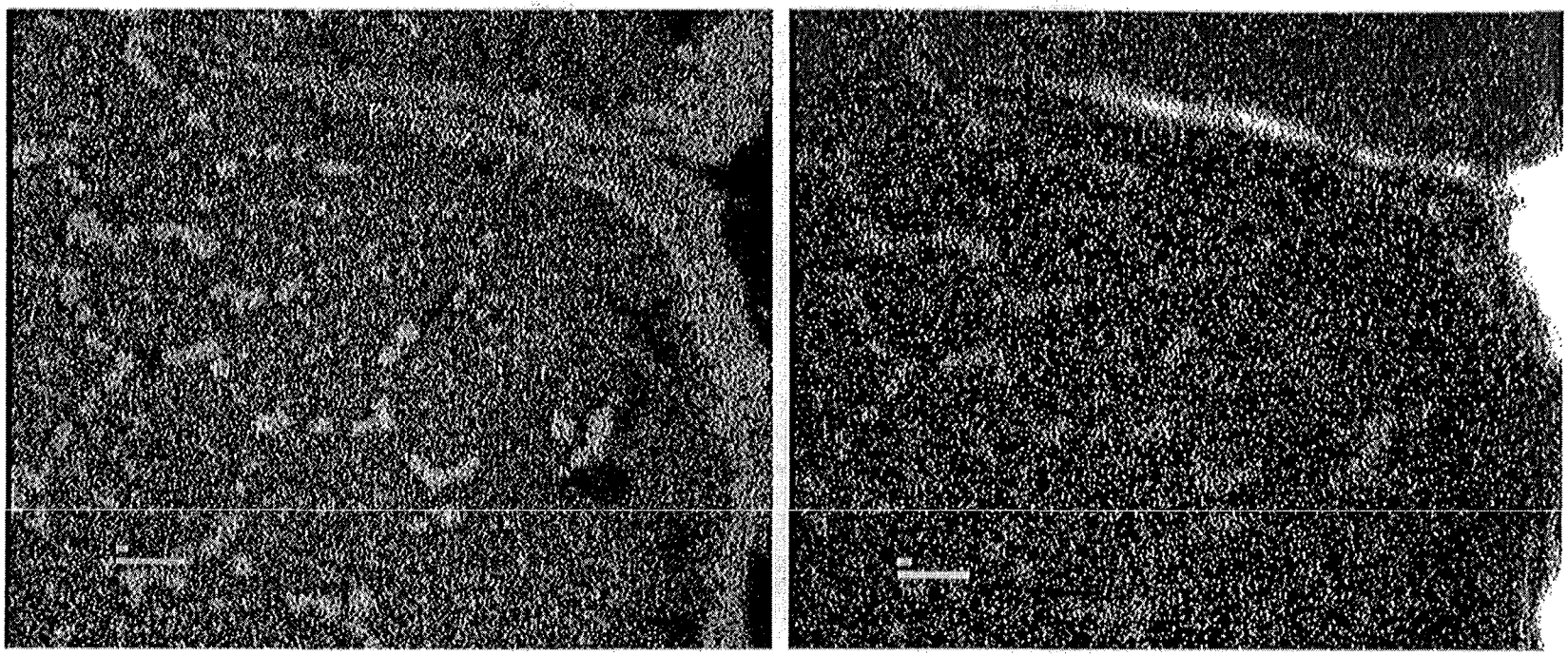

(e) *(f)*

Fig. 26. (*e*) and (*f*) are chromium maps of the region shown in the backscattered electron image shown in (*b*) of Fig. 24 of HU coupon exposed for 258 days in a carburizing batch furnace at Delphi Saginaw.

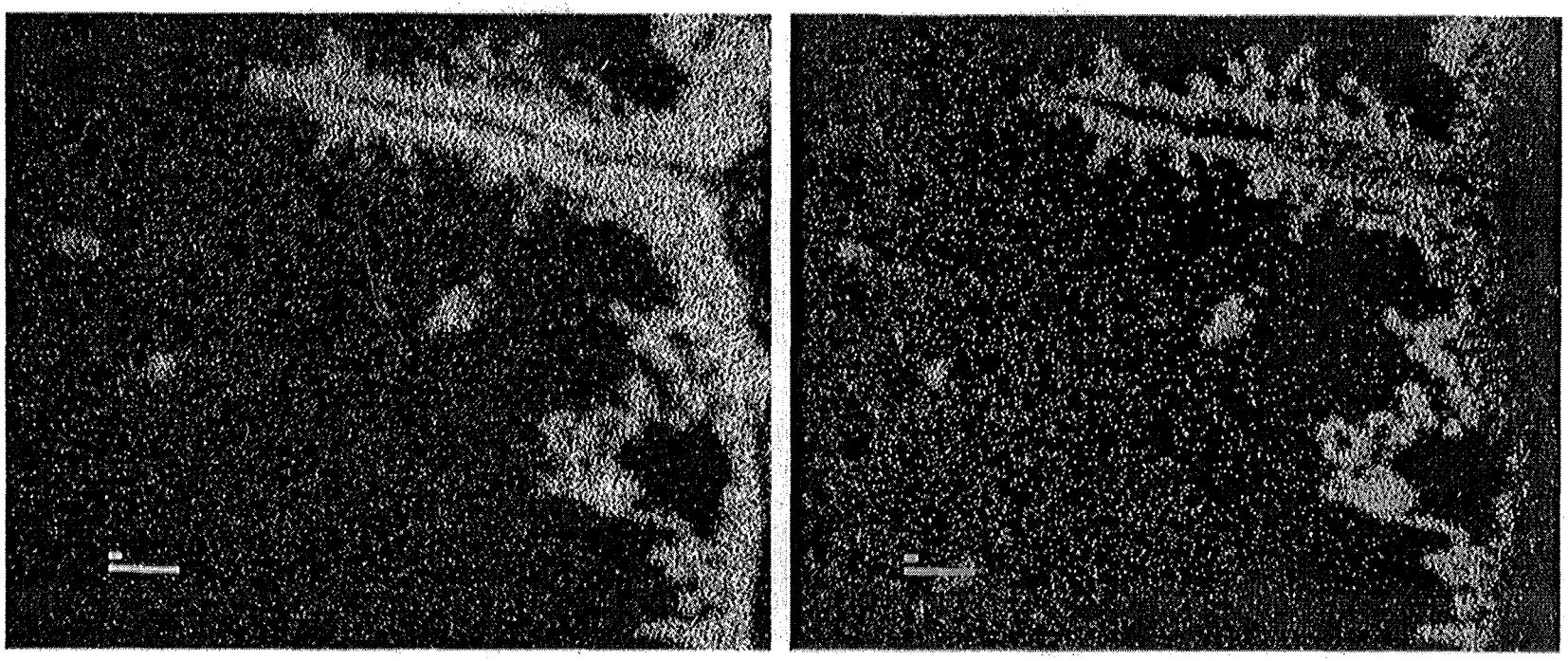

(g) *(h)*

Fig. 27. (*g*) and (*h*) are oxygen and silicon maps of the region shown in the backscattered electron image shown in (*b*) of Fig. 24 of HU coupon exposed for 258 days in a carburizing batch furnace at Delphi Saginaw.

Table 7. Quantitative electron microprobe data from different regions of low-silicon nickel-aluminide coupons exposed in batch and pusher furnaces at Delphi Saginaw

Coupon exposure	Element (weight percent)						
	Al	Ni	Cr	Zr	Si	C	O
Matrix							
68 days in a batch furnace	6.1 ± 0.62	82.47 ± 0.97	7.51 ± 1.06	1.01 ± 0.60	0.04 ± 0.0	0.35 ± 0.29	0.0
57 days in a pusher furnace	5.68 ± 0.29	82.42 ± 0.32	7.17 ± 0.67	0.94 ± 0.48	0.25 ± 0.01	0.66 ± 0.29	0.0
High *Z* inclusions in base material							
68 days in a batch furnace	0.17 ± 0.12	71.06 ± 0.56	1.07 ± 0.17	29.99 ± 0.91	0.05 ± 0.01	0.72 ± 0.15	0.41 ± 0.06
57 days in a pusher furnace	0.19 ± 0.21	70.34 ± 0.50	1.00 ± 0.17	29.67 ± 0.97	0.50 ± 0.03	0.47 ± 0.13	0.26 ± 0.18
Matrix zone adjacent to corrosion layer							
68 days in a batch furnace	6.30 ± 0.34	83.30 ± 0.64	6.52 ± 0.50	1.22 ± 0.23	0.17 ± 0.01	1.12 ± 0.32	0.0
57 days in a pusher furnace	5.46 ± 0.76	85.72 ± 0.57	4.40 ± 0.70	0.44 ± 0.31	0.26 ± 0.02	0.82 ± 0.14	0.0
High *Z* inclusion in zone adjacent to corrosion layer							
68 days in a batch furnace	3.19 ± 1.02	54.25 ± 4.39	11.53 ± 4.39	26.04 ± 7.10	0.05 ± 0.02	7.09 ± 2.81	0.29 ± 0.28
57 days in a pusher furnace	1.89 ± 0.59	45.37 ± 14.31	5.26 ± 2.06	42.21 ± 11.50	0.05 ± 0.02	8.83 ± 2.59	1.41 ± 1.66

Table 7. (continued)

Coupon exposure	Element (weight percent)						
	Al	Ni	Cr	Zr	Si	C	O
Low *Z* inclusion in zone adjacent to corrosion layer							
68 days in a batch furnace	4.28 ± 0.43	57.69 ± 6.95	31.50 ± 3.70	1.08 ± 0.70	0.09 ± 0.01	7.92 ± 2.20	0.0
57 days in a pusher furnace	1.12 ± 0.42	22.26 ± 7.04	69.13 ± 6.71	0.16 ± 0.20	0.06 ± 0.02	13.65 ± 0.43	0.0
Solid band beneath corrosion layer							
68 days in a batch furnace	2.82 ± 0.22	90.60 ± 1.67	4.09 ± 0.27	0.59 ± 0.86	0.10 ± 0.01	0.80 ± 0.15	0.0
57 days in a pusher furnace	2.43 ± 0.64	90.64 ± 1.49	4.80 ± 0.53	0.25 ± 0.26	0.14 ± 0.02	1.06 ± 0.16	0.0
High *Z* material in corrosion layer							
68 days in a batch furnace	0.08 ± 0.15	96.01 ± 1.85	1.90 ± 1.47	0.73 ± 1.13	0.01 ± 0.01	1.06 ± 0.16	0.12 ± 0.26
57 days in a batch furnace	0.02 ± 0.0	93.93 ± 1.33	3.30 ± 0.46	0.40 ± 0.55	0.13 ± 0.07	0.86 ± 0.10	0.0
Low *Z* inclusions in corrosion layer							
68 days in a batch furnace (*a*)	2.03	14.35	50.90	0.36	0.32	7.94	32.57
(*b*)	38.49	5.25	4.86	7.30	0.39	1.23	40.88
57 days in a pusher furnace (*a*)	10.28	1.47	50.61	0.40	0.31	0.32	36.61
(*b*)	41.88	8.88	1.45	0.08	1.42	0.0	47.73

Table 8. Quantitative electron microprobe data from different regions of HU coupons exposed for 258 days in a batch carburizing furnace at Delphi Saginaw

Coupon exposure	Element (weight percent)					
	Fe	Ni	Cr	Si	C	O
Matrix						
258 days in a batch furnace	39.59 ± 0.45	42.12 ± 0.67	14.78 ± 0.85	1.69 ± 0.04	0.57 ± 0.20	0.0
Matrix grain boundaries						
258 days in a batch furnace	12.79 ± 0.24	5.13 ± 0.21	75.78 ± 1.26	0.07 ± 0.04	8.27 ± 0.37	0.0
Matrix near the corrosion layer						
258 days in a batch furnace	41.22 ± 0.71	44.77 ± 0.55	12.67 ± 0.25	0.81 ± 0.27	0.48 ± 0.11	0.0
Grain boundary and points near the corrosion layer						
258 days in a batch furnace	14.52 ± 0.46	5.48 ± 0.32	74.58 ± 1.35	0.08 ± 0.05	7.92 ± 1.15	0.0
Outer corrosion layer						
258 days in a batch furnace	1.37 ± 0.75	0.97 ± 0.82	47.02 ± 9.60	2.56 ± 1.59	0.89 ± 0.32	26.29 ± 1.25
Inner corrosion layer[a]						
258 days in a batch furnace	10.73	9.02	6.70	33.70	1.35	42.05
258 days in a batch furnace	1.06	0.39	6.29	35.10	0.46	48.67

[a]Large variation in data and, thus, two extreme data sets are shown.

July 25, 1994

Dr. Vinod Sikka
Oak Ridge National Laboratory
Bethel Valley Road
Oak Ridge, TN 37830

Dear Dr. Sikka;

Enclosed is ACI HU sample number 8.
Installed July 8, 1993.
Removed July 22, 1994.
Per our estimates this becomes 258 operating days.
Sample was on tray for one ten day period during the year.

Other observations:

- The tray assembly had just gone through a furnace burnoff.
- The Nickel Aluminide tray had significant dirt buildup.
- Most Nickel Aluminide samples were very green. Sample #61 looked white like the HU tray and the two boxes.
- The Nickel Aluminide samples did not have the dirt buildup like they tray.
- There were no cracks in the Nickel Aluminide tray.
- The HU tray looked clean.
- The HU tray had many cracks. The tray's usable life cycle is nearing its end.
- All of the bolts and nuts were in bad shape. Most nuts were cracked. The bolts were very brittle. Seven of the sample bolts were changed.
- The bolt holding Sample # 25 was melted out of the sample. The sample reached a very high temperature around the bolt hole. All other samples had the bold driven out with a punch.
- All box-tray nuts and bolts were cracked.
- The screens in the bottom of the boxes were replaced. They were broken and very dirty.
- The tray width was measured for several trays.

Nickel Aluminide	30 3/16 inches
ACI HU	30 5/16
Scrap	30 5/8
Scrap	30 1/2
Scrap	30 3/4
New	30

The next samples are due to be removed August 22, 1994.

Jerry D. Jablonski

Saginaw Division General Motors Corporation 3900 Holland Road Saginaw, Michigan 48601-9494 (517) 757-5000

Fig. 28. Letter from Mr. Jerry D. Jablonski of GM-Saginaw dated July 25, 1994.

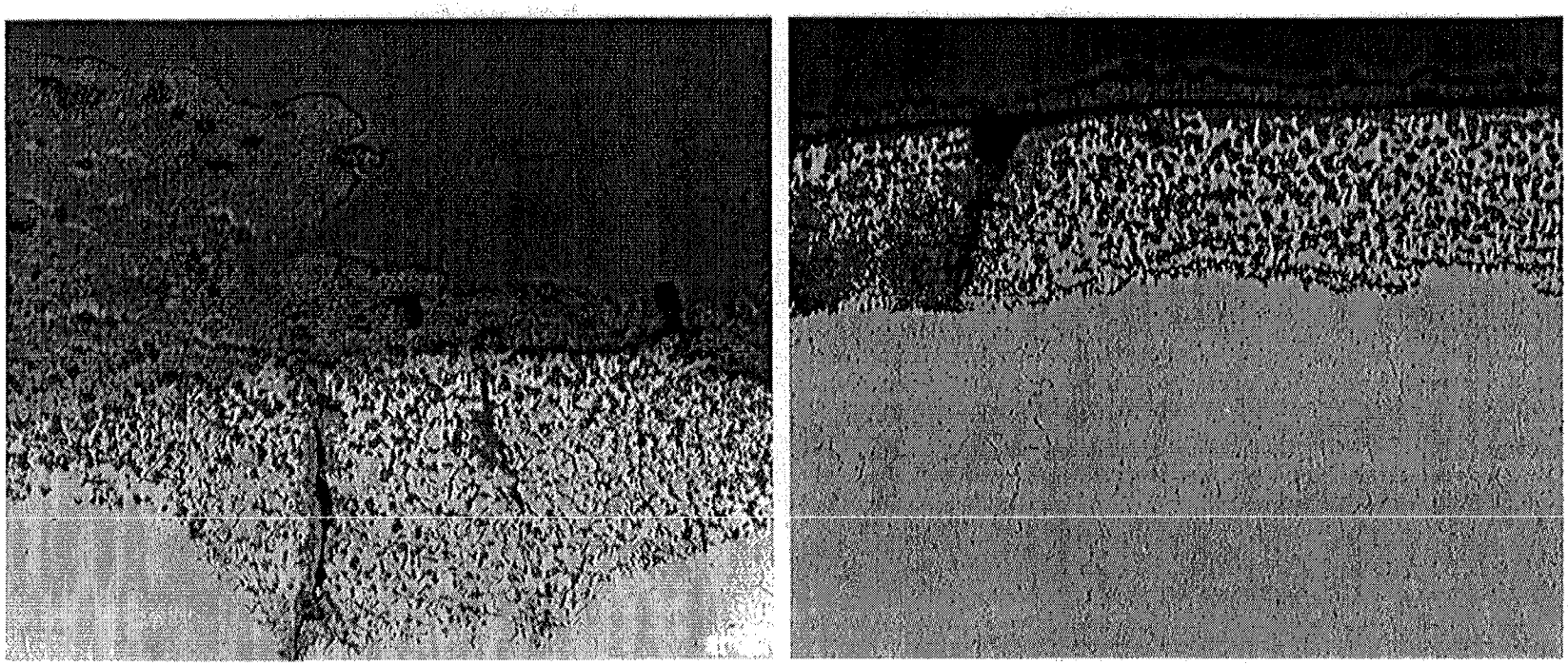

(a) *(b)*

Fig. 29. Optical microstructures of the (*a*) edge and (*b*) center of coupon No. 51. This coupon was exposed in a preoxidized condition for 336 days in a batch carburizing furnace at Delphi Saginaw.

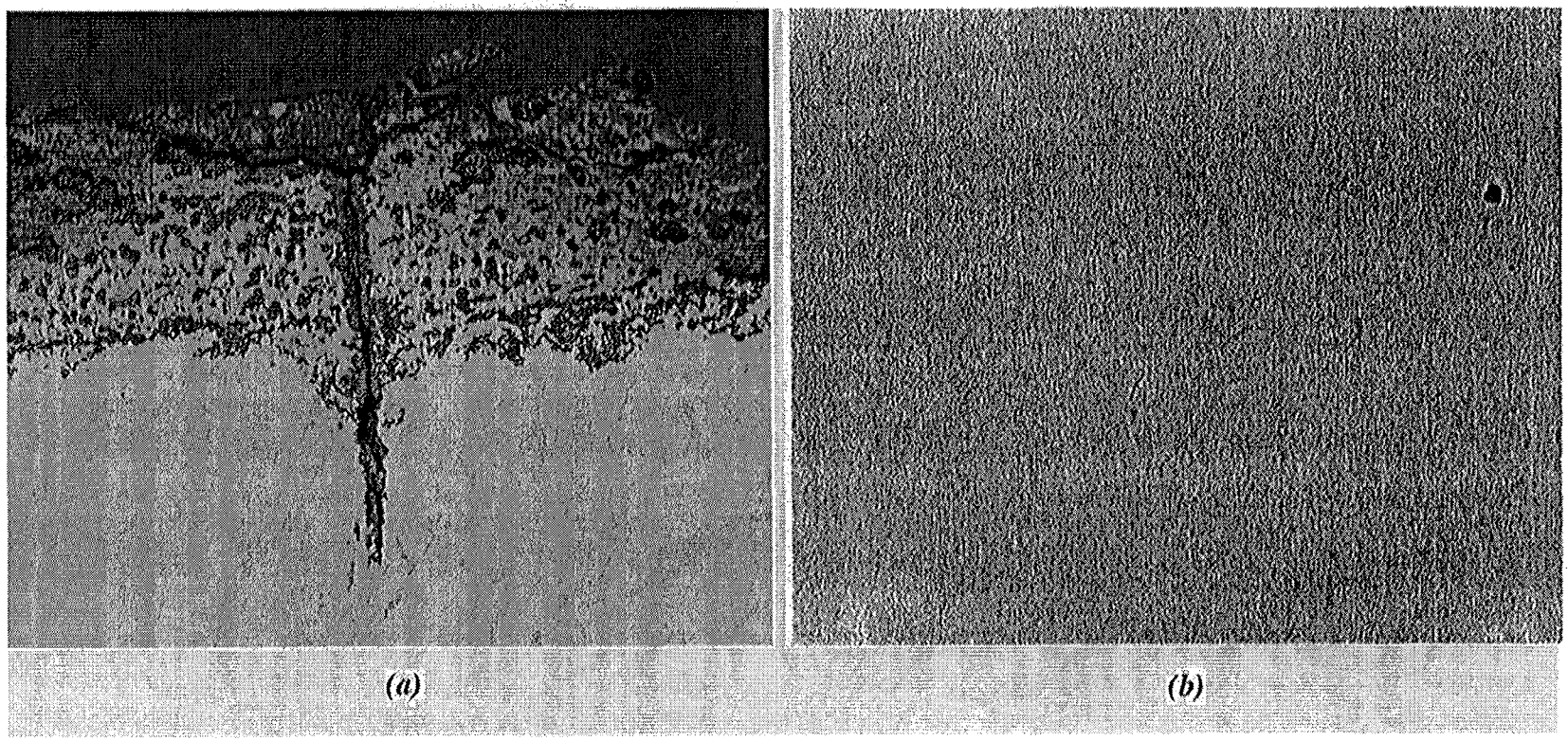

Fig. 30. Optical microstructure of the (*a*) edge and (*b*) center of coupon No. 61. This coupon was exposed in an as-cast condition for 208 days in a batch carburizing furnace at Delphi Saginaw.

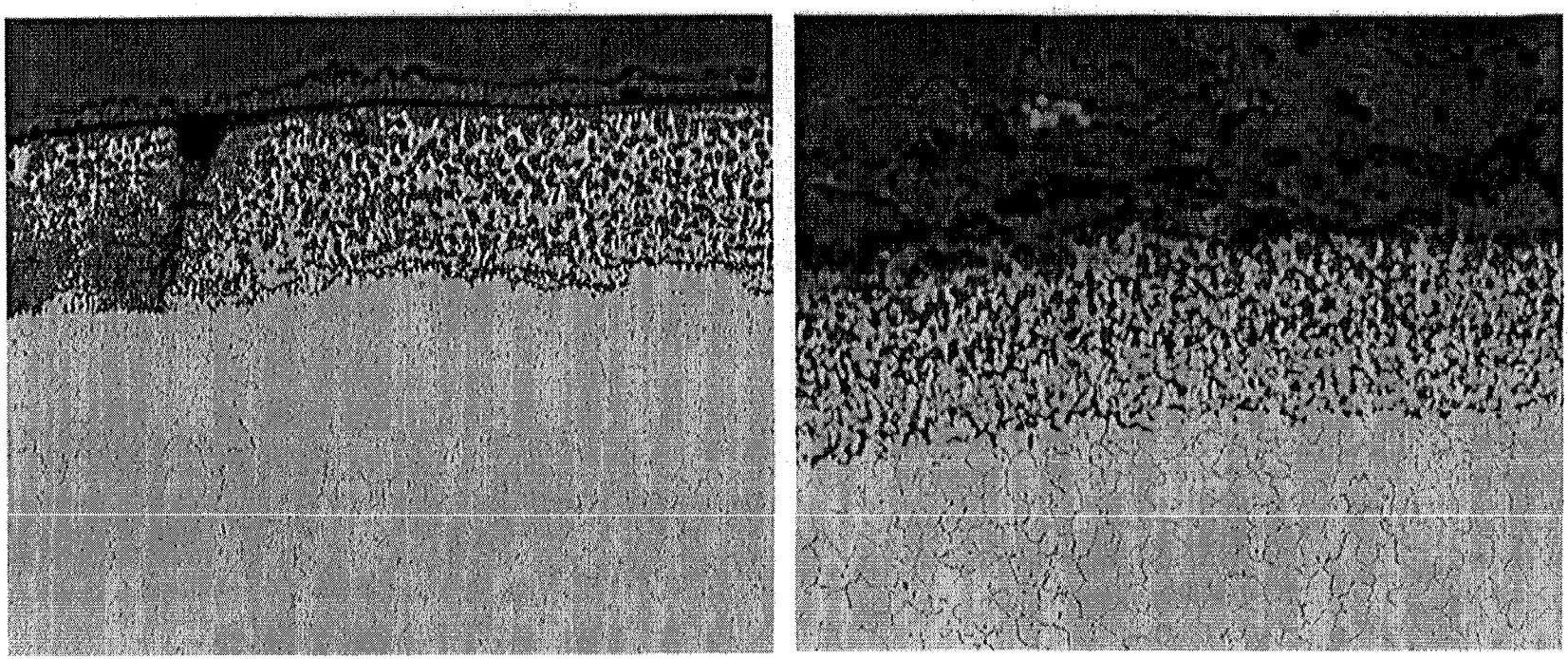

(a) *(b)*

Fig. 31. Optical microstructures comparing the weld crowns of IC-221LA and IC-221W on coupon No. 51 after 336 days of exposure in a batch carburizing furnace at Delphi Saginaw. The welds on the coupon were preoxidized.

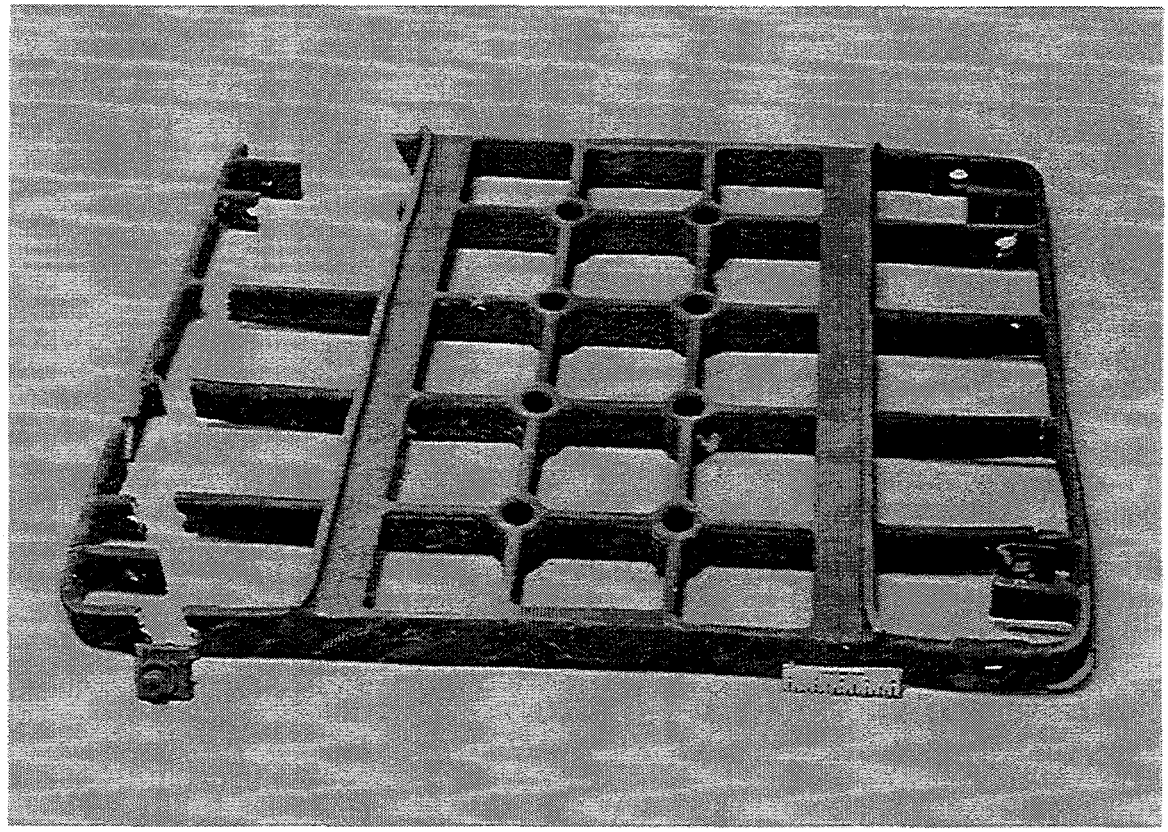

Fig. 32. Broken HU tray removed from a batch carburizing furnace at Delphi Saginaw after 18 months of service.

A total of 63 pusher assemblies were cast to demonstrate commercial production capability. From a total of 63 pusher assemblies, the Oak Ridge National Laboratory (ORNL) paid for 42 assemblies and Delphi Saginaw paid for 21. The 63 pusher assemblies required casting of 63 trays, 63 lower fixtures, 63 upper fixtures, and 252 posts. The production run required melting of a total of 94 heats. Each heat typically weighed 500 lb and was produced by air-induction-melting process. Twenty-six of the 94 heats were produced from virgin stock, and 68 consisted of 50% virgin and 50% revert stock. Detailed chemical analysis of the 94 heats are shown in Table 9. The range of various elements and the average for the virgin and revert heats are compared with the nominal composition for IC-221M in Table 10. The following observations regarding the chemistry of the virgin and revert heats are possible:

1. The average aluminum content of both virgin and revert heats are very similar and approximately 2% lower than its nominal amount.

2. The average chromium content of both the virgin and revert heats are very similar but slightly higher than the nominal amount.

3. The average molybdenum content of the virgin and revert heats matches closely with the nominal amount in the alloy.

4. The average zirconium content of the virgin and revert heats were similar but higher than the nominal amount.

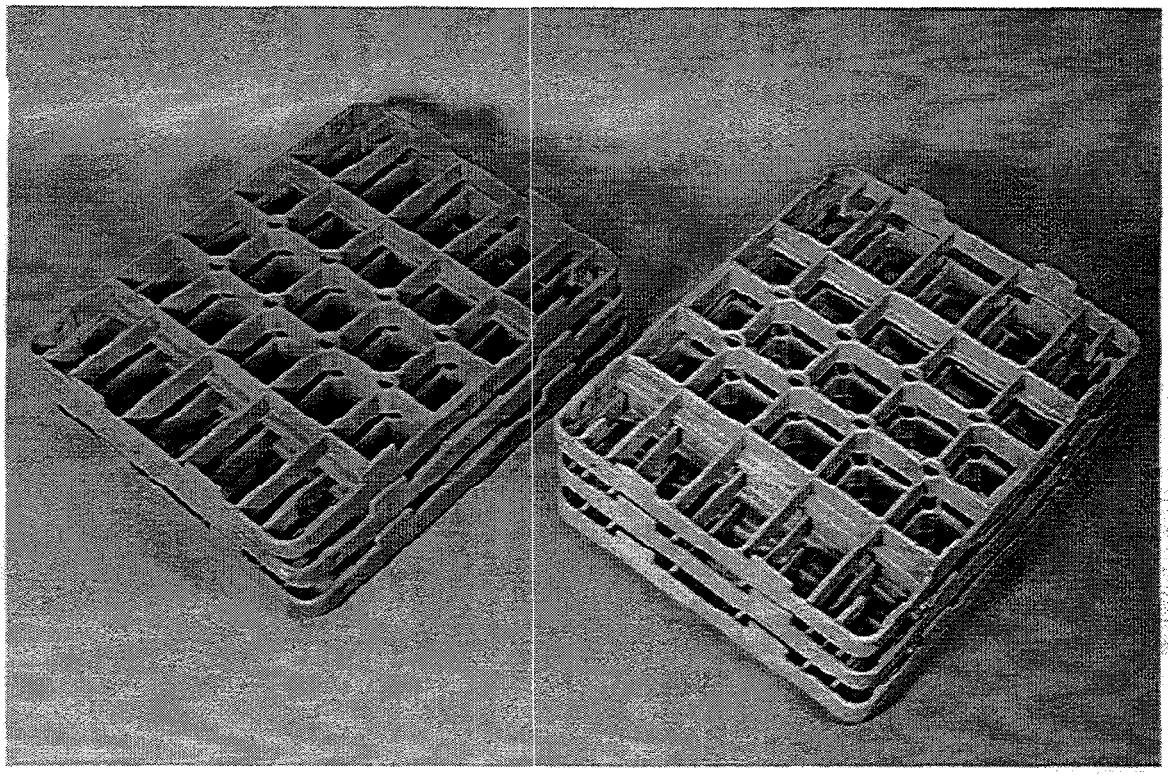

Fig. 33. The preoxidized (left) and as-cast (right) trays of IC-221M for installation in batch furnaces at Delphi Saginaw.

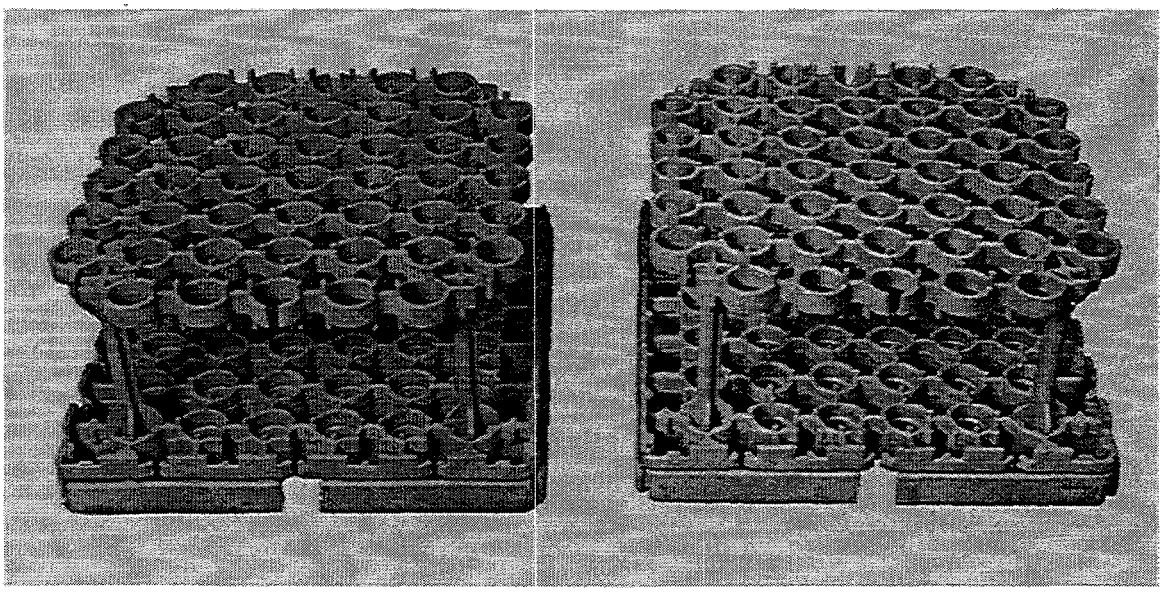

Fig. 34. The preoxidized (left) and as-cast (right) tray and fixture assemblies of IC-221M for installation in a pusher furnace at Delphi Saginaw.

Table 9. Chemical analysis of 94 heats of IC-221M melted to date at Alloy Engineering & Casting Company

Date of melt	Heat No.	Alloy								
		C	Si	Ni	Cr	Mo	Al	Zr	B	Fe
					26 virgin heats					
10/28/96	F2169	0.018	0.055	80.28	7.77	1.46	7.86	1.87	0.005	0.06
	F2170	0.017	0.034	80.24	7.89	1.50	8.19	1.90	0.008	0.03
	F2171	0.019	0.038	81.40	7.81	1.46	8.20	1.79	0.006	0.73
10/29/96	F2172	0.020	0.039	79.90	7.71	1.46	8.16	1.96	0.006	0.06
	F2173	0.023	0.021	80.20	7.93	1.43	8.20	1.96	0.005	0.08
	F2174	0.021	0.050	81.00	7.83	1.46	7.67	1.94	0.005	0.08
	F2175	0.023	0.030	81.10	8.11	1.43	7.50	1.96	0.006	0.041
10/30/96	F2176	0.012	0.043	80.68	7.81	1.45	7.91	2.02	0.005	0.077
	F2177	0.013	0.031	81.20	7.80	1.46	7.70	1.96	0.005	0.15
	F2178	0.014	0.035	80.85	7.76	1.47	7.79	1.98	0.006	0.12
	F2179	0.022	0.031	80.70	7.83	1.44	7.75	1.97	0.006	0.11
10/31/96	F2180	0.016	0.031	80.50	7.89	1.49	7.80	2.02	0.005	0.08
	E2559	0.013	0.032	80.67	7.86	1.43	7.98	1.93	0.004	0.063
11/04/96	F2182	0.021	0.038	80.30	7.63	1.44	7.71	1.93	0.005	0.10
	F2183	0.022	0.026	80.60	7.78	1.38	7.63	1.93	0.005	0.09
	F2184	0.023	0.031	80.70	7.70	1.41	7.72	1.88	0.006	0.52
11/05/96	F2185	0.021	0.032	80.00	7.68	1.42	8.12	1.93	0.005	0.06
	F2186	0.029	0.031	80.60	7.70	1.42	7.95	1.97	0.005	0.07
	F2187	0.030	0.034	80.30	7.68	1.41	8.03	1.96	0.005	0.181

Table 9. (Continued)

Date of melt	Heat No.	Alloy								
		C	Si	Ni	Cr	Mo	Al	Zr	B	Fe
11/08/96	F2188	0.026	0.042	81.10	7.90	1.42	7.70	1.81	0.005	0.15
	F2189	0.023	0.040	81.10	7.73	1.48	7.60	1.73	0.007	0.08
	F2190	0.024	0.032	80.95	7.85	1.46	8.10	1.93	0.005	0.056
	F2191	0.031	0.037	80.05	8.00	1.44	7.90	1.92	0.005	0.034
11/11/96	F2192	0.029	0.049	80.10	7.85	1.47	7.75	1.98	0.005	0.11
	F2193	0.031	0.046	80.05	7.85	1.47	7.75	1.97	0.006	0.067
	F2194	0.032	0.040	80.90	7.81	1.45	7.80	1.93	0.005	0.066
		50% revert heats								
11/18/96	F2195	0.021	0.051	80.40	7.82	1.41	8.08	1.96	0.006	0.05
	F2196	0.025	0.045	80.20	7.71	1.43	8.10	1.96	0.005	0.045
11/19/96	F2197	0.031	0.053	80.90	7.68	1.43	7.60	1.94	0.006	0.06
	F2198	0.021	0.052	80.60	7.90	1.50	7.63	1.77	0.007	0.05
11/20/96	F2199	0.020	0.046	81.10	7.80	1.46	8.01	1.80	0.006	0.11
	F2200	0.031	0.056	80.27	7.78	1.51	7.90	1.91	0.007	0.16
11/22/96	K1241	0.016	0.050	80.50	7.70	1.49	7.30	1.90	0.008	0.11
	K1242	0.018	0.055	81.00	7.76	1.46	7.80	1.83	0.006	0.13
11/26/96	F2202	0.020	0.063	81.05	7.76	1.40	7.68	1.85	0.005	0.07
	F2204	0.031	0.063	80.87	7.90	1.41	7.60	1.93	0.006	0.086

Table 9. (Continued)

Date of melt	Heat No.	Alloy								
		C	Si	Ni	Cr	Mo	Al	Zr	B	Fe
11/27/96	F2205	0.021	0.068	80.25	7.75	1.43	7.80	1.96	0.006	0.081
	F2206	0.024	0.051	80.04	8.01	1.42	7.71	1.94	0.006	0.056
	F2207	0.023	0.051	80.50	7.91	1.44	7.71	1.85	0.006	0.12
12/02/96	F2208	0.023	0.046	80.76	7.93	1.43	7.81	1.73	0.005	0.04
	F2209	0.024	0.051	80.50	7.88	1.44	7.79	1.85	0.006	0.05
12/03/96	F2211	0.031	0.029	79.91	8.30	1.45	7.30	1.70	0.003	0.03
	F2212	0.025	0.026	80.17	8.50	1.42	7.50	1.90	0.003	0.04
	F2213	0.031	0.045	79.69	8.10	1.56	7.88	1.85	0.004	0.04
12/04/96	F2214	0.041	0.091	78.97	7.66	1.43	7.91	1.98	0.006	0.55
	F2215	0.036	0.128	79.26	7.67	1.41	7.80	1.89	0.006	0.80
	F2216	0.050	0.119	79.57	7.82	1.34	7.30	1.93	0.007	0.70
	F2217	0.045	0.155	78.64	7.61	1.45	8.30	2.03	0.006	0.39
12/10/96	K1243	0.016	0.069	81.00	7.80	1.40	7.81	1.90	0.005	0.47
	K1244	0.020	0.058	80.72	7.65	1.45	7.60	1.93	0.006	0.36
	K1245	0.018	0.046	80.90	7.90	1.43	7.71	1.85	0.005	0.91
12/11/96	F2218	0.025	0.060	80.40	7.75	1.45	7.75	1.89	0.006	0.82
	F2219	0.023	0.070	80.50	7.93	1.41	7.93	1.95	0.006	0.52
	F2220	0.022	0.063	80.30	7.89	1.45	7.89	1.90	0.005	0.80
12/12/96	F2221	0.016	0.060	80.76	7.95	1.43	7.60	1.75	0.006	0.61
	F2222	0.020	0.058	80.05	7.65	1.40	7.75	1.81	0.006	0.11
	F2223	0.021	0.050	80.60	7.85	1.45	7.80	1.90	0.005	0.13
	F2224	0.026	0.061	80.50	7.81	1.41	7.68	1.73	0.005	0.25

Table 9. (Continued)

Date of melt	Heat No.	Alloy								
		C	Si	Ni	Cr	Mo	Al	Zr	B	Fe
12/18/96	F2226	0.025	0.060	80.10	7.68	1.39	7.70	1.78	0.005	0.19
	F2227	0.026	0.057	80.80	7.71	1.41	7.81	1.80	0.006	0.21
12/19/96	F2228	0.026	0.041	81.00	7.87	1.36	7.50	1.75	0.005	0.07
	F2229	0.025	0.045	80.50	7.90	1.43	7.40	1.80	0.004	0.09
	F2230	0.030	0.036	10.80	7.76	1.42	7.70	1.85	0.005	0.11
	F2231	0.029	0.041	80.80	7.99	1.41	7.60	1.83	0.005	0.22
	F2232	0.023	0.041	80.80	7.75	1.39	7.71	1.80	0.005	0.15
12/20/96	F2233	0.025	0.058	80.80	7.98	1.40	7.63	1.88	0.006	0.07
	F2234	0.023	0.053	80.20	7.85	1.38	7.76	1.90	0.005	0.08
	F2235	0.024	0.056	80.80	7.98	1.41	7.60	1.84	0.006	0.069
	F2236	0.027	0.057	81.30	8.20	1.46	7.89	1.86	0.005	0.055
	F2237	0.030	0.048	80.50	7.96	1.45	7.81	1.92	0.005	0.044
	F2238	0.031	0.059	80.20	7.90	1.49	7.91	2.00	0.006	0.11
12/23/96	F2239	0.010	0.078	80.80	8.09	1.46	7.85	1.98	0.004	0.09
	F2240	0.010	0.077	79.84	8.06	1.43	7.76	1.82	0.004	0.06
	F2241	0.010	0.065	80.58	8.16	1.46	7.66	2.00	0.005	0.11
	F2242	0.010	0.72	80.71	8.02	1.43	7.83	1.80	0.005	0.11
	F2243	0.010	0.066	80.13	8.26	1.47	7.63	1.80	0.004	0.13
12/24/96	F2244	0.010	0.070	80.26	8.15	1.43	8.00	1.77	0.005	0.09
	F2245	0.010	0.091	79.55	7.56	1.45	7.41	1.90	0.006	0.066
	F2246	0.010	0.082	80.54	8.08	1.50	8.05	1.62	0.005	0.13
	F2247	0.010	0.050	79.40	7.83	1.50	7.69	1.97	0.005	0.05

Table 9. (Continued)

Date of melt	Heat No.	Alloy								
		C	Si	Ni	Cr	Mo	Al	Zr	B	Fe
01/06/97	F2249	0.025	0.053	79.95	7.85	1.41	7.75	1.99	0.006	0.088
	F2250	0.031	0.060	80.50	7.76	1.44	7.65	1.92	0.005	0.09
	F2251	0.026	0.056	80.48	7.79	1.41	7.77	1.91	0.006	0.45
01/07/97	F2252	0.030	0.056	80.20	7.81	1.42	7.60	1.86	0.005	0.2
	F2253	0.025	0.061	80.40	7.96	1.36	7.70	1.75	0.005	0.15
	F2254	0.031	0.060	80.70	7.79	1.38	7.65	1.73	0.005	0.07
	F2255	0.029	0.056	80.20	7.80	1.41	7.71	1.93	0.005	0.06
	F2256	0.030	0.051	80.40	8.01	1.42	7.80	1.96	0.006	0.11
01/08/97	F2257	0.025	0.061	80.40	7.89	1.38	7.65	2.05	0.005	0.08
	F2258	0.021	0.060	80.60	7.70	1.40	8.10	1.78	0.006	0.06
01/20/97	F2259	0.025	0.061	80.10	7.95	1.35	8.01	1.75	0.005	0.04
	F2260	0.021	0.065	80.12	8.00	1.34	7.68	1.73	0.005	0.03
	F2261	0.025	0.060	80.10	7.90	1.40	7.90	1.80	0.006	0.6
01/22/97	F2262	0.030	0.090	80.10	7.93	1.35	7.60	1.71	0.005	0.12

Table 10. Comparison of nominal chemical analysis of IC-221M with the range observed for heats made using virgin and revert stock in a pilot commercial melt run of 94 heats carried out at Alloy Engineering & Casting Company

Element	Nominal (wt %)	Virgin heats (wt %)		Revert heats (wt %)[a]	
		Range	Average	Range	Average
Al	8.0	7.5 – 8.2	7.86	7.3 – 8.3	7.74
Cr	7.7	7.63 – 8.11	7.81	7.56 – 8.5	7.88
Mo	1.43	1.38 – 1.50	1.45	1.34 – 1.56	1.43
Zr	1.70	1.73 – 2.02	1.93	1.62 – 2.05	1.86
B	0.0080	0.004 – 0.008	0.0054	0.003 – 0.008	0.0054
C	--	0.012 – 0.032	0.022	0.01 – 0.05	0.024
Si	--	0.021 – 0.055	0.036	0.026 – 0.155	0.061
Fe	--	0.03 – 0.15	0.077	0.03 – 0.91	0.194
Ni	81.1	*b*	80.81	*b*	80.81

[a]50% virgin and 50% revert.
[b]Balance.

5. The average boron content of the virgin and revert heats were similar but slightly lower than the target.

6. The silicon and iron contents of the revert heats were significantly higher than the virgin heats. The carbon content was not affected by changing from virgin to revert heats.

The melting of 94 heats demonstrated that the nickel aluminide alloy IC-221M can be melted successfully under commercial conditions from the virgin and revert stock. The only concern was about the silicon and iron pickup in the revert heats. The silicon pickup above 0.05 wt % is detrimental to weldability, and a too high an iron content (≥0.5 wt %) lowers the high temperature. However, Alloy Engineering & Casting Company indicated that with proper procedures, better control of these elements can be achieved.

In order to determine the dimensional reproducibility, the length and width of all 63 trays and the lower and upper fixtures were measured, and this is summarized in Table 11. These data show that dimensionally, the fixtures were highly reproducible. Detailed inspection of the fixtures showed only minor casting details, which could be weld-repaired using the ORNL-developed IC-221LA weld wire.

All 63 pusher furnace fixtures were preoxidized at 1100°C for 1 h in air prior to shipping to Delphi Saginaw. Since ORNL and Delphi Saginaw paid for them, the fixtures were identified by the letter O for ORNL and without any mark for Delphi Saginaw. It was thought that the casting marked by the letter O would be returned to ORNL for detailed microstructural analysis after periodic intervals. After preoxidation, all of the fixtures were delivered to Delphi Saginaw in early January 1997. They were installed in the production pusher carburizing furnaces during March 1997. In addition to the 63 assemblies, one each of the as-cast and preoxidized assemblies were installed in another pusher furnace in January 1996.

Operating Experience in Pusher Carburizing Furnaces

The visual inspection in September 1996 of the two assemblies installed in January 1996 at Delphi Saginaw revealed that they were both free from bowing and cracking (typical deformation and failure mode for the HU assemblies). However, the as-cast assemblies were found to show more loose carbon dust on the casting surface as opposed to the preoxidized one. Since the preoxidized fixtures did not show the base carbon dust, it is believed that it comes from the reduction of furnace carbon atmosphere (CO and CO_2) by aluminum in the alloy. Based on these results, the 63 assemblies from the commercial production were preoxidized at 1100°C for 1 h.

An inspection of the 63 pusher furnace assemblies during January 1998 revealed that they were operating without indication of any likely failure mode. Some of the HU assemblies in the same furnace showed bowing of the upper fixtures after only ten months of service. To our surprise, even after preoxidation, the fixtures were showing loose carbon dust. The only difference between the preoxidation treatment between the initial two assemblies and the 63 production assemblies was that the latter was carried out by a commercial vendor. It is possible that the commercial vendor did not achieve the proper preoxidation conditions. The details of the preoxidation treatment are being sought from the vendor to confirm the oxidation conditions used.

Table 11. Variability of casting dimensions for a pilot commercial run of 63 sets of IC-221M castings

Component deviation	Average ± standard deviation (length)	Average ± standard (width)
Tray	672.7 ± 0.7	672.5 ± 1.2
Lower fixture	657.7 ± 1.8	657.4 ± 1.9
Upper fixture	632.8 ± 2.2	632.3 ± 2.0

Larger Batch Furnace Test

In addition to the large pusher furnace test, it was recognized that the large batch furnace test can provide the statistical operating experience in a shorter time frame than the pusher furnace because the trays go through three quench cycles per day in the batch furnace versus only one per day in the pusher furnace. The six (three as-cast and three preoxidized) batch furnace trays shown in Fig. 33 were produced for the larger batch furnace test. However, they were not installed for a long time because each nickel aluminide tray needed to be bolted or attached to an HU (HT) tray. During the end of 1996, Delphi Saginaw supplied ORNL with six HU trays to prepare the assemblies with the nickel aluminide. The assemblies were prepared by using nickel aluminide pins between the HU and the nickel aluminide trays. The assembled pair of batch furnace trays are shown in Fig. 35. All six pairs have been operating in the batch furnaces at Delphi Saginaw since March 1997. Of these batch furnace trays, no known failures have occurred, and they continued to be used in production.

Physical and Mechanical Properties of IC-221M Used for Batch Furnace Trays and Pusher Furnace Fixtures

As described in this report, the nickel aluminide alloy IC-221M was used for the casting of batch and pusher furnace trays and assemblies. The physical and mechanical properties data on the cast alloy are essential for developing its additional applications. The data available to date have been summarized in Table 12 for this purpose.

Summary and Conclusions

The superior carburization and oxidation resistance and higher high-temperature strength were the driving force for evaluating the possible use of trays and fixtures of Ni_3Al-based alloy IC-221M in batch and pusher carburizing furnaces at Delphi Saginaw. These were used to compare with the same components fabricated from the HU material. However, prior to any possible replacement of HU by IC-221M, the following needed to be demonstrated:

1. Melting and casting of IC-221M alloy using the conventional foundry practice.
2. Weld repairability of castings.
3. Testing of HU and IC-221M coupons in batch and pusher carburizing furnaces.
4. Testing of trays and fixtures in production carburizing furnaces.

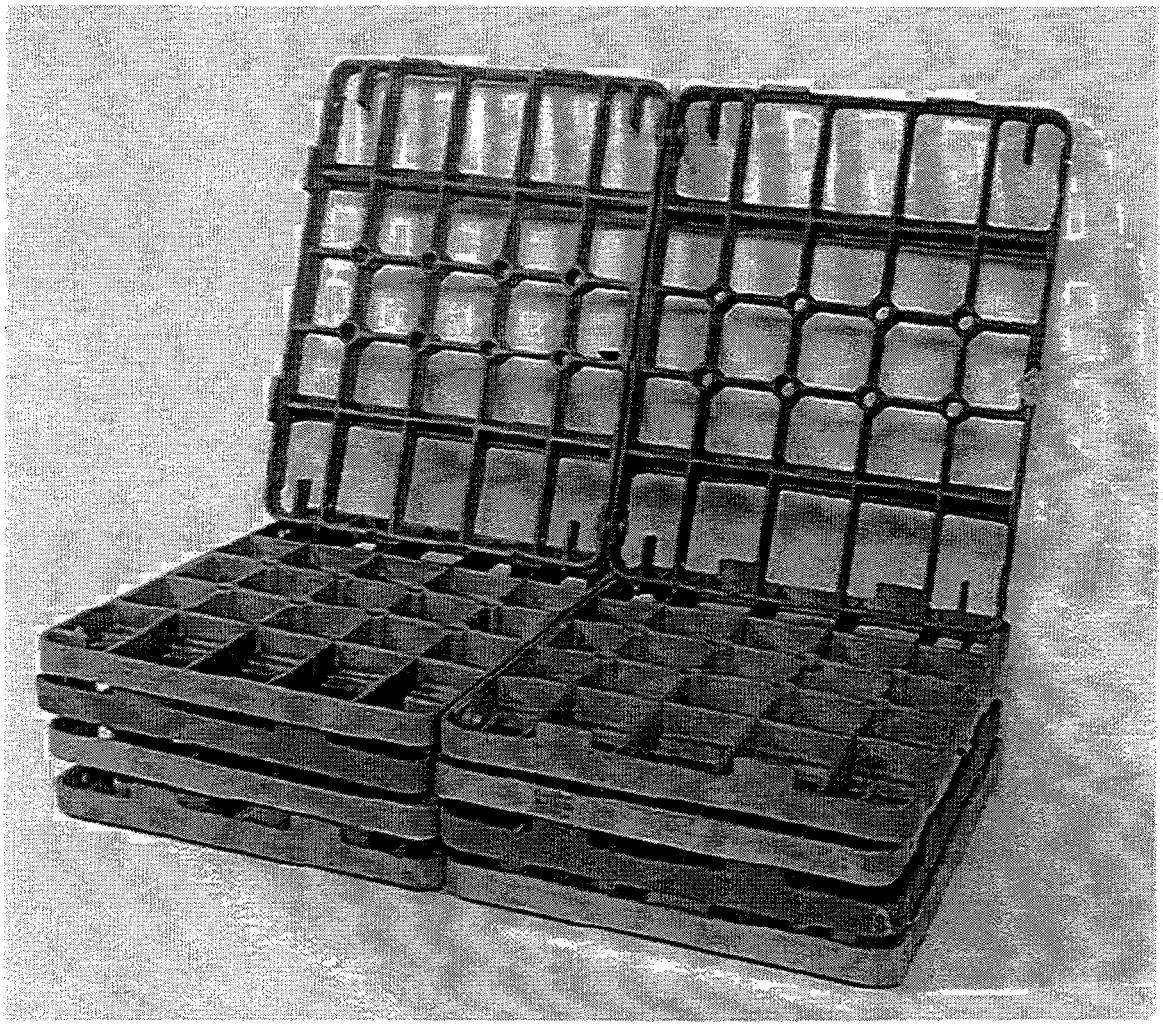

Fig. 35. Assembled pair of batch furnace trays.

The work to date has met most of the demonstration requirements with the following conclusions:

1. The Ni_3Al-based alloy IC-221M can be melted using the Exo-Melt ™ process along with the normal foundry practice. The molten metal from the Exo-Melt™ process can be sand cast into trays, fixtures, and posts using practices similar to those used for HU. The solidification modeling has guided the foundry with more details of actual mold pouring for Ni_3Al-based alloy.

2. The weld repair of trays and fixtures was demonstrated. The IC-221LA wire looks quite acceptable for all situations.

3. The coupon testing has been conducted in both batch and pusher furnaces. The longest exposure time reached has been 336 days for IC-221M in a batch furnace.

Table 12. Physical and mechanical properties of Ni_3Al-based cast alloy IC-221M

Property	Temperature (°C)							
	Room	200	400	600	800	900	1000	1100
Density (g/cm^3)	7.86	--	--	--	--	--	--	--
Hardness (R_C)	30	--	--	--	--	--	--	--
Microhardness (dph)	260	270	280	290	280	230	120	--
Modulus (GPA)	200	190	174	160	148	139	126	114
Mean Coefficient of thermal expansion (10^{-6}/°C)	12.77[a]	13.08[b]	13.72[b]	14.33[b]	15.17[b]	15.78[b]	16.57[b]	--
Thermal conductivity (w/m • k)	11.9	13.9	16.7	20.3	25.2	27.5	30.2	--
0.2% Tensile yield strength (MPa)	555	570	590	610	680	600	400	200
Ultimate tensile strength (Mpa)	770	800	850	850	820	675	500	200
Total tensile elongation (%)	14	14	17	18	5	5	7	10
10^2 h Rupture strength (MPa)	--	--	--	--	252	124	55	28

Table 12. (Continued)

Property	Temperature (°C)							
	Room	200	400	600	800	900	1000	1100
10^3 h Rupture strength (MPa)	--	--	--	--	172	83	36	18
10^4 h Rupture strength (MPa)	--	--	--	--	124	55	24	11
Charpy impact toughness (J)	40	40	40	35	15	10	--	--
Fatigue 10^6 cycle life (MPa)	--	--	--	630[c]	--	--	--	--
Fatigue 10^7 cycle life (MPa)	--	--	--	550[c]	--	--	--	--

[a]Room temperature to 100°C.
[b]Room temperature to specified temperature.
[c]Data at 650°C for investment-cast test bars.

4. The IC-221M showed a surface corrosion layer. However, the penetration was limited to short distances, as opposed to the HU coupons which showed deep penetrations after short exposure times. The preoxidized coupon appears to show even less carburization penetration than the as-cast coupon.

5. The testing of the HU and IC-221M trays in the batch furnace at Delphi Saginaw has confirmed the results from the coupon study in that the HU trays have cracked and the Ni_3Al-based alloy tray is relatively unaffected.

6. Initial installation of one batch furnace tray at Delphi Saginaw was extended to two pusher furnace fixtures during January 1996.

7. A commercial production run of 63 pusher furnace assemblies was completed. This production run used a total of 94 heats, 26 of which were from virgin stock and 68 were made up of 50% virgin and 50% revert stocks.

8. The 63 pusher furnace fixtures from the production run have been operating at Delphi Saginaw since March 1997 and is still operating without any noticeable change.

9. Six batch furnace trays of nickel aluminide, bolted to HU trays, have been operating at Delphi Saginaw in the six-batch furnace since March 1997.

10. The results of this CRADA have shown that the nickel aluminide alloy, IC-221M, can be cast into trays and fixtures under production conditions. Furthermore, these trays and fixtures are continuing to operate without reflecting the possible failure mode.

Evaluation of Nickel Aluminide (IC-221M) and HU Fixtures Removed from Carburizing Furances at Delphi Saginaw

This deals with the metallographic characterization of a fixture of nickel aluminide alloy IC-221M removed from a pusher furnace after 14 months of service and a broken tray of HU alloy that was taken from a batch furnace after 18 months of service. The photograph of the broken HU tray is shown in Fig. 32. The tray surface is very black with carbon tightly bonded to the surface. The photograph of the IC-221M fixture is shown in Fig. 36. this photo shows three pieces of the fixture that were plasma cut from a fixture that was removed from service after 14 months. The as-removed fixture was very black in color as seen in Fig. 36(*a*). The other two pieces [shown in Figs. 36(*b*) and 36(*c*)] were sand blasted, which seemed to remove the black dusty surfaces easily. Thus, it is believed that the black surface of the fixture is loose dust.

A careful examination of the sand-blasted fixtures of IC-221M shows the initiation of small surface cracks near the intersections. Two small pieces were sectioned from the fixture for chemical analysis and detailed metallography.

The chemical analysis of the IC-221M sample from the fixture is compared with the nominal composition in Table 13. The data in this table show that the exposed fixture has picked up carbon, which increased from a nominal value of 0.02 to 0.17 wt %. More details of the carbon distribution and its form in the alloy will become clearer in the detailed metallurgical analysis section. It is also worth noting that the aluminum content of the

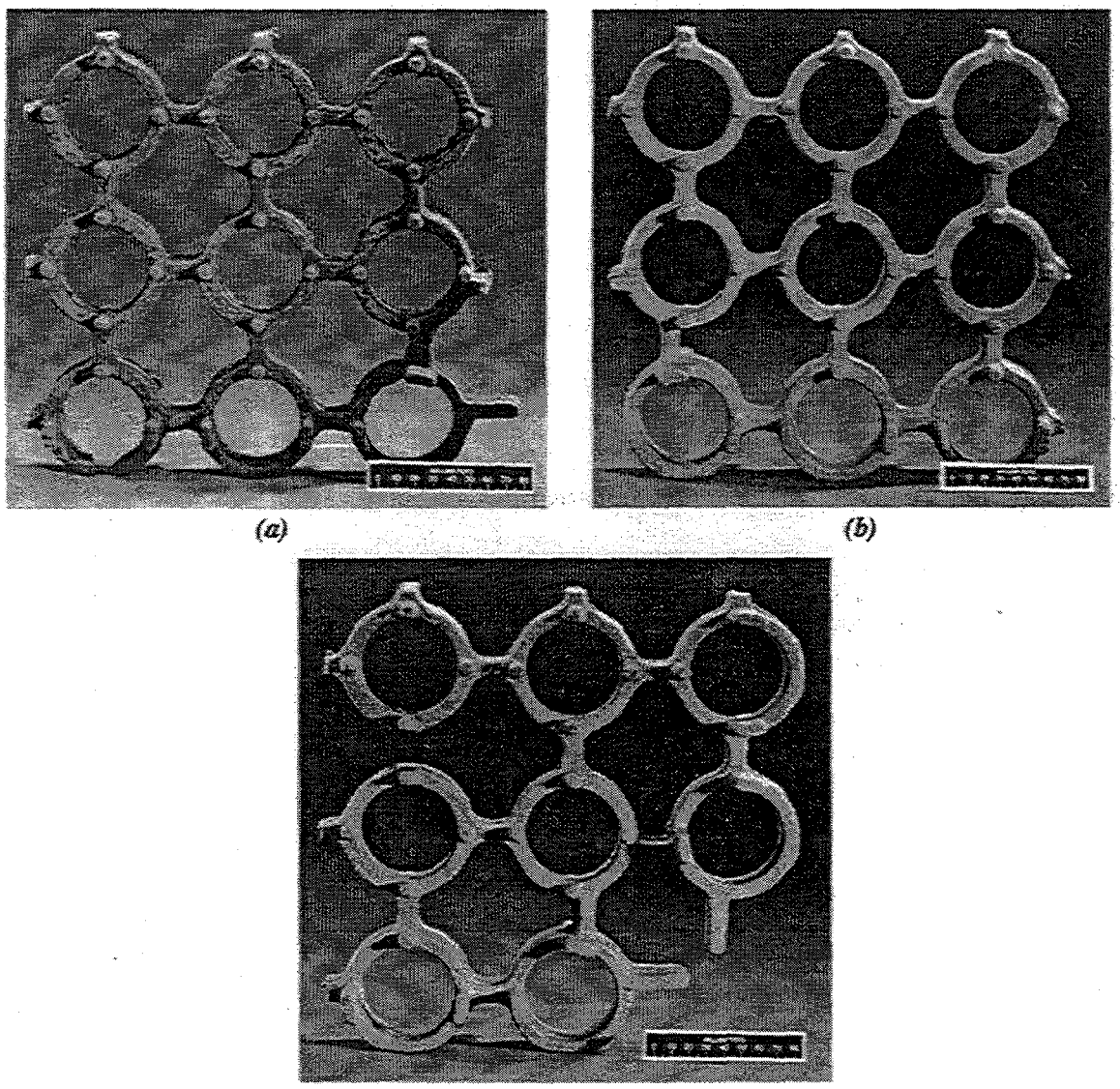

Fig. 36. Photograph of three pieces of IC-221M in pusher furnace at Delphi Saginaw: (*a*) as-removed and (*b*) and (*c*) sand blasted.

Table 13. Comparison of chemical analysis[a] of nickel aluminide fixture and HU tray removed from carburizing furnace at Delphi Saginaw with the nominal composition of the alloys

Element	Alloy (weight percent)			
	IC-221M		HU	
	Nominal	Exposed[b]	Nominal	Exposed[c]
Al	8.0	7.0	--	0.03
Cr	7.7	7.54	18.0	21.3
Mo	1.43	1.29	0.5 max	0.14
Zr	1.7	1.77	--	--
Mn	--	0.02	2.0 max	0.86
P	--	--	--	0.022
Si	--	0.06	2.0 max	1.40
B	0.008	<0.001	--	--
C	*d*	0.17	0.55	1.00
Fe	--	0.79	42.45	37.25
Ni	81.1	81.32	39.00	39.2
Cu	--	0.11	--	0.11
N_2	--	0.011	--	0.043
O_2	--	0.002	--	0.045

[a]Chemical analysis by ABB-CE Services Inc., Chattanooga, Tennessee
[b]Fixture from pusher furnace after 14 months of service.
[c]Broken tray from batch furnace after 18 months of service.
[d]Average carbon level of 0.02 in virgin and revert heats.

exposed sample is about 1 wt % lower than the nominal composition. Analysis of 94 heats (Table 10) shows that aluminum varied from 7.3 to 8.3 wt % in the trays and fixtures before they went into service. Thus, the lower aluminum in the exposed sample is real, but the reason for it being lower is not clear. None of the other elements showed any significant difference between the nominal and the exposed fixtures.

The chemical analysis of the exposed HU tray from the batch furnace are compared in Table 13 above. This table shows that the carbon content of the HU tray increased to 1% as opposed to a nominal value of 0.55 wt % in the alloy. The exact distribution of carbon across the tray section thickness will be described in a later section. The only other element significantly different from the nominal composition is chromium. Its value is 3% higher than the nominal. The exact reasons for this difference are not clear unless the actual composition of the new HU tray did contain 3% higher chromium than the nominal [which would still be within the allowed range for chromium in the HU alloy (19 to 23 wt %)].

The carbon scan, using the microprobe analyses, is shown for the IC-221M fixture and HU tray in Fig. 37. It is clear from this figure that carbon enrichment near the surface occurs in both alloys. However, the enrichment effect for IC-221M is different from HU in two respects: (1) its value at the surface is 60% lower and peak value near the surface is approximately 30% lower than in HU, and (2) the depth of penetration of carbon for the IC-221M is half that of HU. The results of the microprobe analysis are consistent with the bulk chemical analysis in that the carbon level for the exposed IC-221M is 0.17 as opposed to 1.0% for HU.

The microhardness traverses for the exposed IC-221M and HU are compared in Fig. 38. This figure shows: (1) region of carbon enrichment in Fig. 37 shows increased hardness for both IC-221M and HU; (2) the increased hardness is for nearly two times deeper for HU than IC-221M, which is consistent with the results of carbon profile depth (Fig. 37); (3) exposure in carburizing furnace increases the hardness of the HU tray from the base value of 160 to 240 HV. In comparison to HU, the hardness of the exposed IC-221M fixture dropped slightly from its baseline value. The observations of differences in hardness profiles for IC-221M and HU suggest that the two alloys respond differently to the furnace environment (HU increases in its hardness and IC-221M hardness either remains the same or drops slightly).

Data in Fig. 38 also show that the near surface region affected by carbon results in slightly higher hardness values than observed for HU. Since an increase in hardness is a result of carbide precipitation, the higher hardness is a result of carbide precipitation, the higher hardness for IC-221M may be a result of zirconium-carbon precipitation. The exact nature of carbides in exposed samples of IC-221M and HU will be examined in a later section.

Optical Metallography of Exposed HU Tray

The optical micrographs of the unetched and etched sections of the broken HU tray exposed for 18 months are shown in Figs. 39 through 46. These micrographs show the surface reaction with carbon and localized regions of cracks that penetrate significantly into the base metal. The cracks facilitates carbon penetration into the base metal. The etched microstructures of the base metal show depleted regions and coarse microstructural features which are typical of thermally exposed material.

The unetched and etched micrographs of sections of the IC-221M fixture after 14 months exposure are shown in Figs. 47 through 52. These micrographs show the surface reaction with carbon. The actual depth of carbon attack for HU and IC-221M are compared in Table 14. The general corrosion layer for the HU tray after 18 months exposure in the batch furnace showed a nominal thickness of 200 μm with a region as much as 800 μm thickness in some cases. For IC-221M after 14 month exposure in the pusher furnace, the general corrosion layer was 220 μm with a depleted layer of 40 μm underneath. There were several cracks propagating in the HU tray after 18 months exposure in the batch furnace. The cracks ranged in lengths of 500 to 1800 μm. The IC-221M showed very few cracks with one crack of 820 μm in length in the specimen examined for metallography.

Backscattered electron image of the sample from the HU tray after 18 months exposure in the batch furnace is shown in Figs. 53 through 55. These figures show three different magnifications of the near surface region affected by the carburizing environment. Elemental mapping of the area in Fig. 55 is shown in Figs. 56 through 61. The map in Fig. 56 shows only nine small regions of carbon enrichment (white regions). Figure 57 shows the presence of some silicon in the reacted regions. The chromium is the key

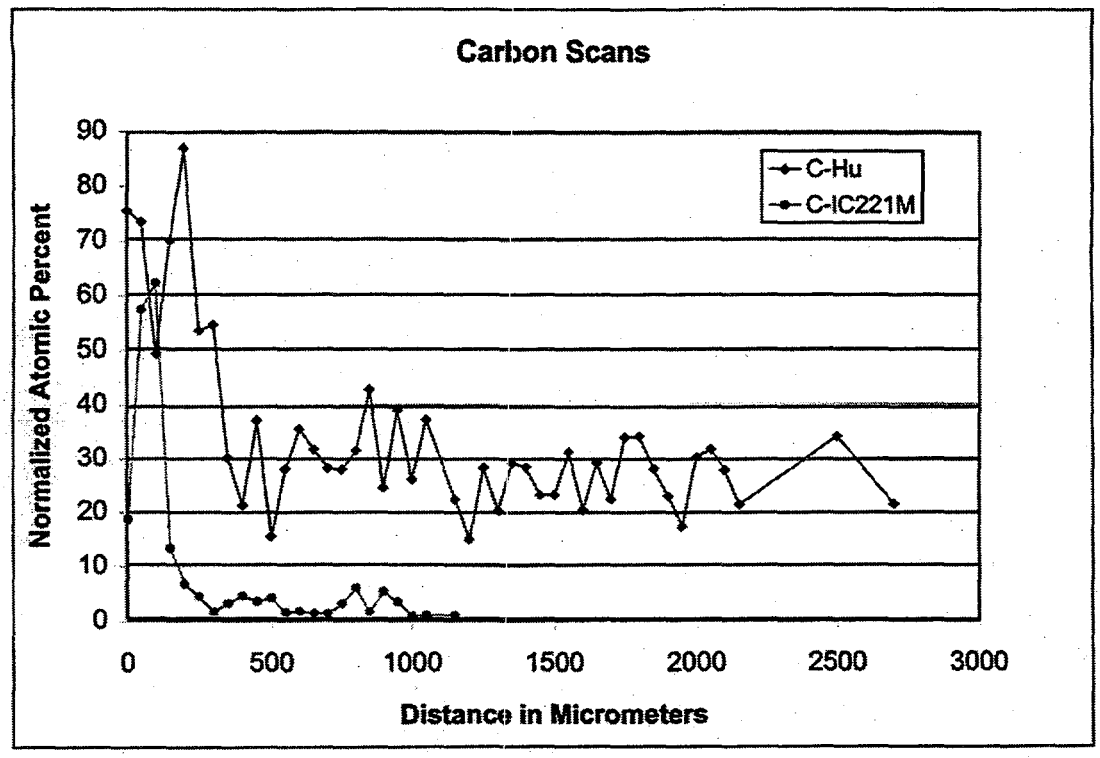

Fig. 37. Comparison of carbon traverse as a function of distance for broken HV tray and the IC-221M fixture removed from pusher carburizing furnace at Delphi Saginaw after 14 months of service.

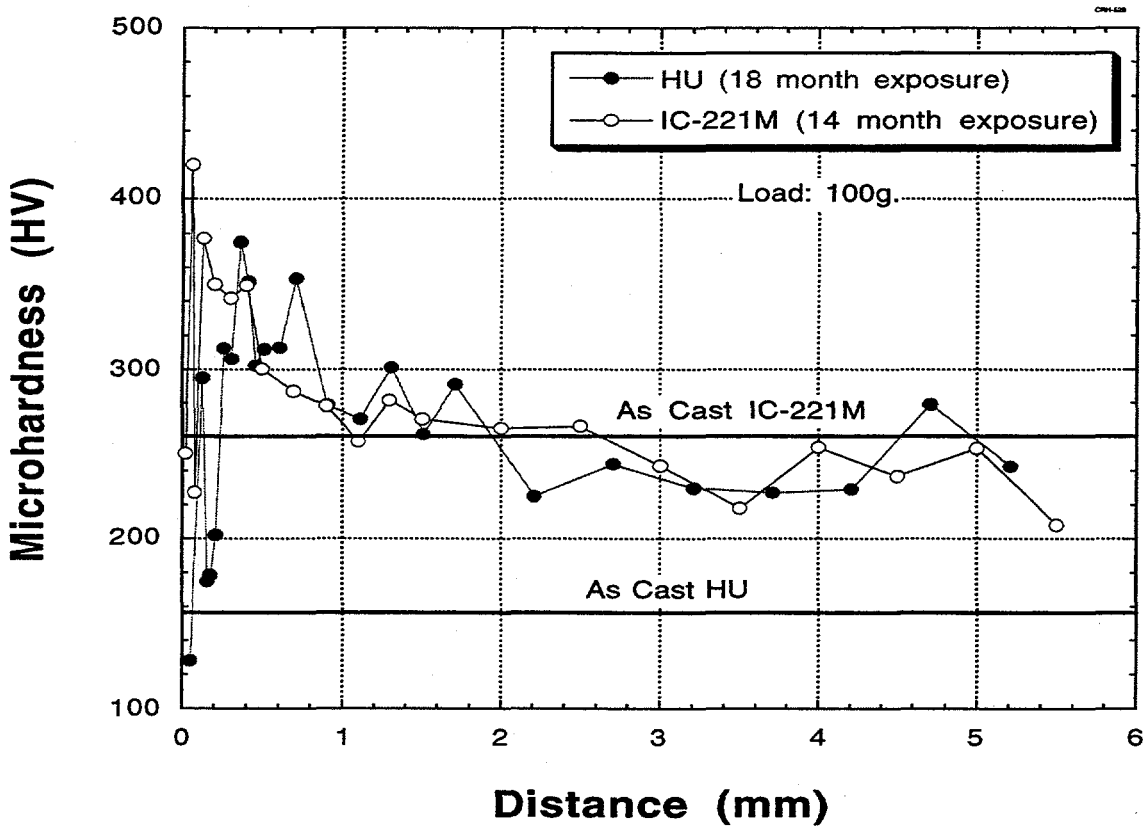

Fig. 38. Comparison of microhardness traverse as a function of distance for broken HU tray and the IC-221M fixture removed from pusher carburizing furnace at Delphi Saginaw after 14 months of service.

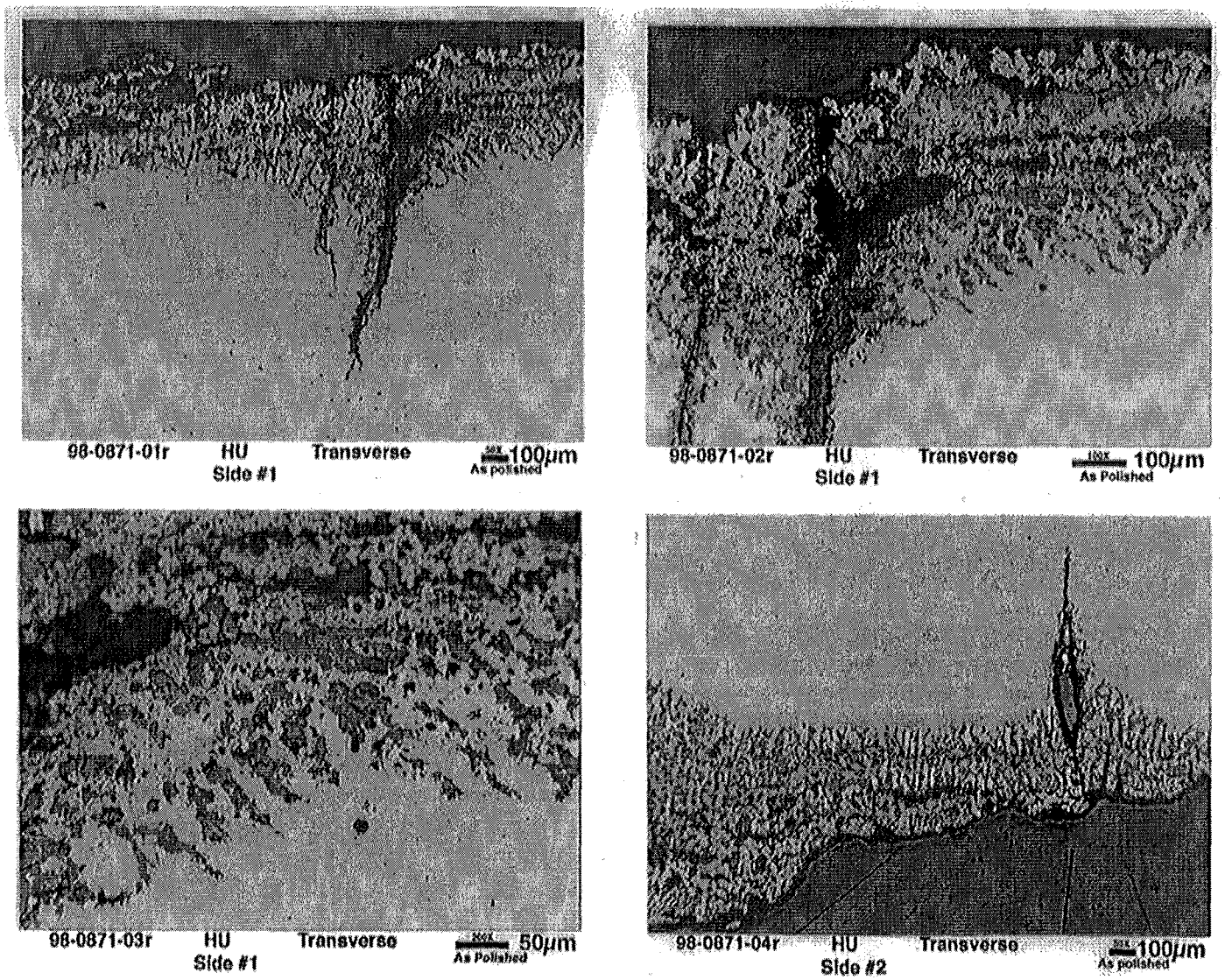

Fig. 39. Optical micrographs of the broken HU tray (sides 1 and 2) in the transverse untetched condition.

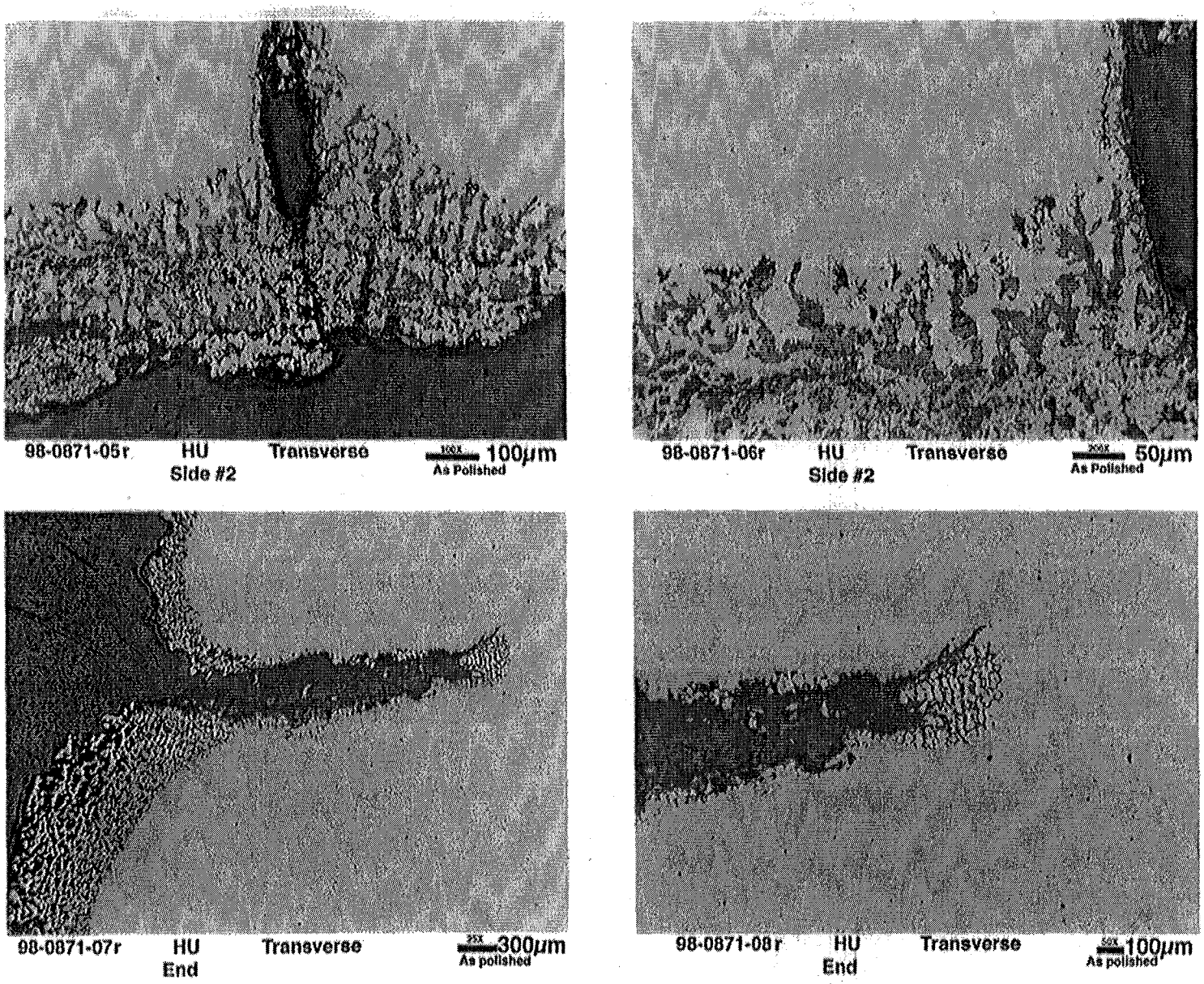

Fig. 40. Optical micrographs of the broken HU tray (side 2 and end) in the transverse untetched condition.

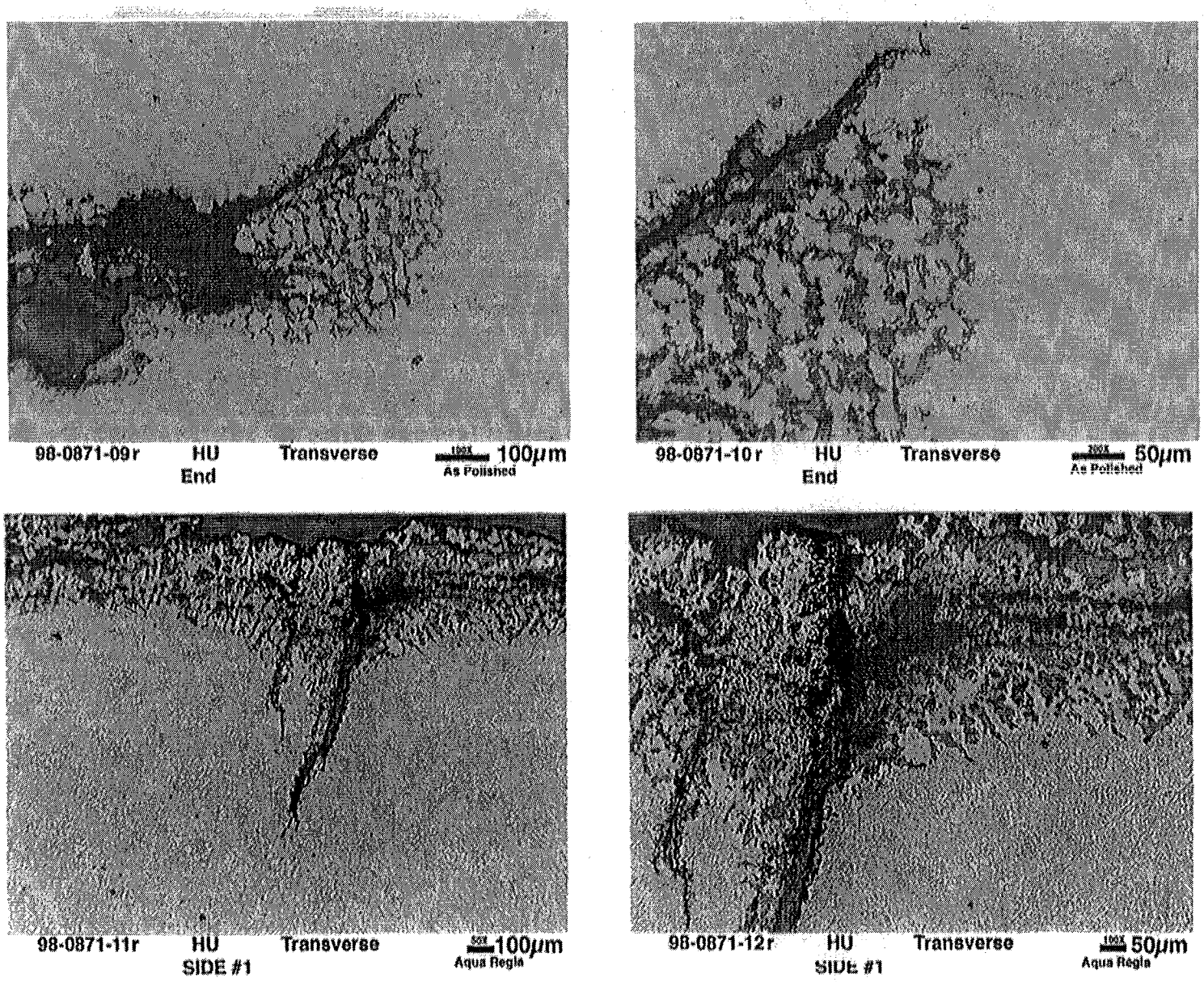

Fig. 41. Optical micrographs of the broken HU tray (end and side 1) in the transverse untetched and etched conditions.

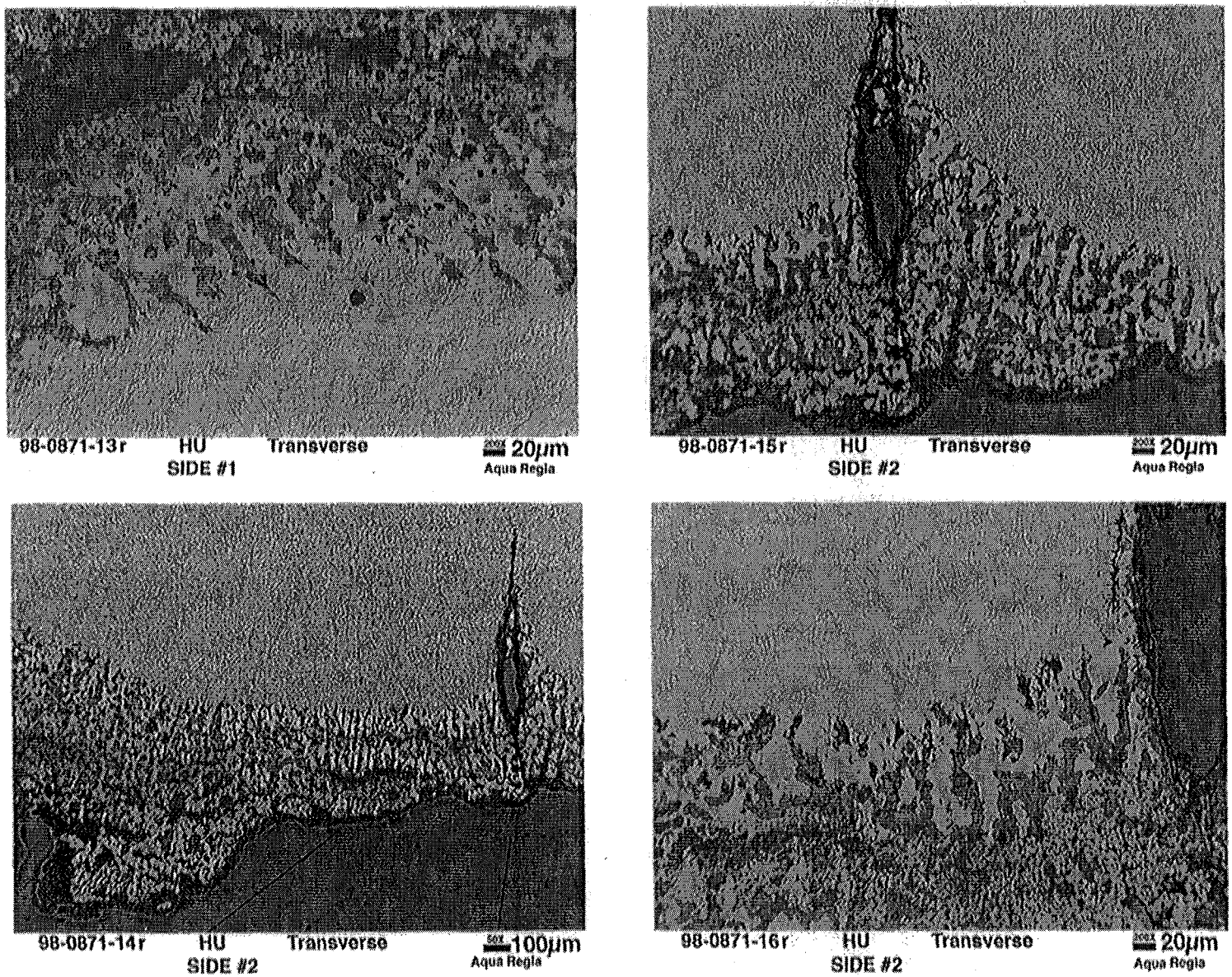

Fig. 42. Optical micrographs of the broken HU tray (sides 1 and 2) in the transverse etched condition at both low and high magnification.

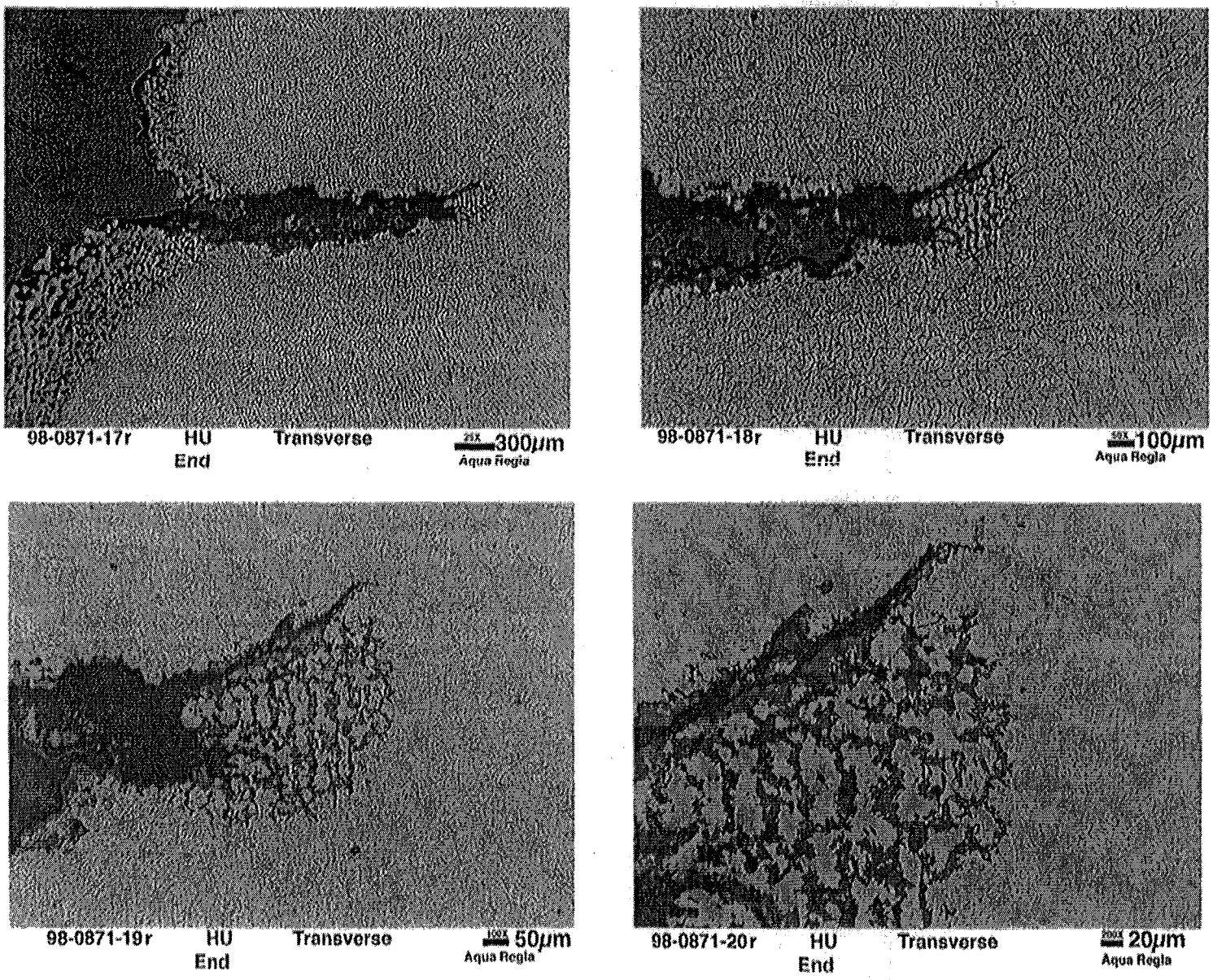

Fig. 43. Optical micrographs of the broken HU tray (end section) in the transverse etched condition at both low and high magnification.

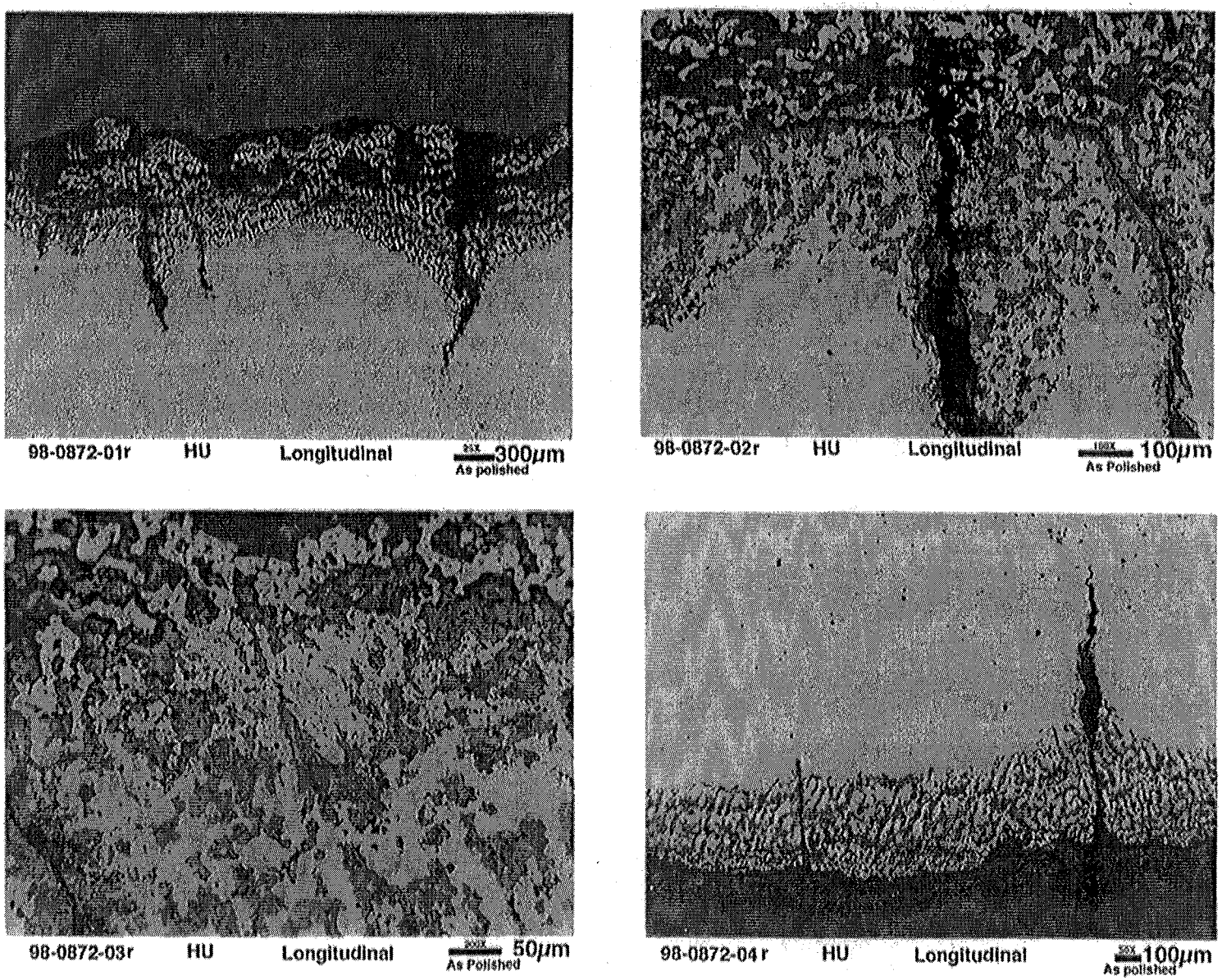

Fig. 44. Optical micrographs of the broken HU tray in the longitudinal unetched condition.

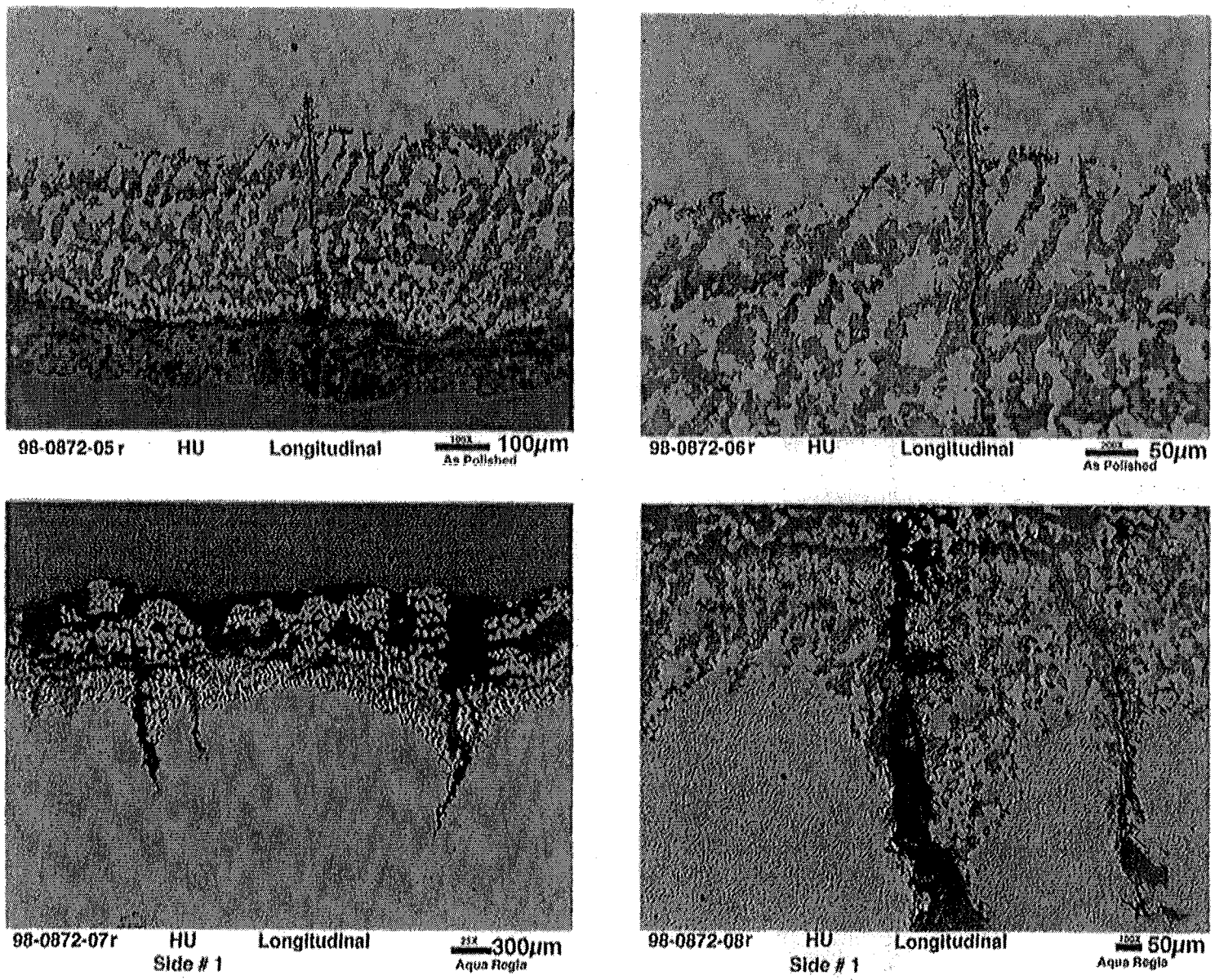

Fig. 45. Optical micrographs of the broken HU tray (side 1) in the longitudinal unetched and etched conditions.

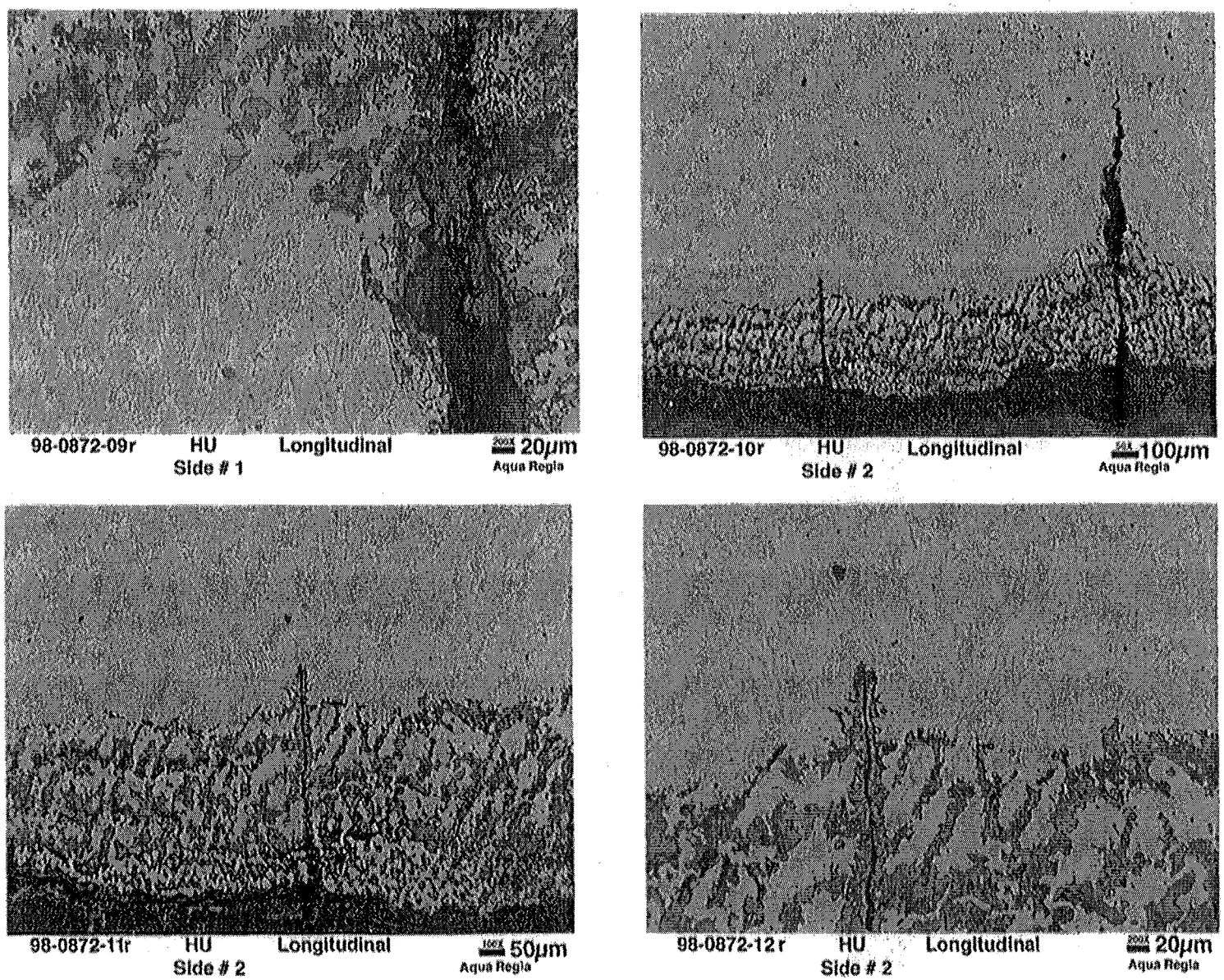

Fig. 46. Optical micrographs of the broken HU tray (sides 1 and 2) in the longitudinal etched condition.

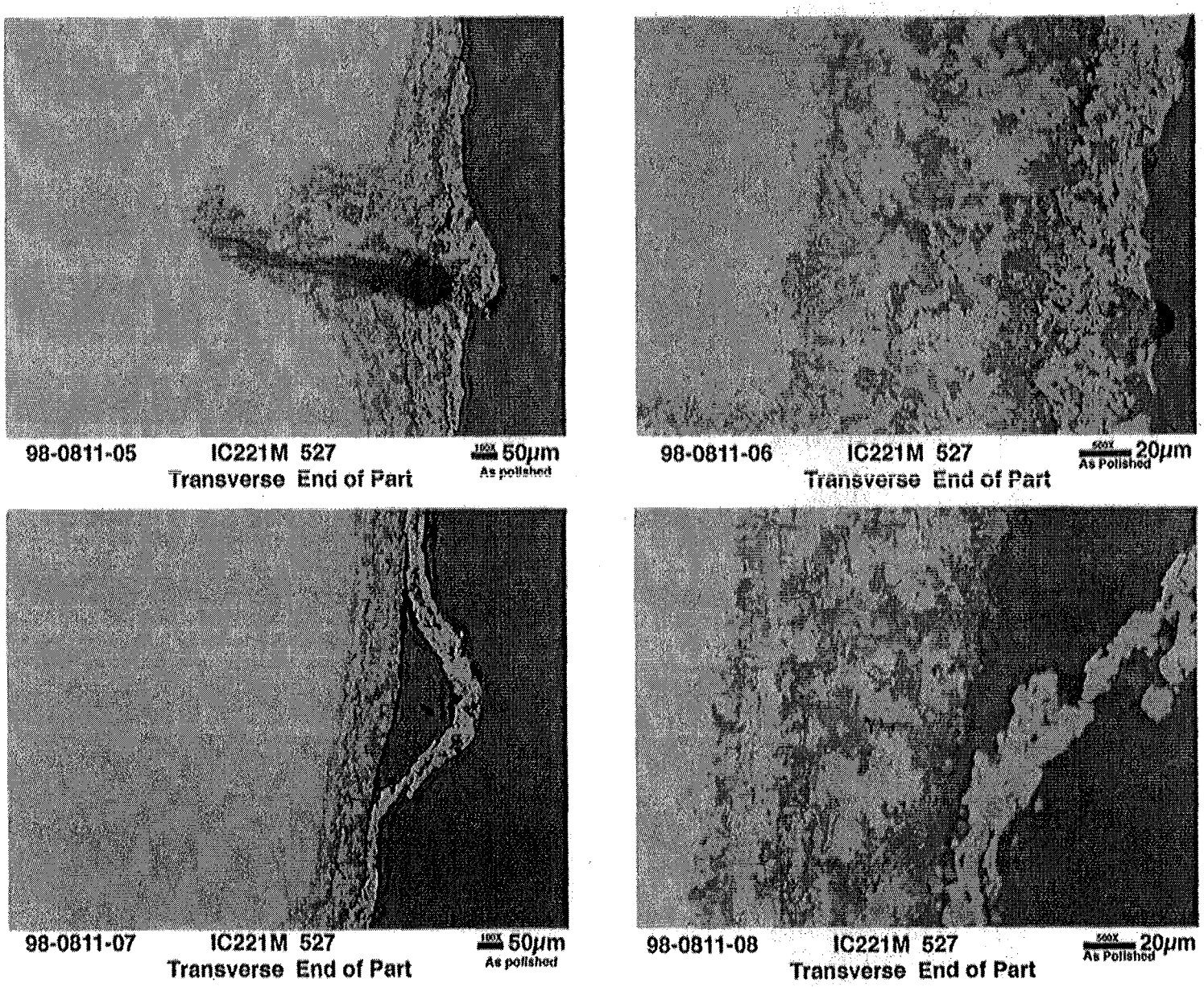

Fig. 47. Optical micrographs of the IC-221M fixture (unetched transverse end section) and removed from pusher carburizing furnace at Delphi Saginaw after 14 months of service.

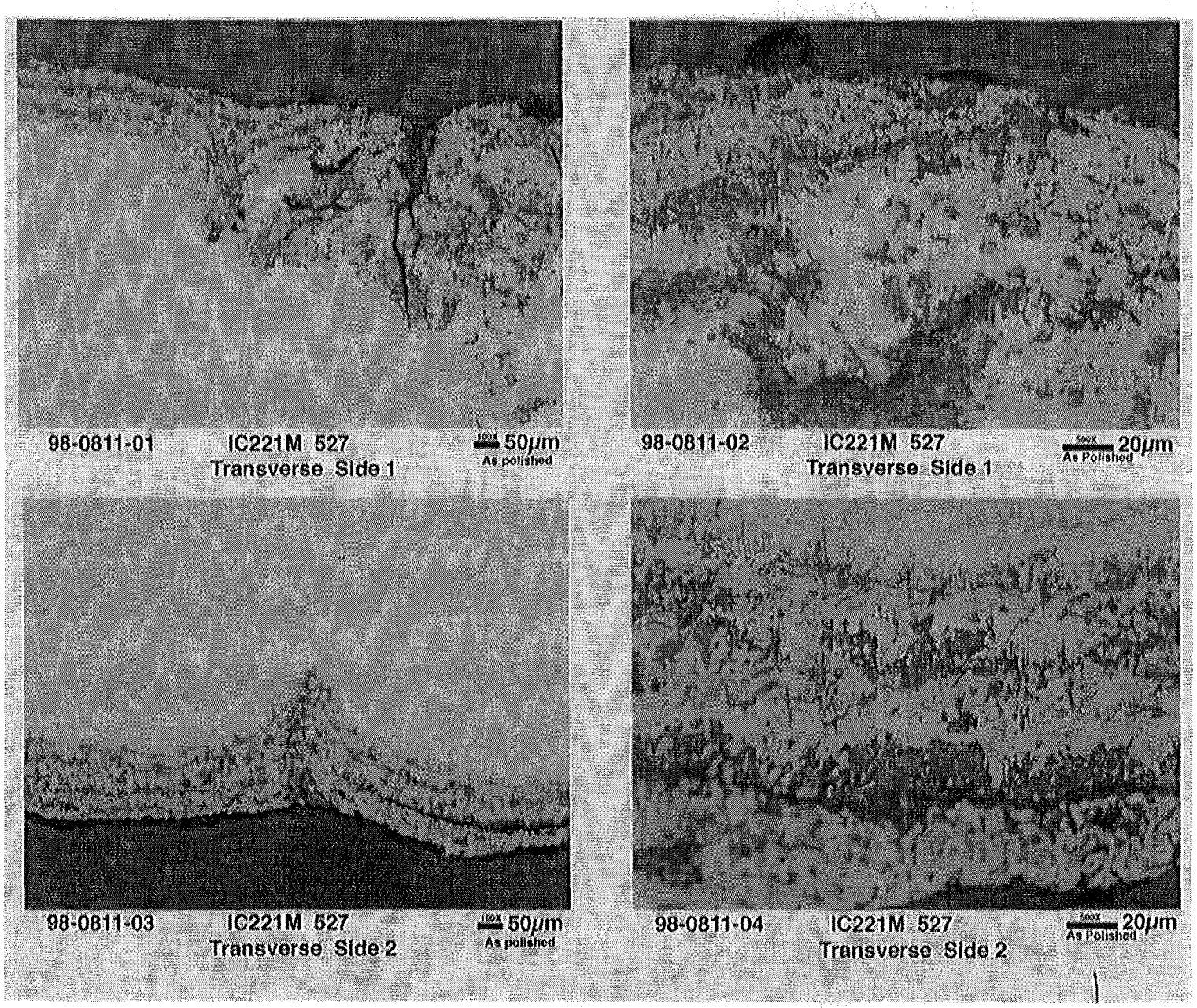

Fig. 48. Optical micrographs of the IC-221M fixture (sides 1 and 2) removed from pusher carburizing furnace at Delphi Saginaw after 14 months of service.

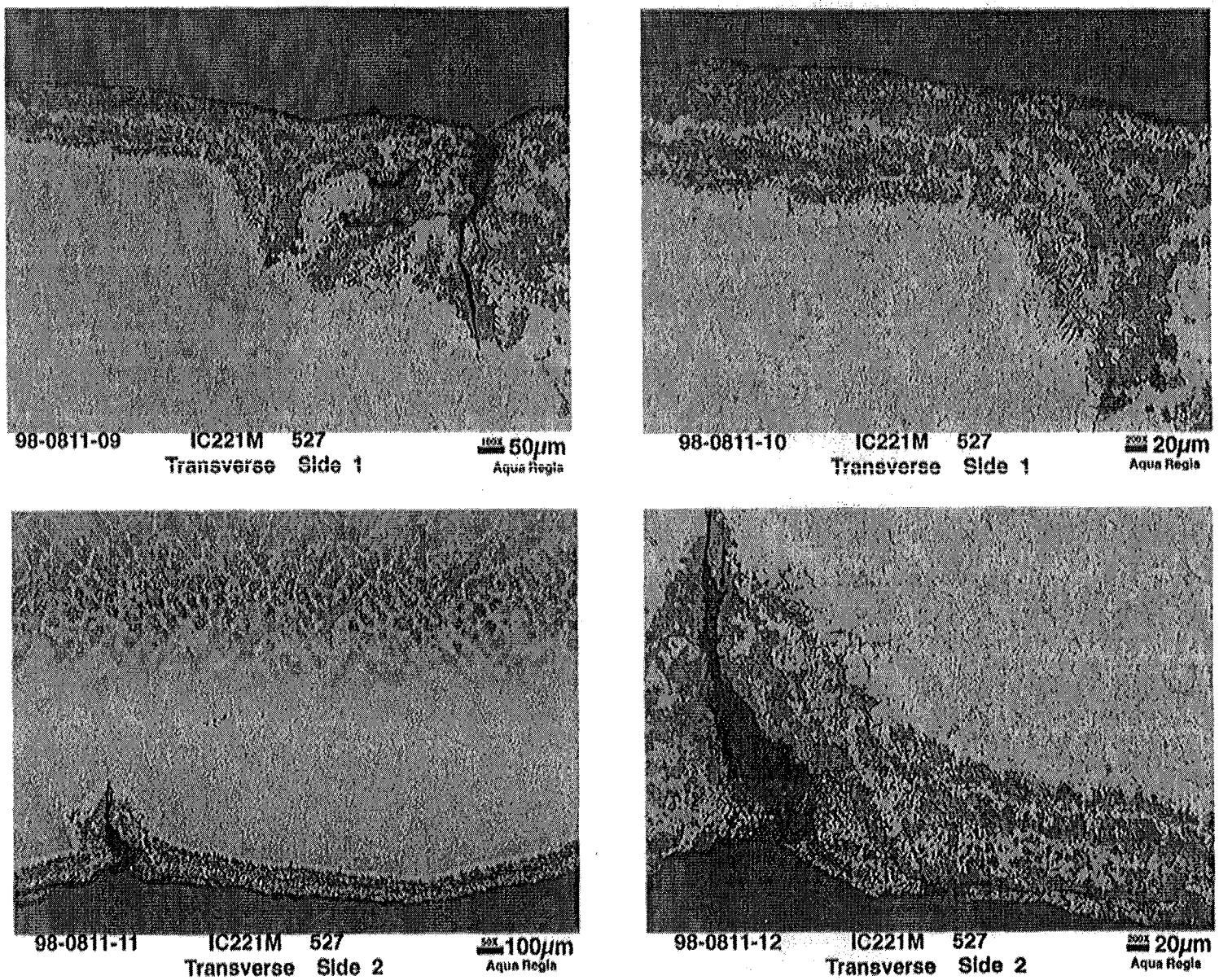

Fig. 49. Optical micrographs of the IC-221M fixture (etched at transverse sides 1 and 2 locations) removed from pusher carburizing furnace at Delphi Saginaw after 14 months of service.

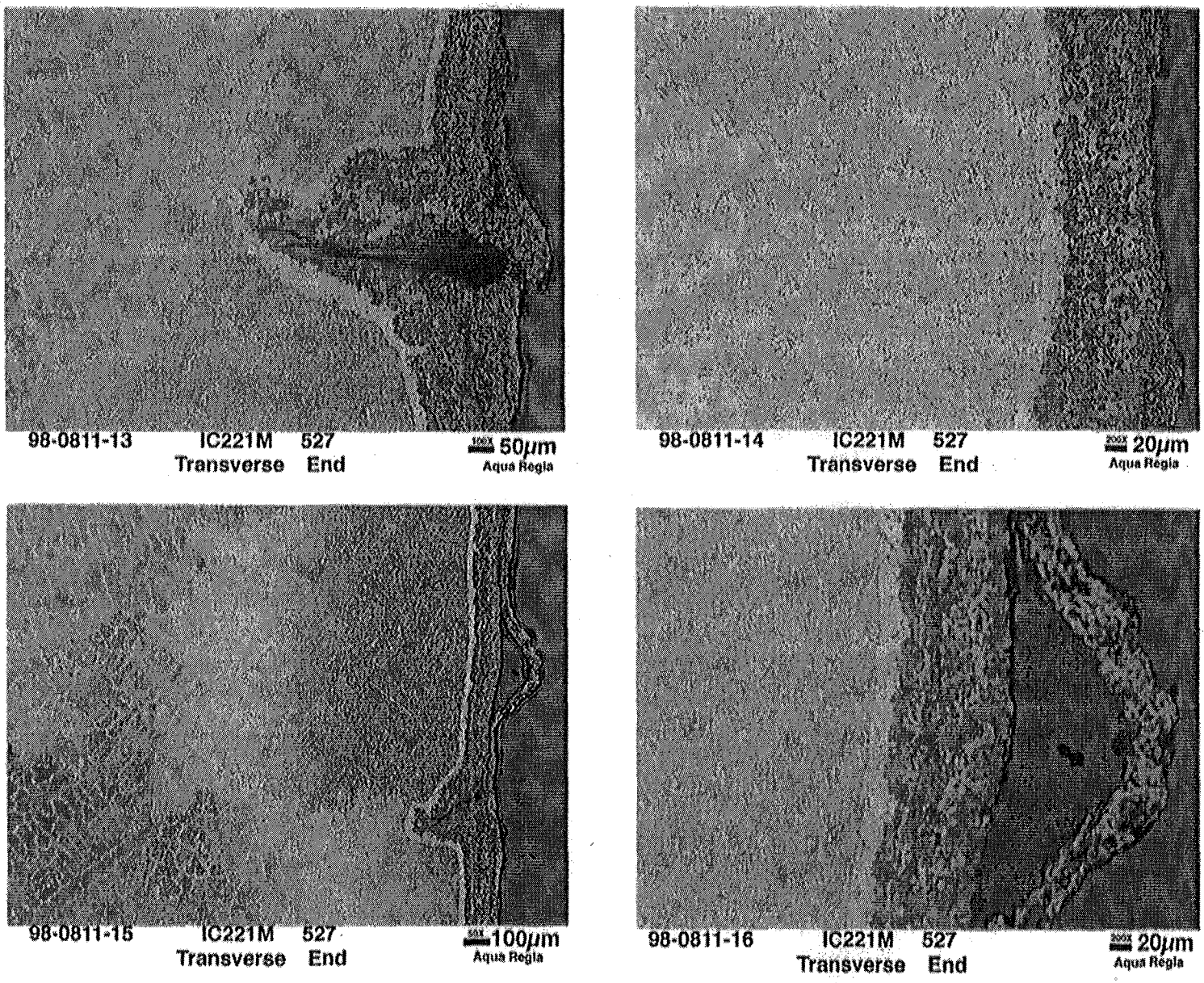

Fig. 50. Optical micrographs of the IC-221M fixture (etched at transverse end) removed from pusher carburizing furnace at Delphi Saginaw after 14 months of service.

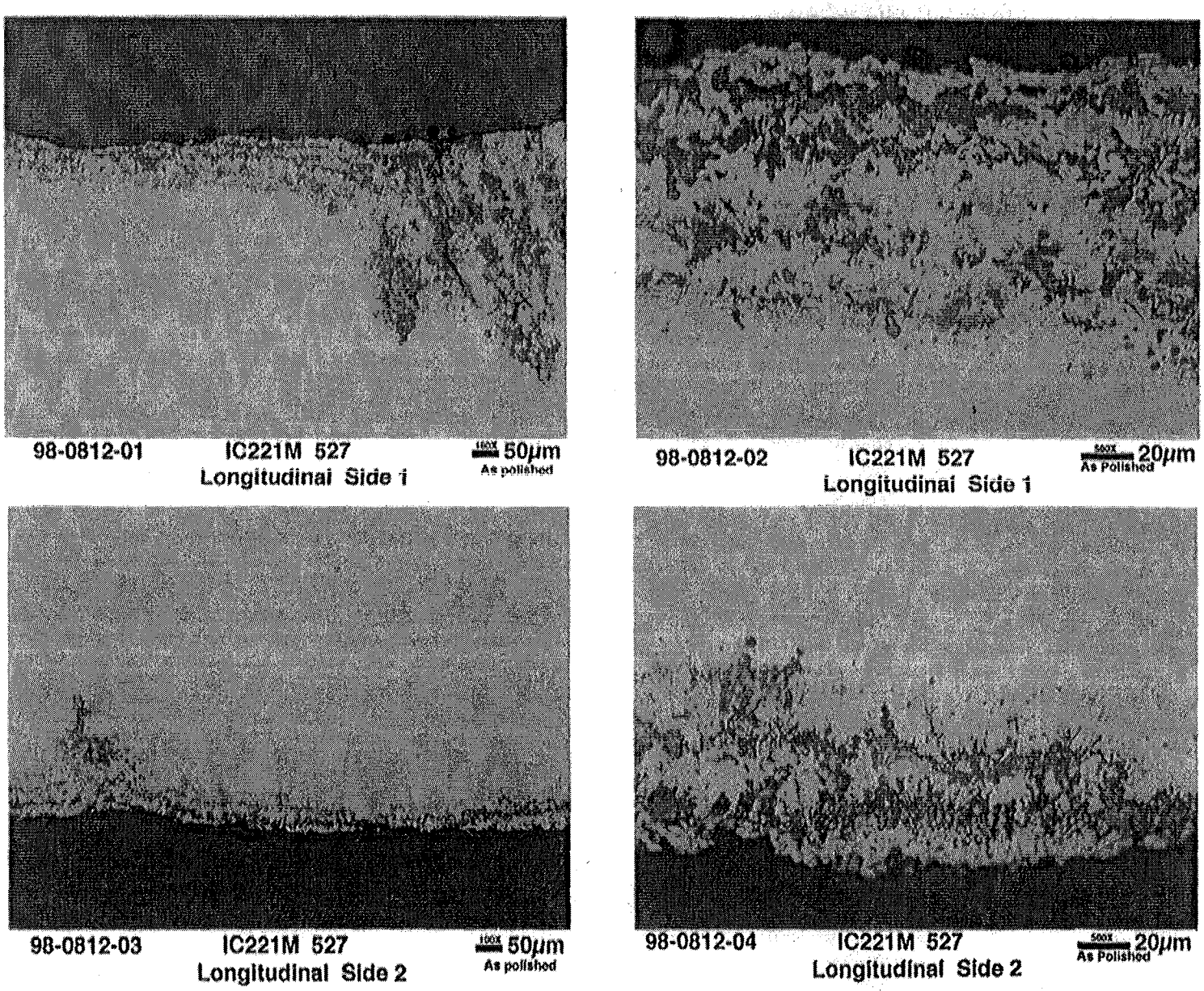

Fig. 51. Optical micrographs of the IC-221M fixture (unetched at longitudinal sides 1 and 2) removed from pusher carburizing furnace at Delphi Saginaw after 14 months of service.

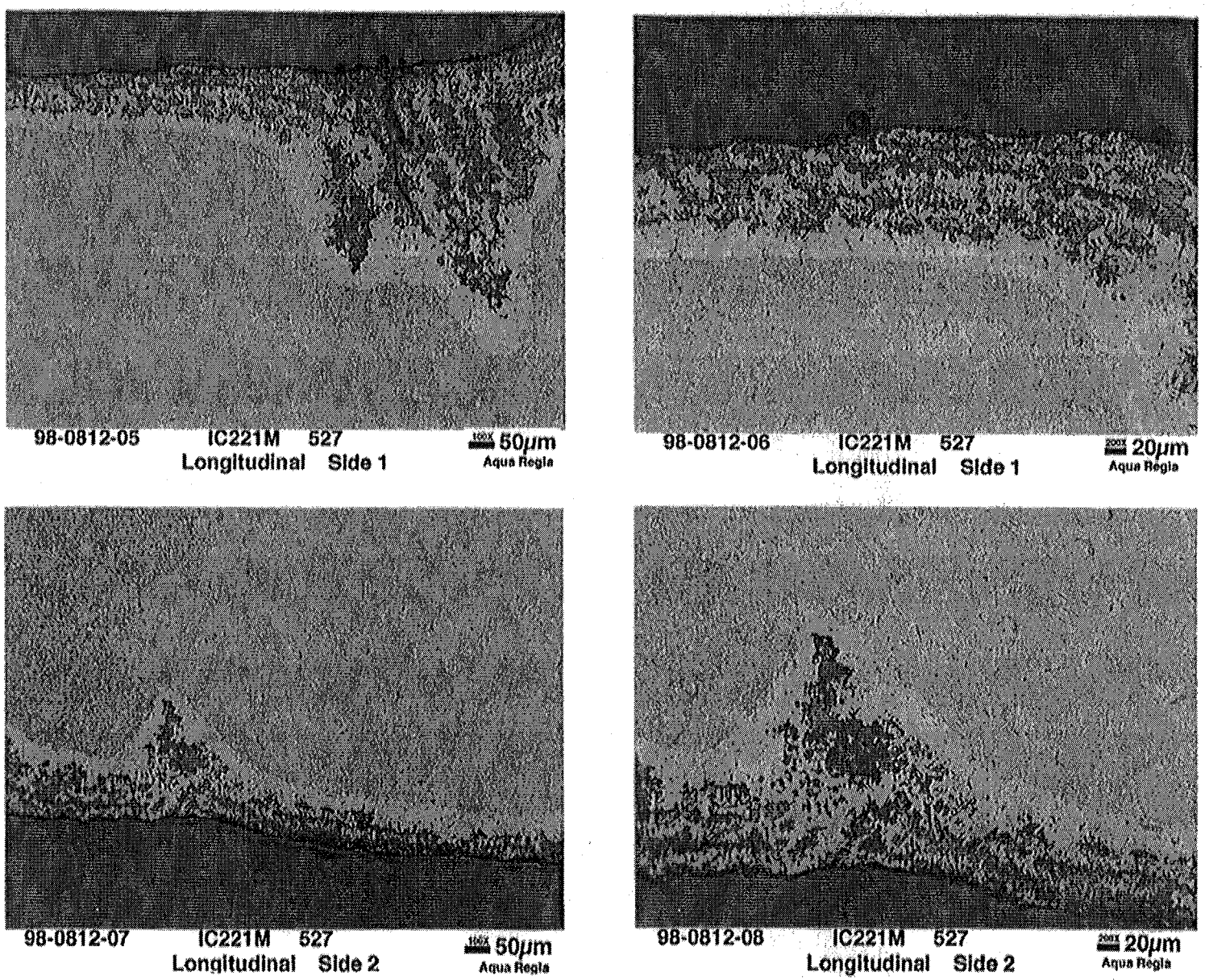

Fig. 52. Optical micrographs of the IC-221M fixture (etched at longitudinal sides 1 and 2) removed from pusher carburizing furnace at Delphi Saginaw after 14 months of service.

Table 14. Thickness of general corrosion layer and depth of cracks in HU after 18 months exposure and IC-221M after 14 months exposure

Sample identification	Carbon-affected layer				Comments
	General corrosion		Depth of crack		
	microns	mils	microns	mils	
HU after 18 Months Exposure					
98-0871-01	200	7.9	600	23.6	Delamination of surface layer. Two cracks side by side.
98-0871-04	200	7.9	500	19.7	Penetrating bulky carbide layer.
98-0872-01	800	31.5	1480 1160 1800	58.3 45.7 70.9	Three propagating cracks.
98-0872-04	200	7.9	540	21.3	Longest crack.
IC-221M after 14 Months Exposure					
98-0811-01	220	8.7	820	32.3	Layered attack. Longest crack is branched.
98-0811-09	220 40	8.7 1.6			Depleted layer underneath. General corrosion layer

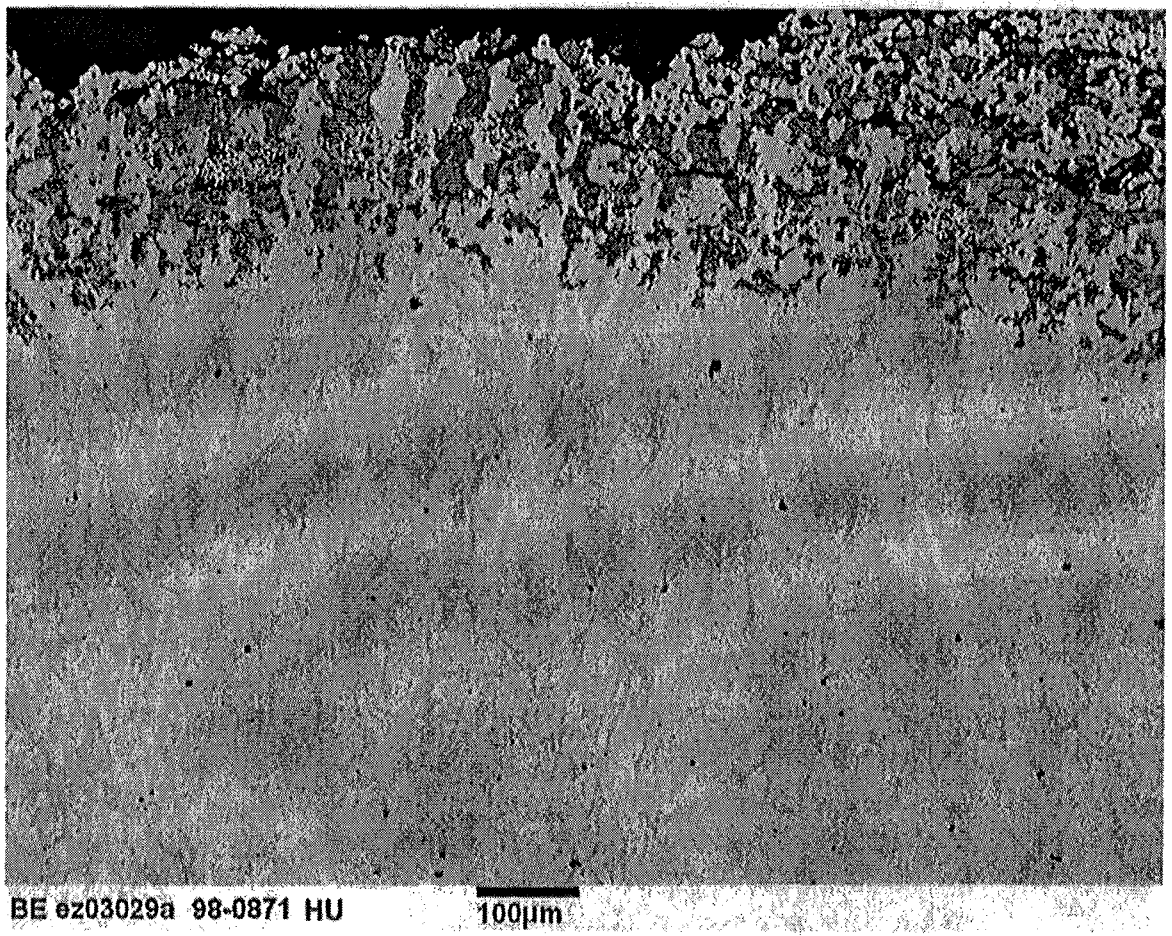

Fig. 53. Backscattered electron image of the sample from HU tray after 18 months of exposure in the batch furnace at Delphi Saginaw. Low magnification showing corrosion layer at surface.

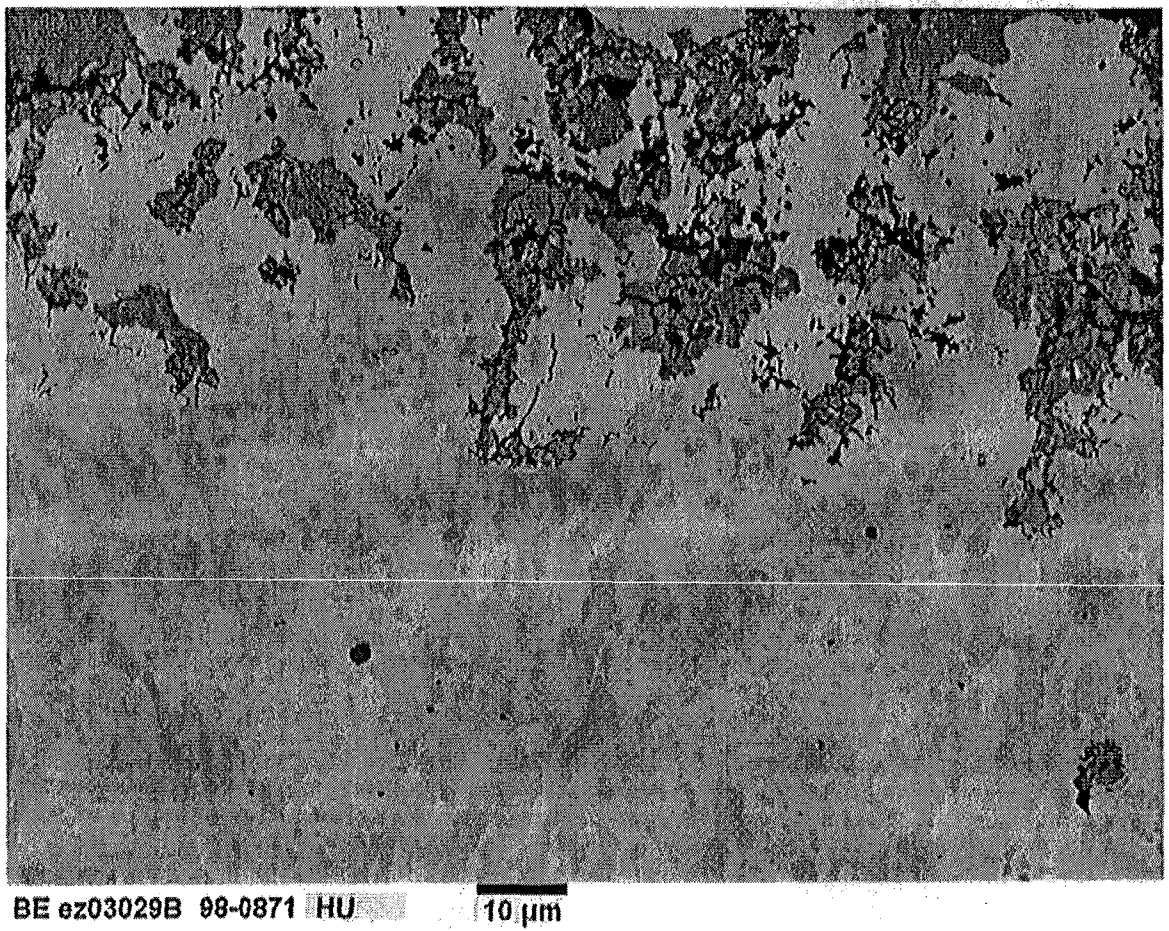

Fig. 54. Backscattered electron image of the sample from HU tray after 18 months of exposure in the batch furnace at Delphi Saginaw. High magnification showing metal/corrosion layer at surface.

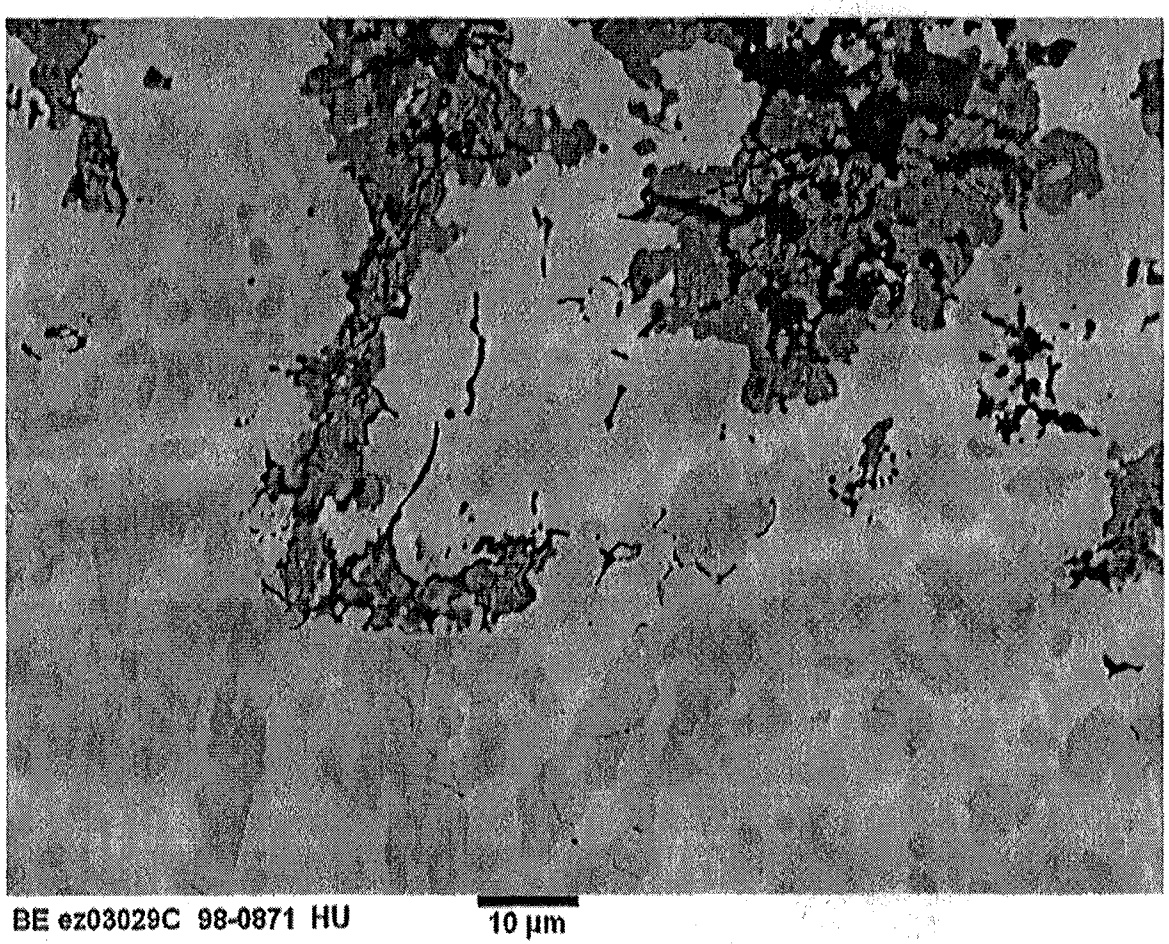

Fig. 55. Backscattered electron image of the sample from HU tray after 18 months of exposure in the batch furnace at Delphi Saginaw. High magnification showing more details of corrosion product into the base metal.

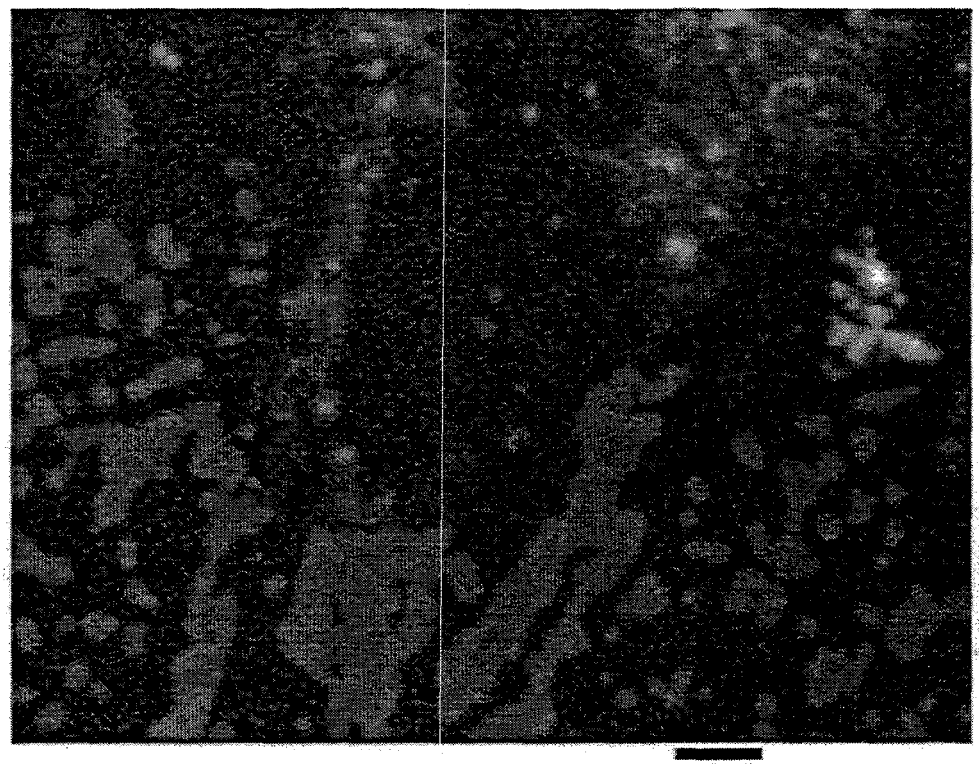

Fig. 56. Carbon elemental map of the backscattered electron image for the HU sample in Fig. 55.

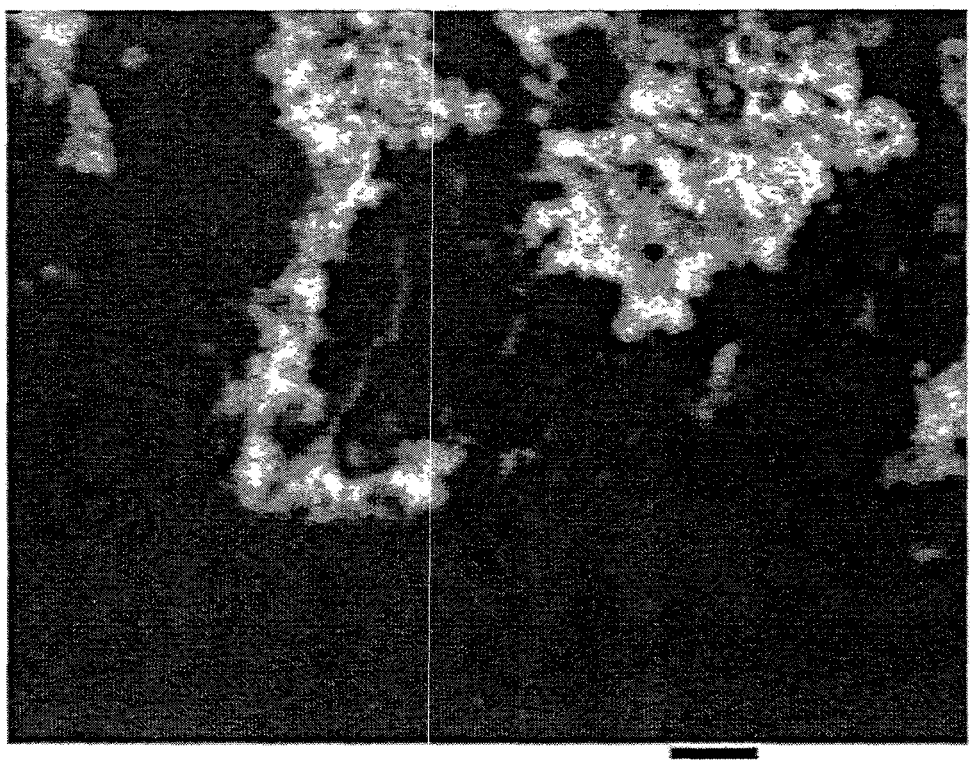

Fig. 57. Oxygen elemental map of the backscattered electron image for the HU sample in Fig. 55.

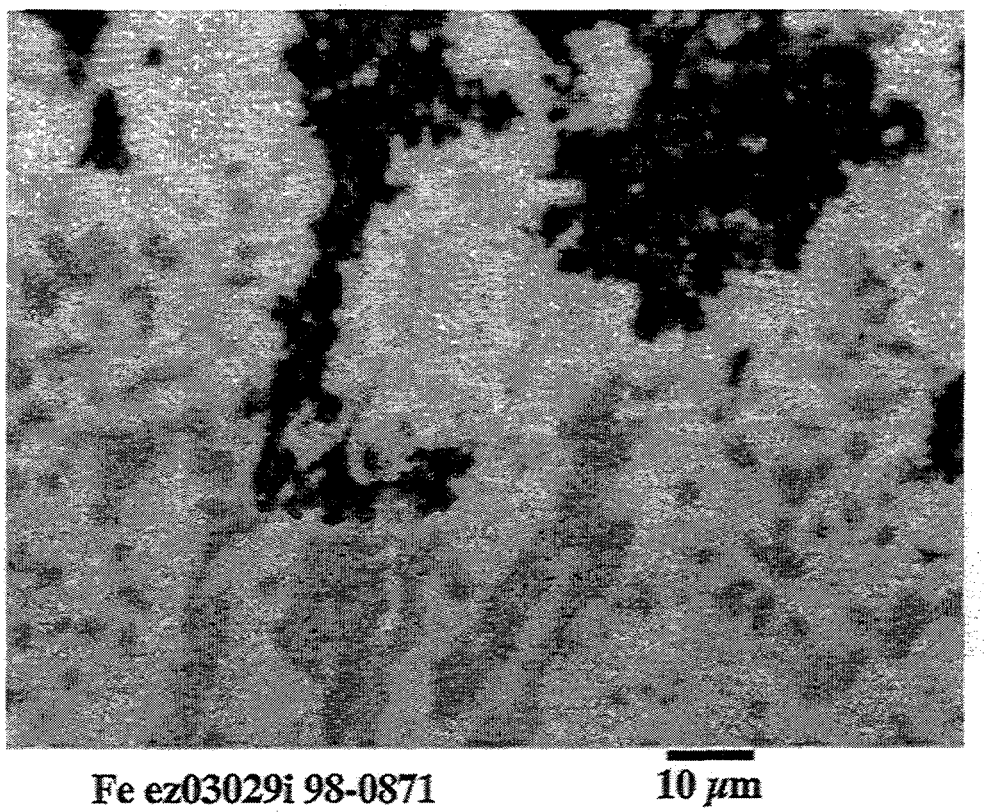

Fig. 58. Iron elemental map of the backscattered electron image for the HU sample in Fig. 55.

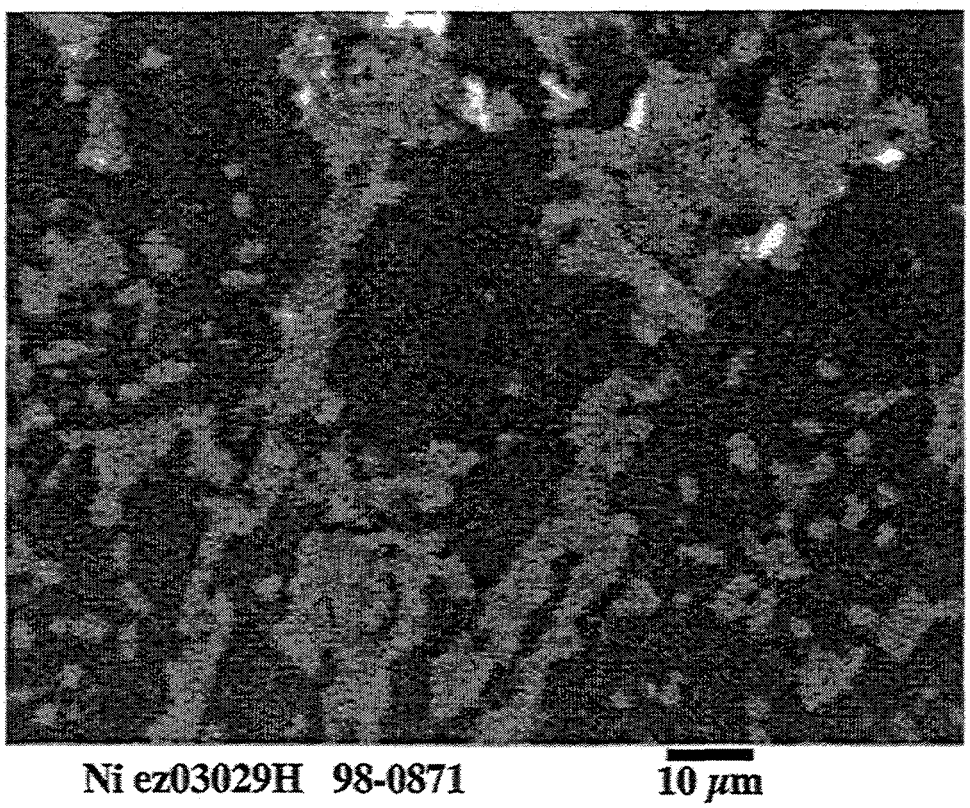

Fig. 59. Nickel elemental map of the backscattered electron image for the HU sample in Fig. 55.

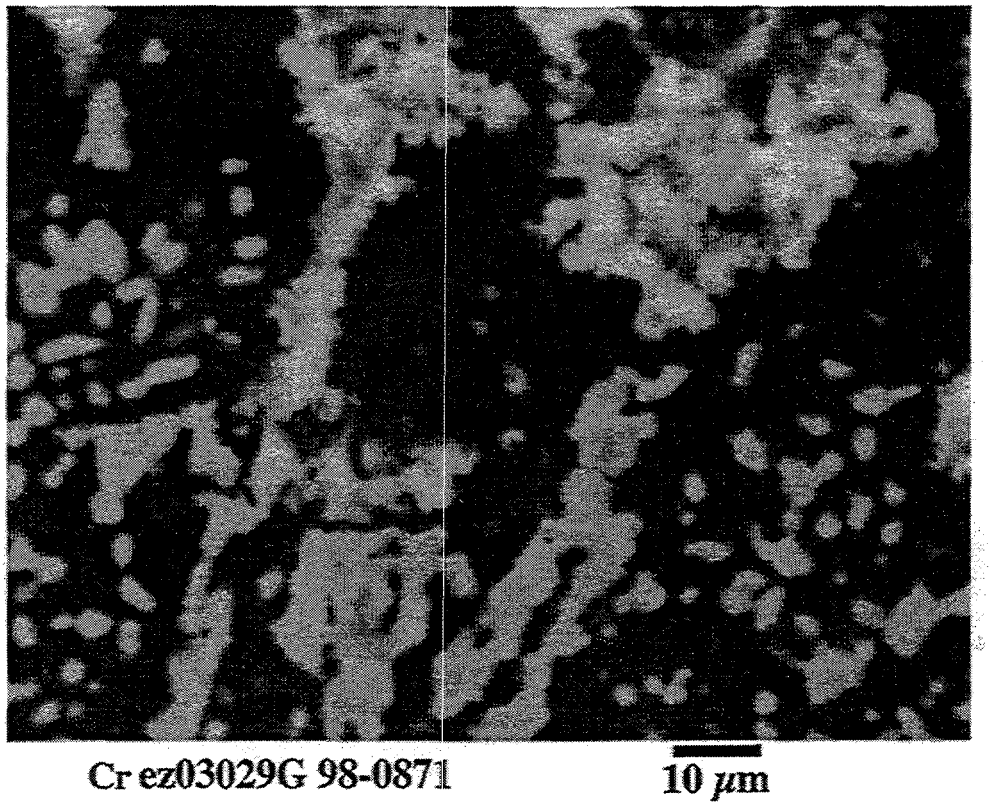

Fig. 60. Chromium elemental map of the backscattered electron image for the HU sample in Fig. 55.

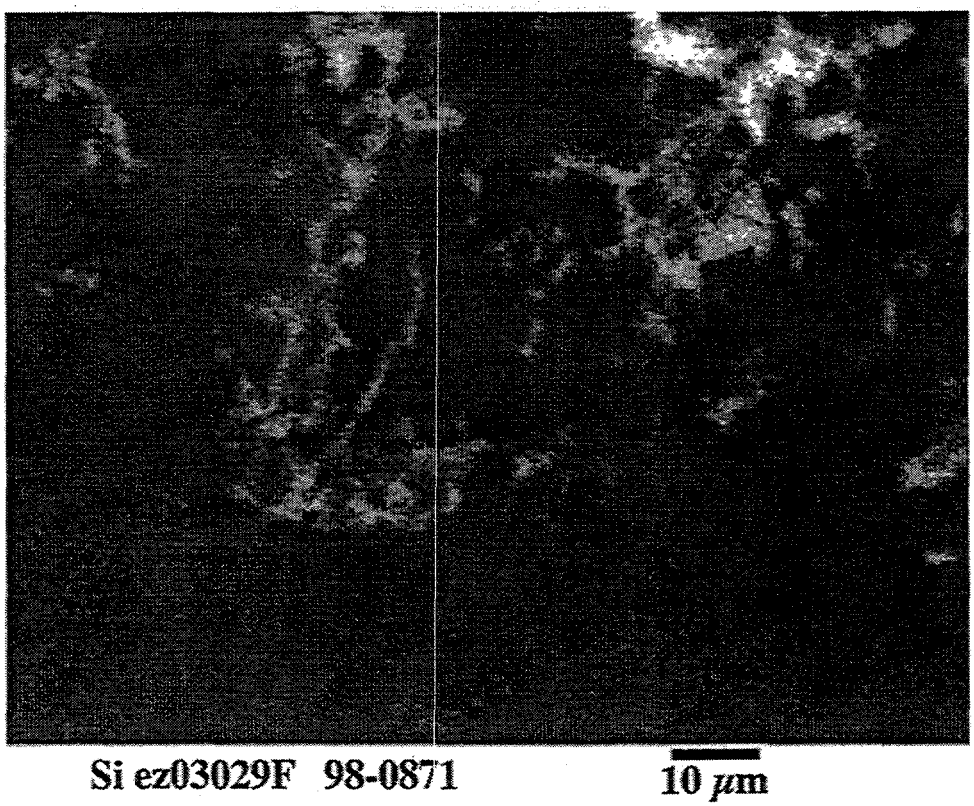

Fig. 61. Silicon elemental map of the backscattered electron image for the HU sample in Fig. 55.

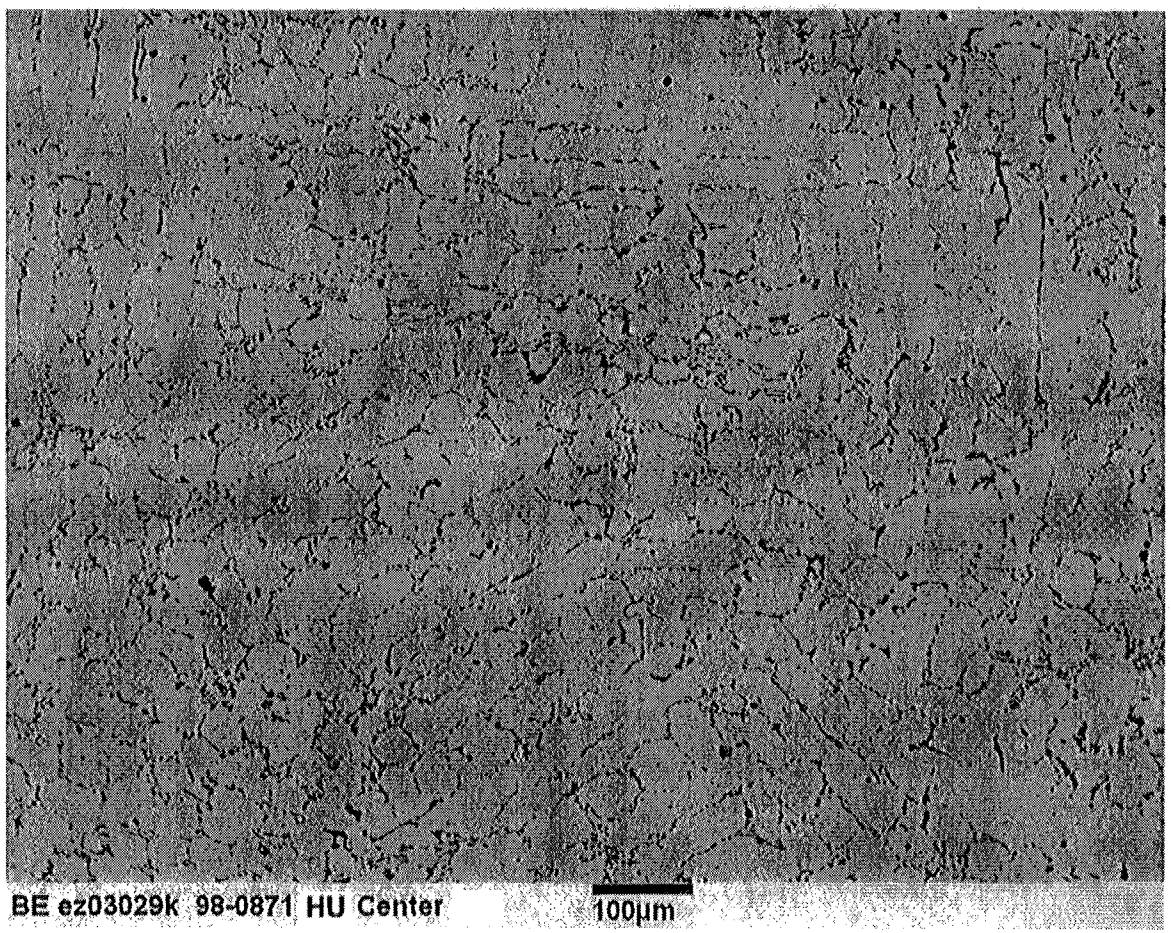

Fig. 62. Backscattered electron image of the sample from the HU tray after 18 months of exposure in the batch furnace at Delphi Saginaw. Low magnification showing center of the tray section (base metal).

element present in both the reacted and unreacted regions in Fig. 58. Nickel is also present to some extent in the regions enriched with chromium as shown in Fig. 59. The reacted area is totally free from iron in Fig. 60. The reacted area enriched with chromium is also enriched with oxygen as shown in Fig. 61.

The backscattered electron images for the center of the HU specimen after 18 months exposure in the batch furnace is shown in Figs. 62 through 64. The elemental maps for the region in Fig. 64 are shown in Figs. 65 through 69. The carbon-enriched regions are shown in Fig. 65. Areas enriched with carbon in Fig. 65 are the same areas that are enriched with chromium shown in Fig. 67. High chromium areas also are enriched in nickel as shown in Fig. 68. Areas enriched with chromium, nickel, and carbon are free of iron and shown in Fig. 69.

In summary, data presented above show that the affected area near the surface in the HU specimen is along the regions enriched with nickel and chromium. The reaction product is an oxide rather than a carbide. However, in the specimen center, the enriched areas with nickel and chromium are enriched with carbon, reflecting the carbide forming.

The backscattered electron images of the IC-221 fixture after 14 months exposure in the carburizing furnace are shown in Figs. 70 through 73. These images show the surface exposed to the carburizing environment. The exposed surface has a banded or layered structure parallel to the metal edge. The layered structure appearance is different from the penetrating attack observed for the HU tray in Fig. 53. The layered structure also has a depleted layer underneath and is shown in Figs. 70 through 73. Each layer, including the depleted layer, is essentially the same thickness. The higher magnification backscattered electron image in Fig. 71 shows the following unusual feature of the layers: (1) the top or first layer from the exposed surface has a penetrating microstructure underneath, (2) the second layer microstructure also exhibits initiation of a penetrating microstructure underneath, and (3) the second and third layers appear to have started as depleted layers prior to nucleation of feathery features. More details are presented on these features in a later section of this report.

Elemental maps of the depleted layer in Fig. 73 were taken. The depleted region is completely free of carbon, with carbon indications in the matrix under the depleted region, Fig. 74. The presence of zirconium in the depleted region and the matrix are shown in Fig. 75. As shown in Fig. 76, the depleted region is absent of any aluminum-rich phases, and the penetrating structure underneath the secondary layer is aluminum-rich. However, the feathery features shown in Fig. 76 are free of aluminum. The feathery features in the layer above the depleted layer are chromium-rich as shown in Fig. 77. No chromium-containing features are observed in the depleted region. The matrix does show the chromium-containing particles. The aluminum-, chromium-, or zirconium-containing features in Figs. 74 through 77 did not contain nickel as shown in Fig. 78. The oxygen distribution is shown in Fig. 79. This figure also shows oxygen to be absent in the depleted and matrix regions. The chromium in the feathery and aluminum in the penetrating features underneath the second layer are both associated with oxygen, Fig. 79. The chromium and zirconium features in the matrix are associated with carbon. The zirconium in the depleted layer does not match with either carbon or oxygen. There is an interesting particle 'A' which has a core that matches with zirconium and carbon and outside matches with aluminum and oxygen. This suggests that the particles are zirconium-carbide with Al_2O_3 film on them.

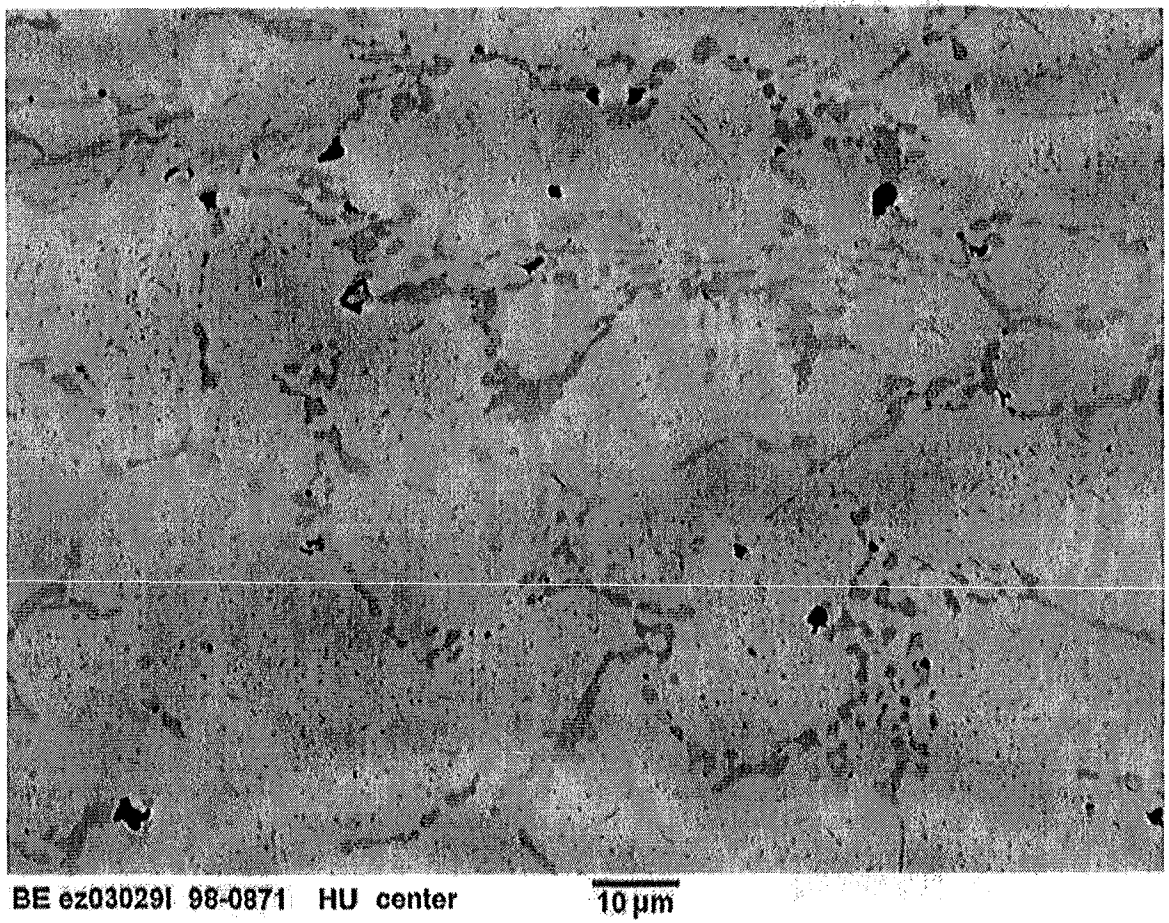

Fig. 63. Backscattered electron image of the sample from the HU tray after 18 months of exposure in the batch furnace at Delphi Saginaw. High magnification showing center of the tray section (base metal).

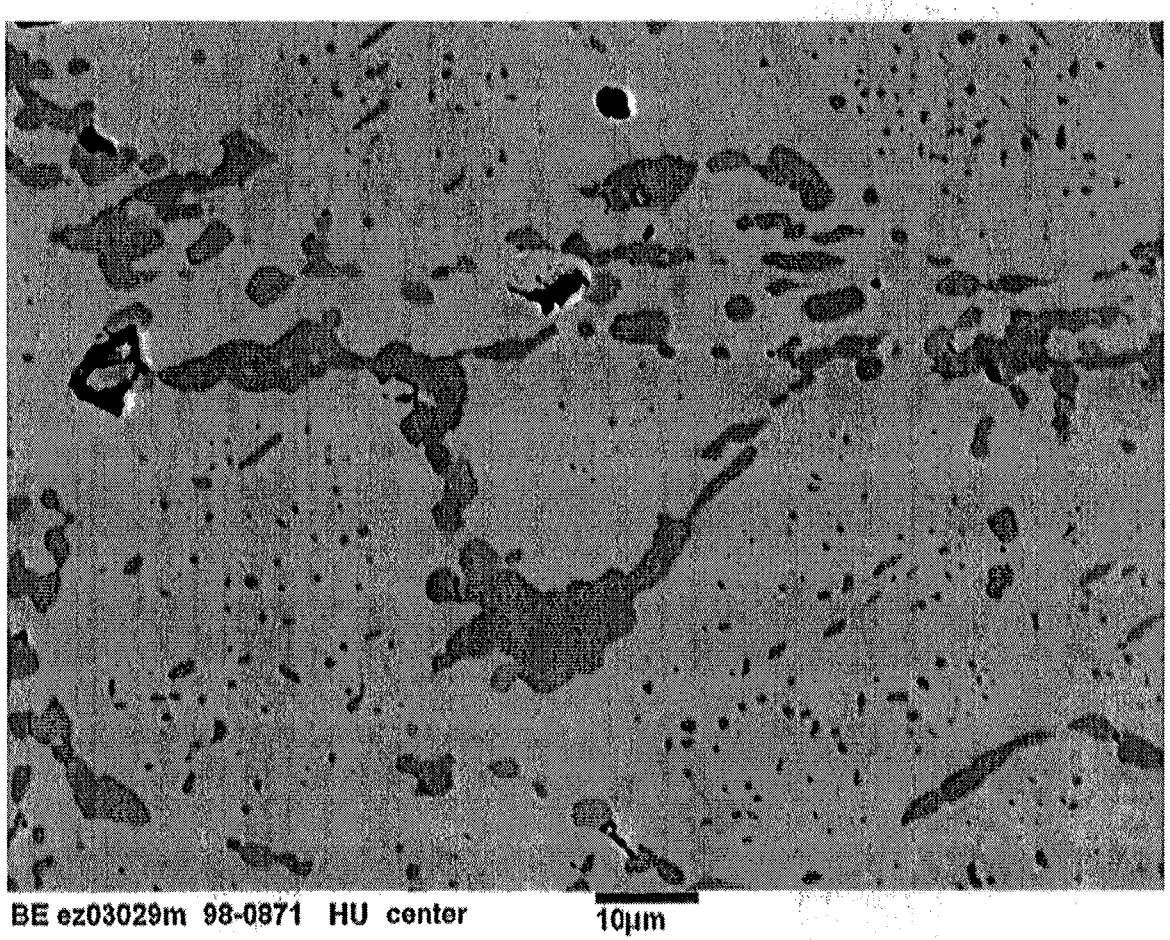

Fig. 64. Backscattered electron image of the sample from the HU tray after 18 months of exposure in the batch furnace at Delphi Saginaw. Highest magnification showing center of the tray section (base metal).

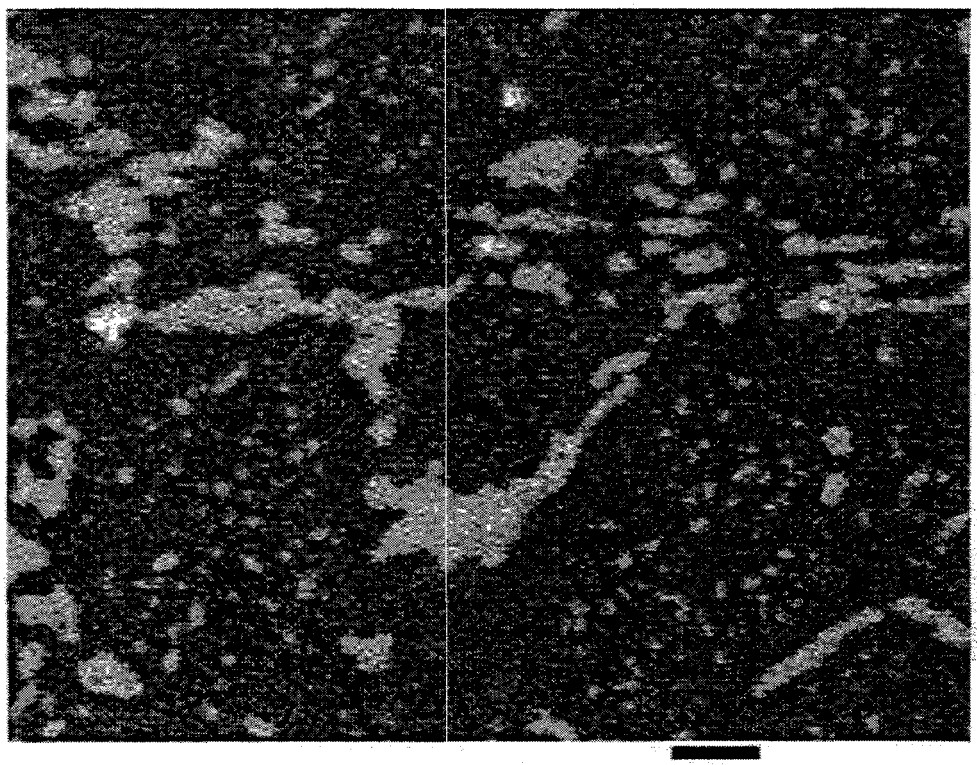

Fig. 65. Carbon elemental map for enlarged region in Fig. 64.

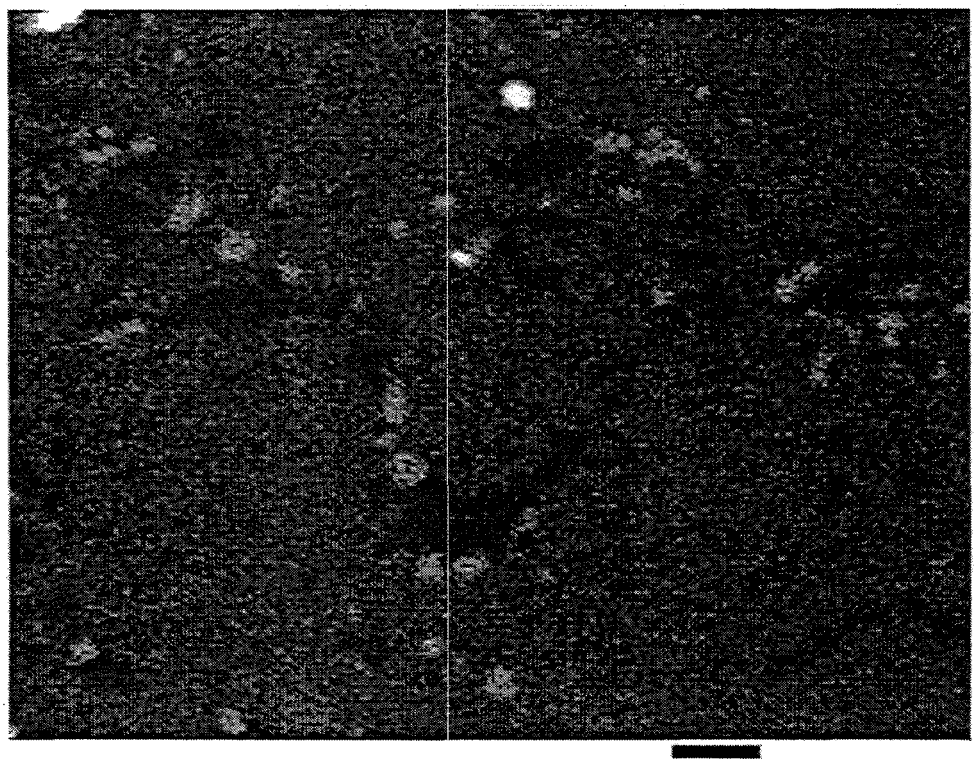

Fig. 66. Silicon elemental map for enlarged region in Fig. 64.

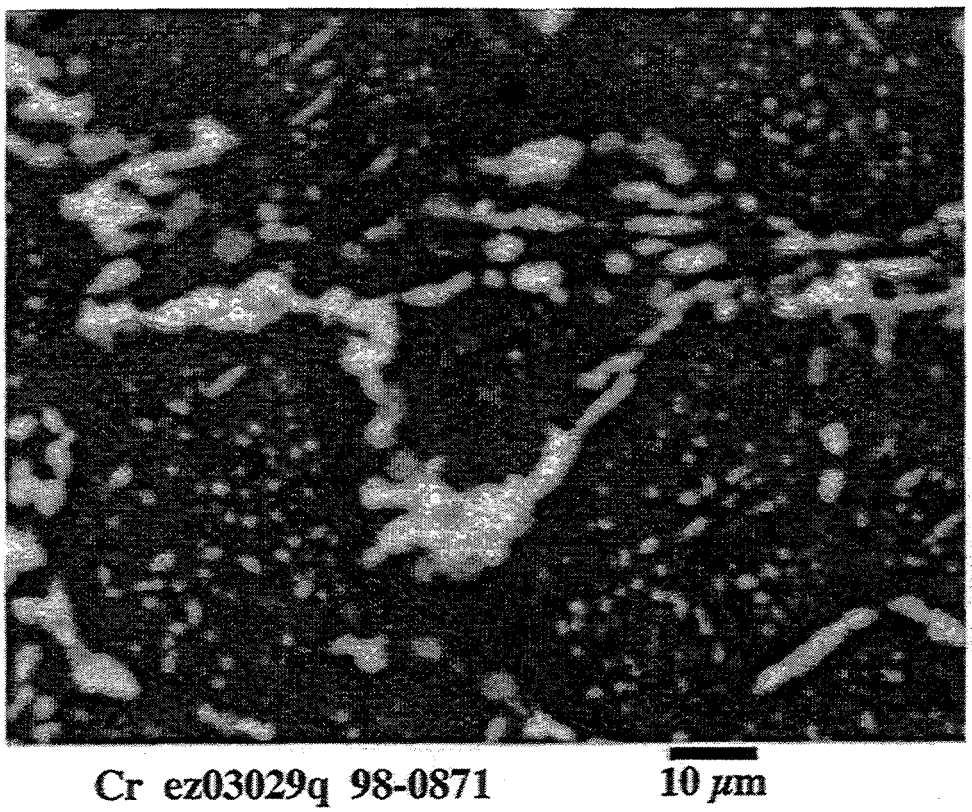

Fig. 67. Chromium elemental map for enlarged region in Fig. 64.

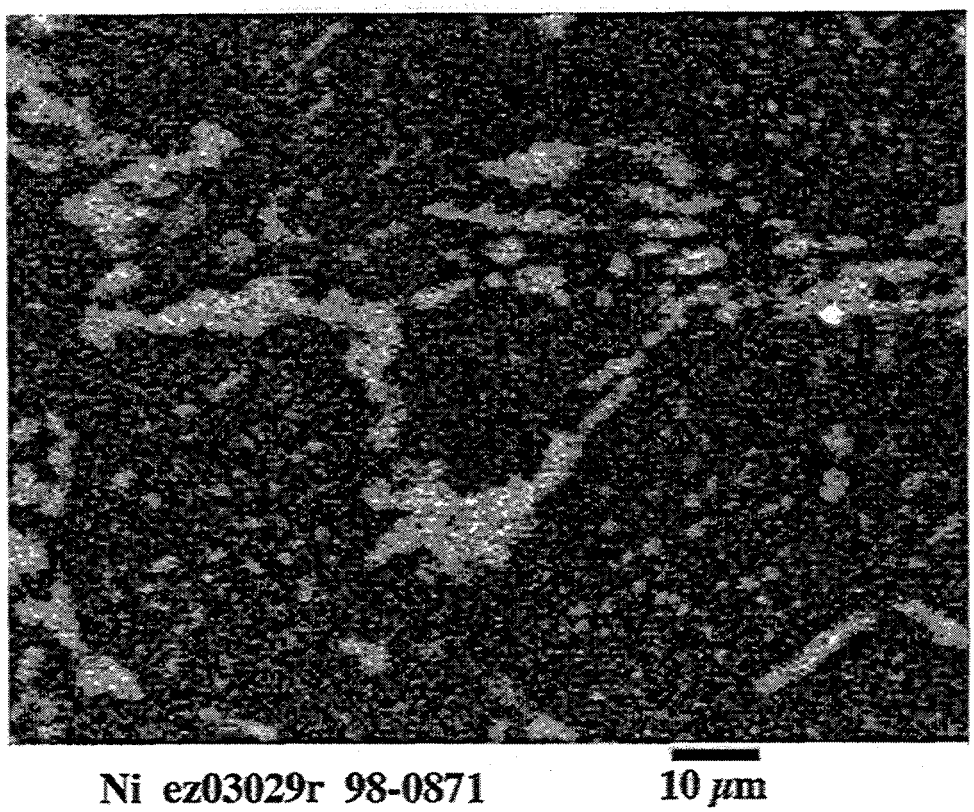

Fig. 68. Nickel elemental map for enlarged region in Fig. 64.

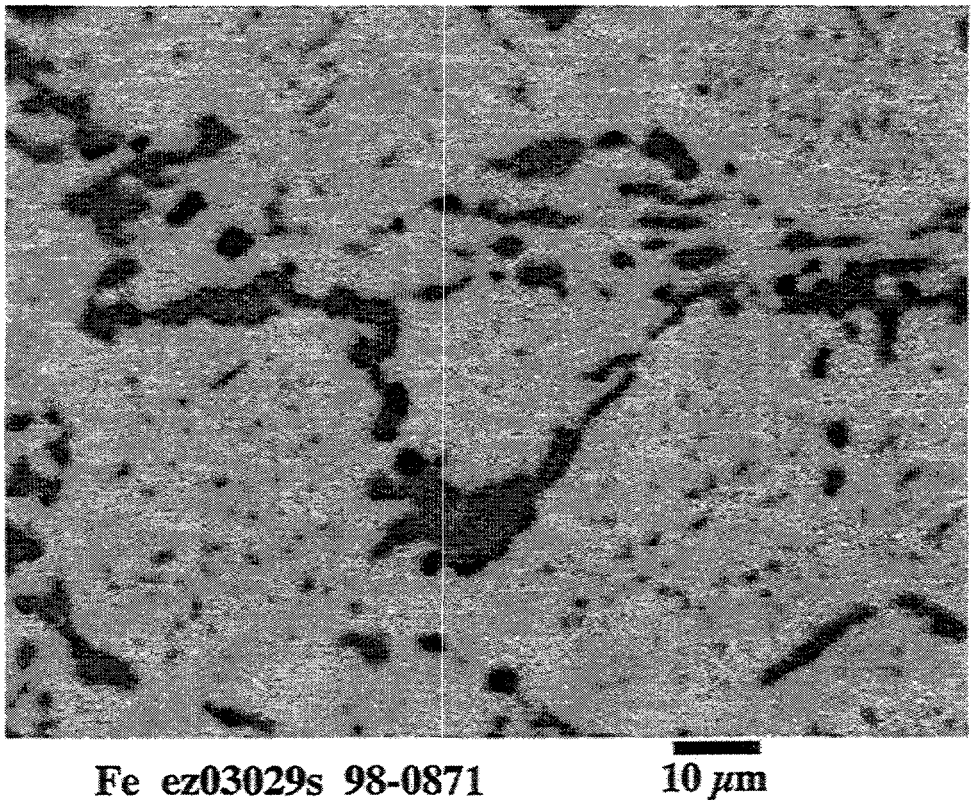

Fig. 69. Iron elemental map for enlarged region in Fig. 64.

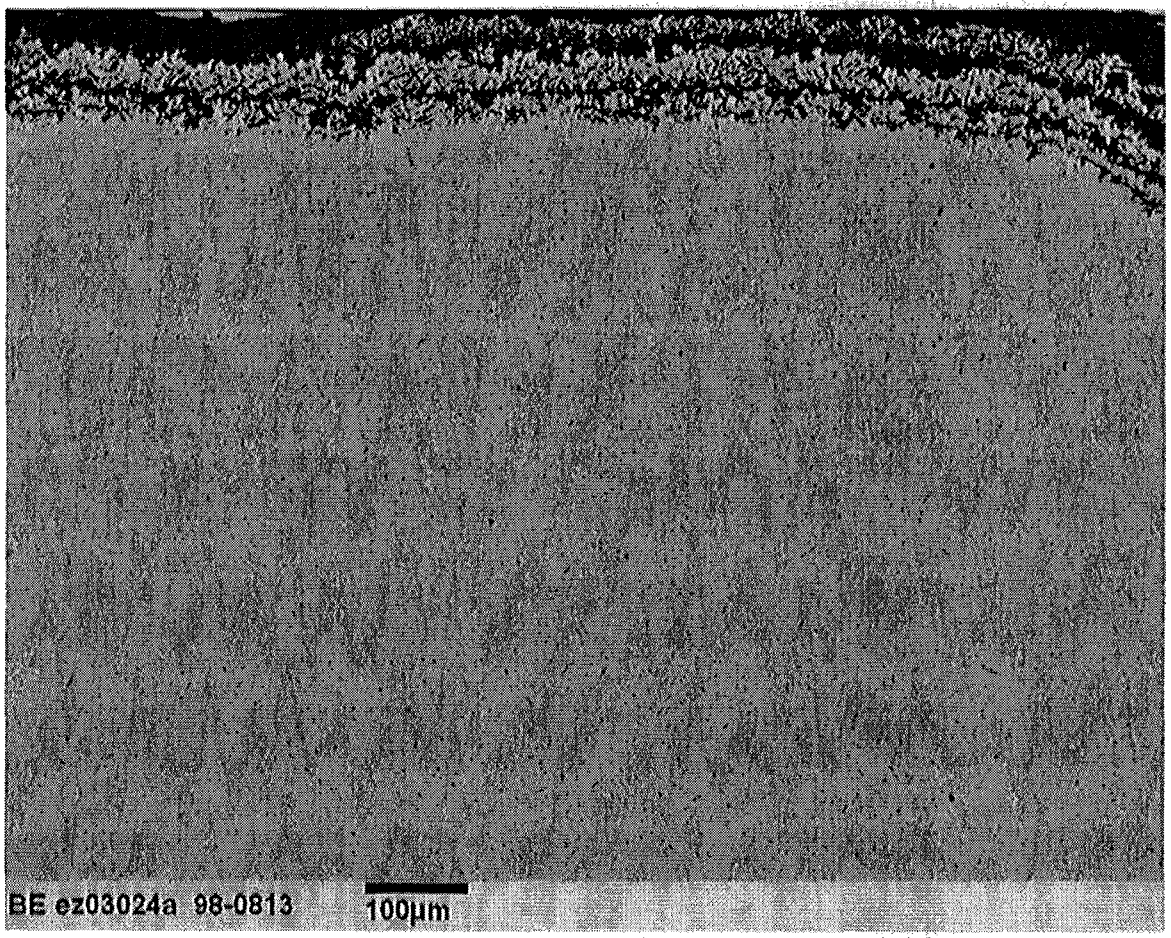

Fig. 70. Backscattered electron image of the surface of IC-221M fixture removed from pusher carburizing furnace after 14 months of service from Delphi Saginaw. Low magnification.

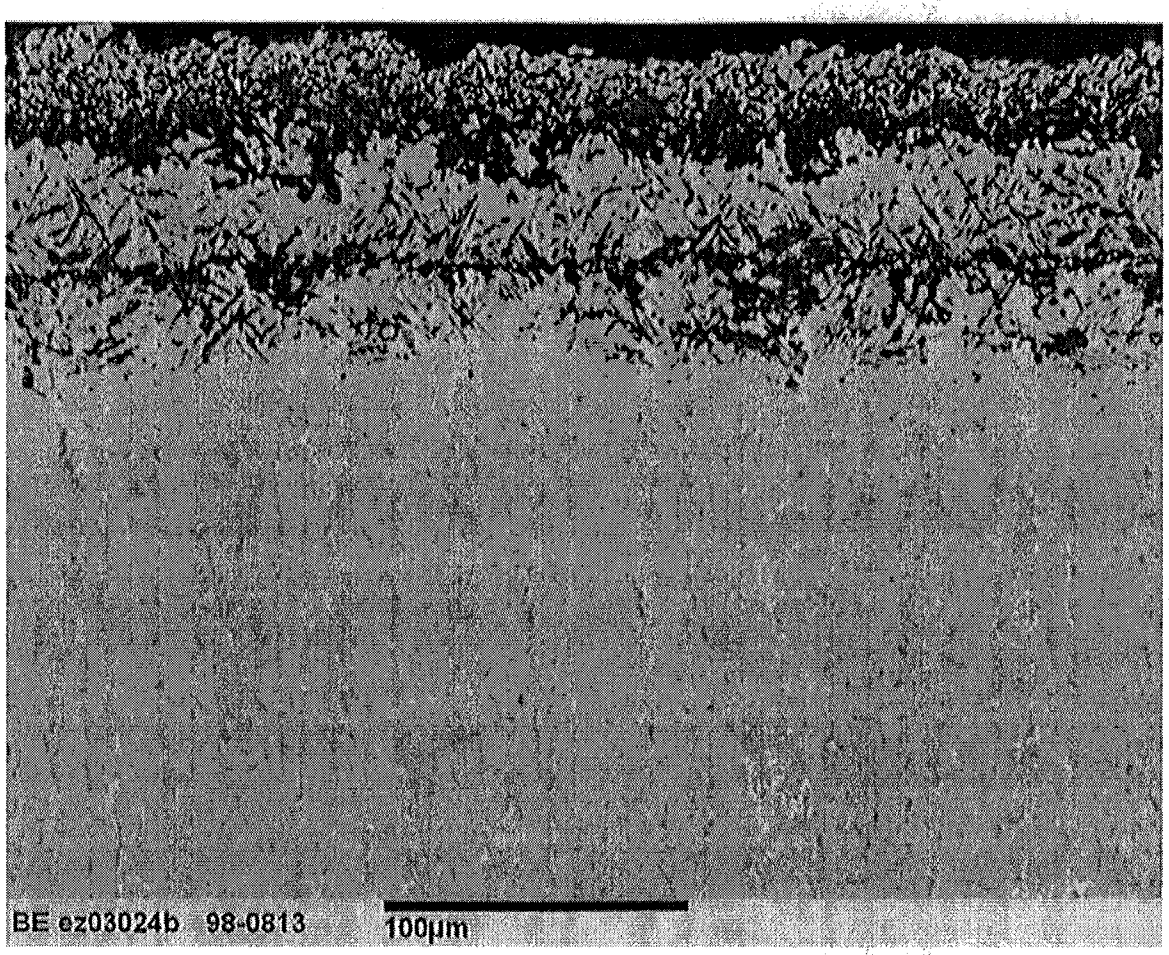

Fig. 71. Backscattered electron image of the surface of IC-221M fixture removed from pusher carburizing furnace after 14 months of service from Delphi Saginaw. High magnification.

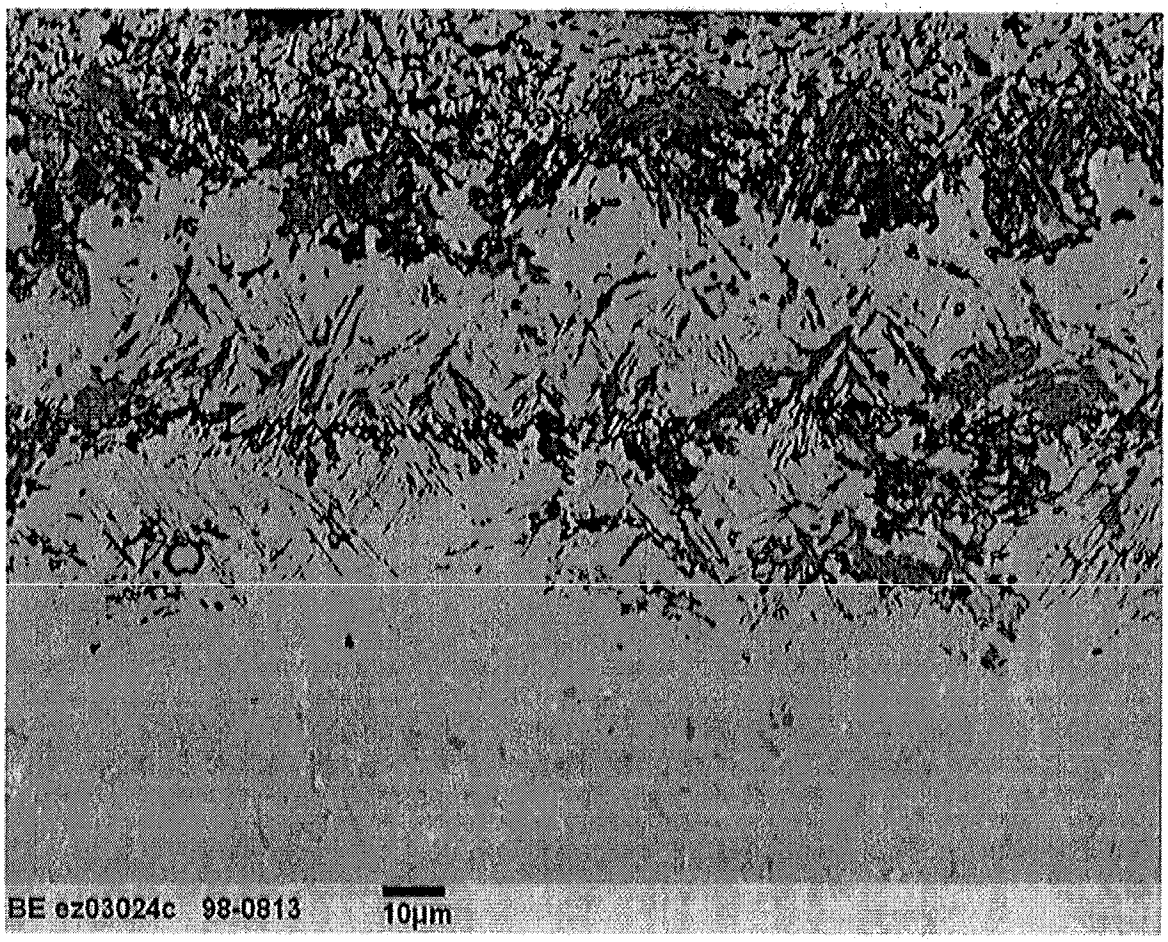

Fig. 72. Backscattered electron image of the surface of IC-221M fixture removed from pusher carburizing furnace after 14 months of service from Delphi Saginaw. Highest magnification.

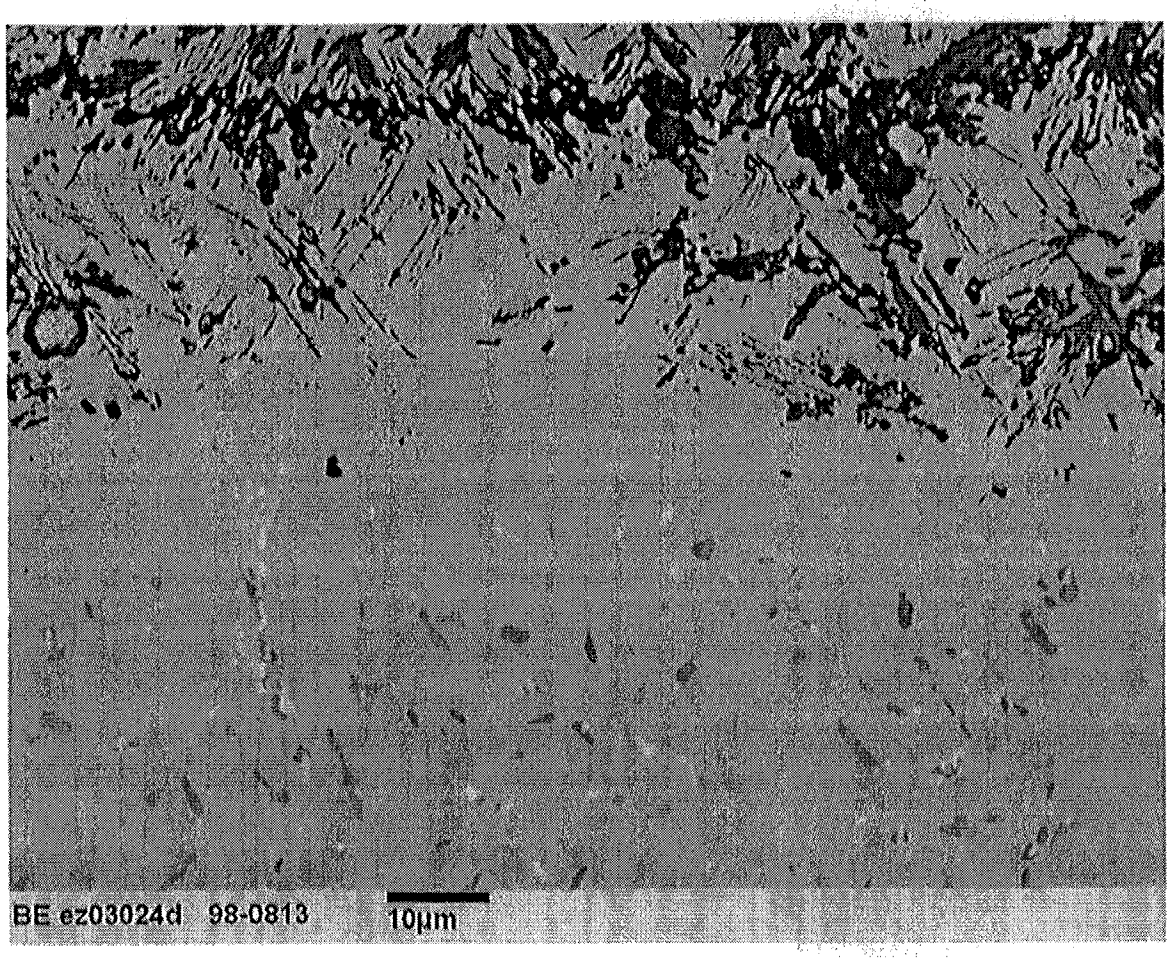

Fig. 73. Backscattered electron image of the depleted region at the base metal/surface reacted layer of IC-221M fixture removed from pusher carburizing furnace after 14 months of service from Delphi Saginaw. High magnification.

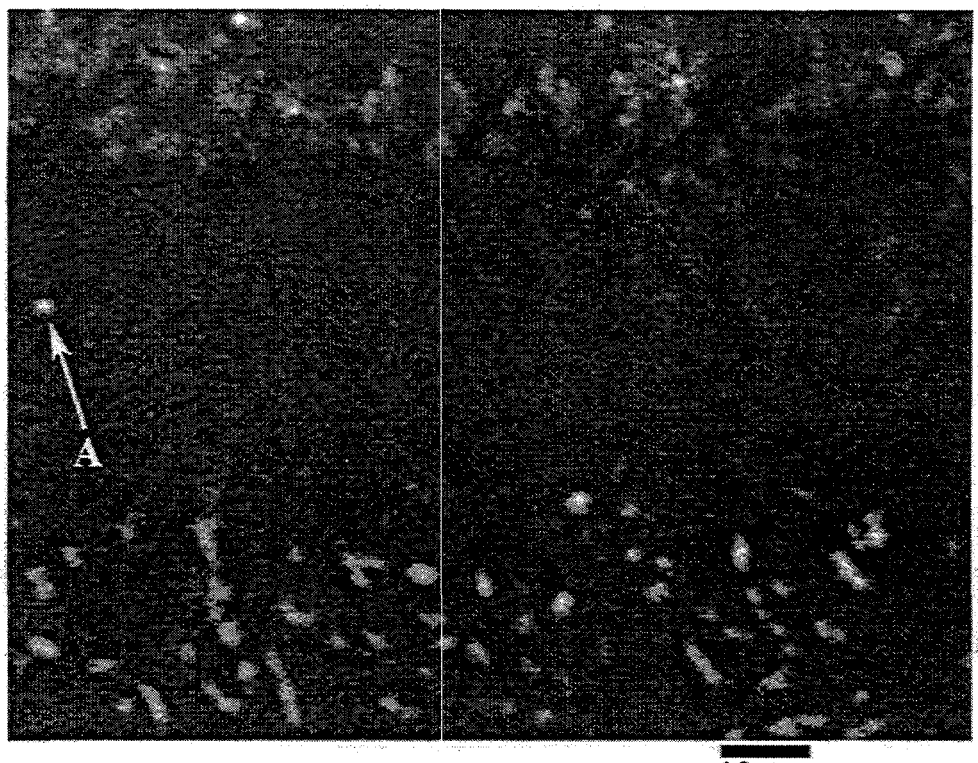

Fig. 74. Carbon elemental map of region shown in Fig. 73.

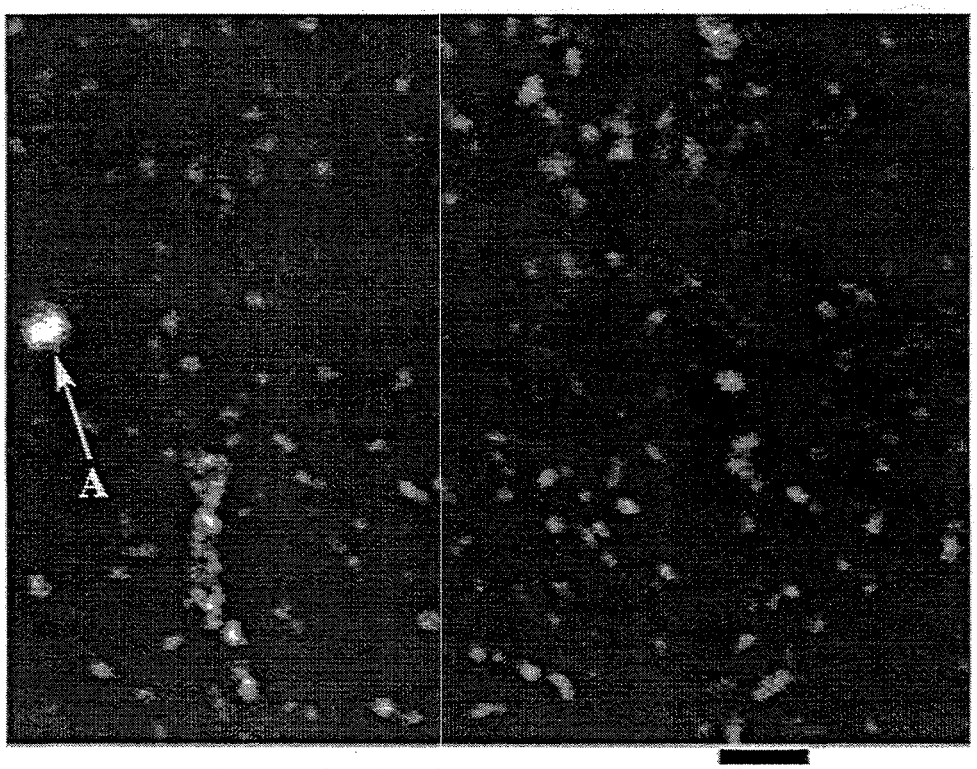

Fig. 75. Zirconium elemental map of region shown in Fig. 73.

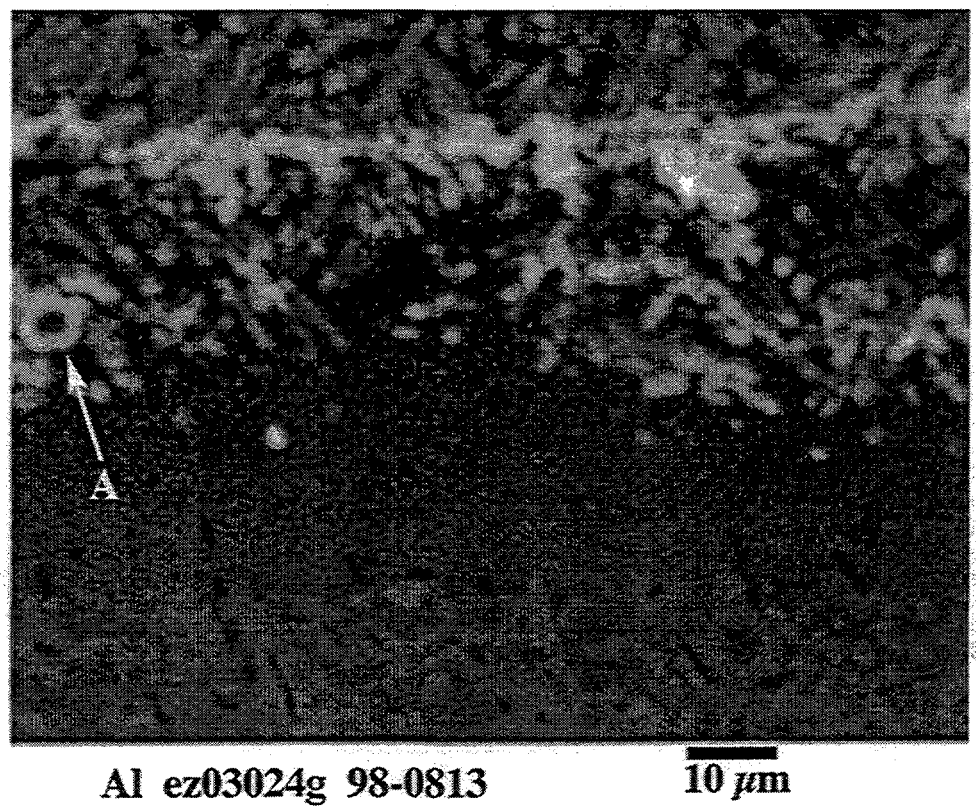

Fig. 76. Aluminum elemental map of region shown in Fig. 73.

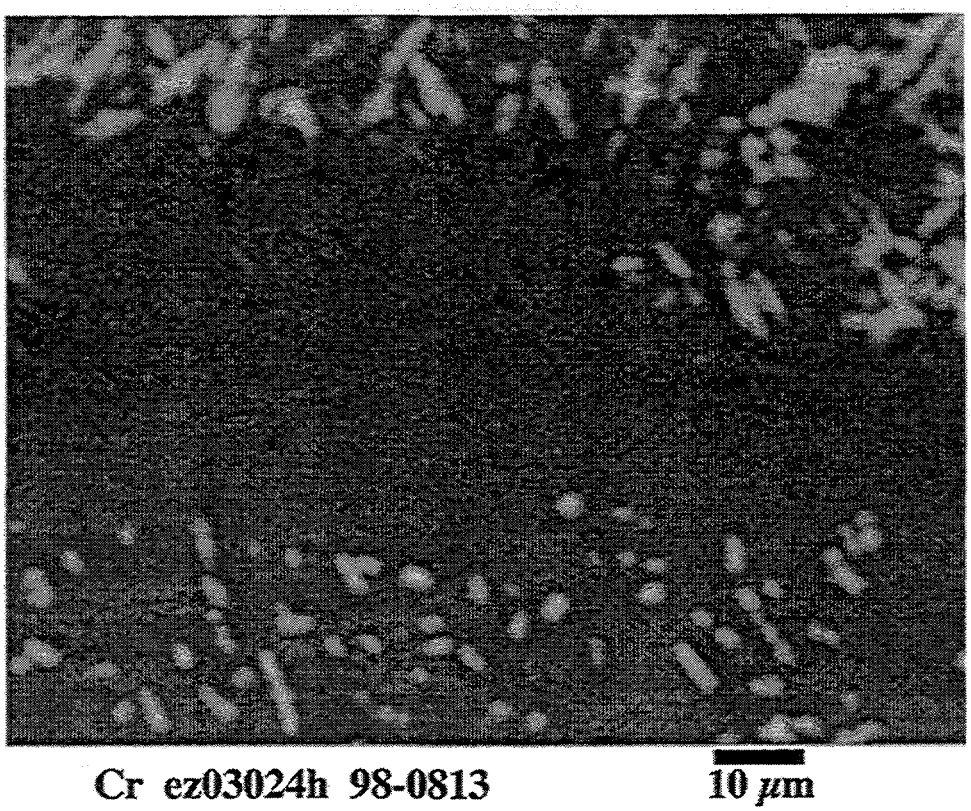

Fig. 77. Chromium elemental map of region shown in Fig.73.

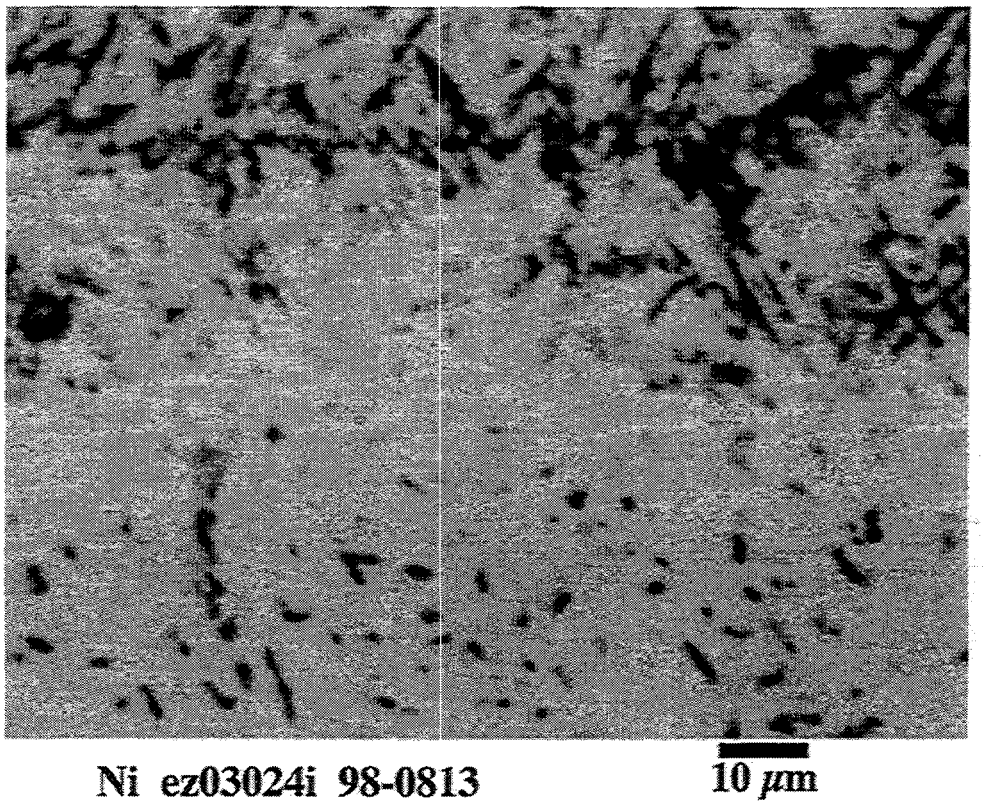

Fig. 78. Nickel elemental map of region shown in Fig. 73.

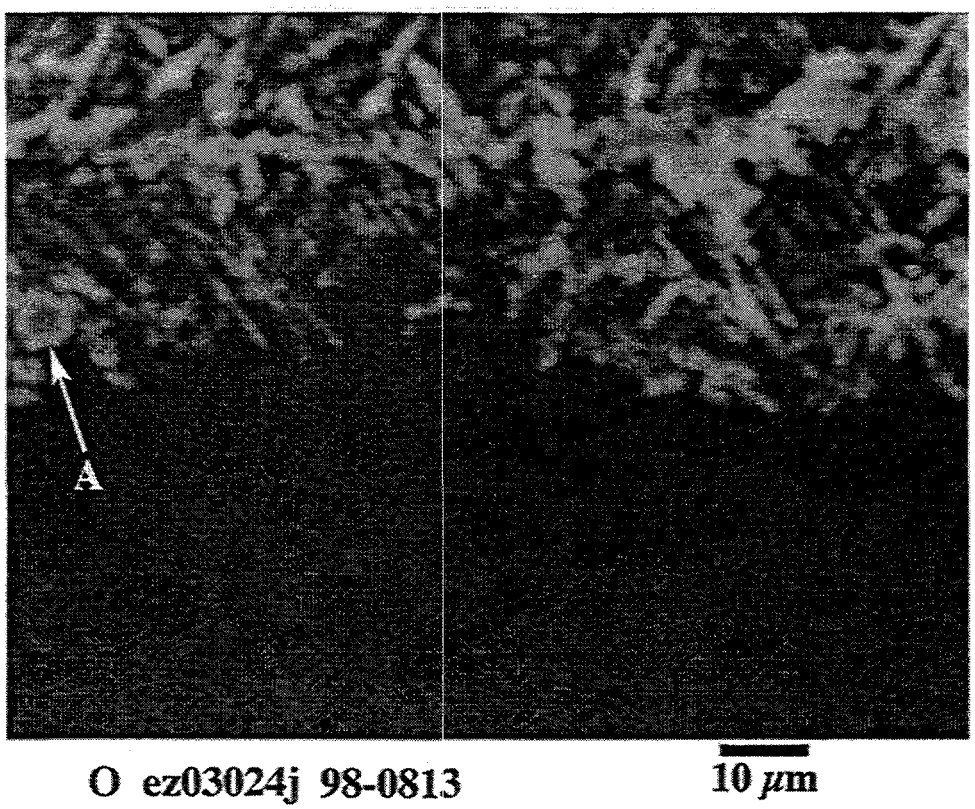

Fig. 79. Oxygen elemental map of region shown in Fig. 74.

In summary, Figs. 74 through 79 show the following interesting and important features for near-surface IC-221M: (1) both the feathery and penetrating features underneath the second layer are oxides. The feathery features are Cr_2O_3, and the penetrating features are Al_2O_3. The depleted region is free of aluminum and chromium but contains some zirconium-rich features which are neither matched with chromium or oxygen. The zirconium and chromium in the matrix are clearly associated with carbon. The chromium and aluminum features associated with oxygen are free of molybdenum as shown in Fig. 80.

The backscattered electron images of the specimen from the center of IC-221M after 14 months exposure are shown in Figs. 81 and 83. The elemental maps for carbon, zirconium, chromium, and nickel are shown in Figs. 84 through 87. Comparison of the elemental maps shows that all of the zirconium and chromium particles show perfect match with the carbon particles, indicating that the carbon diffused into the nickel aluminide is present as zirconium and chromium carbides.

A microprobe scan of elements nickel, aluminum, chromium, zirconium, and carbon is shown in Fig. 88. This figure shows that the peaks in carbon match with the peaks in chromium and valleys in nickel, which implies that the chromium-carbide-forming regions are lower in nickel than other regions with lower carbon content. The other trend in Fig. 88 is the variation of chromium and aluminum. The higher aluminum regions are consistently lower in chromium content and vice versa.

The detailed microprobe analysis of various elements from the exposed surface in towards the matrix are presented in Tables 15 and 16 for HU and IC-221M. The atomic percent values from these tables were used to arrive at an estimate of extra carbon present in the exposed HU and IC-221M trays and fixtures, respectively. The assumption in the analysis for HU is that all of the chromium reacts with carbon to form $Cr_{23}C_6$, all of the iron reacts with carbon to form Fe_3C, and all of the silicon reacts with carbon to form SiC. For IC-221M, the assumption is that all of the chromium reacts with carbon to form $Cr_{23}C_6$, all of the zirconium reacts with carbon to form zirconium-carbon, all of the silicon reacts with carbon to form SiC, and all of the iron reacts with carbon to form Fe_3C.

Based on the above assumptions, the carbon tied up for various elements and the excess carbon are tabulated in Table 17. Data in this table show that all HU locations have significantly more excess carbon than in the IC-221M locations. It is this significantly lower excess carbon in IC-221M may be the reason for its higher resistance to embrittlement and cracking as compared to HU.

Conclusions

A HU tray after 18 months exposure in a batch carburizing furnace and a IC-221M fixture after 14 months exposure in a pusher furnace at Delphi Saginaw were analyzed. The analysis focused on physical appearance, microhardness traverses, optical microstructure, and detailed microprobe analysis. The following are the observations and conclusions from this study.

1. The HU tray after 18 months exposure had broken. The visual observation showed its surface to be extremely dark. The broken pieces showed that the carbon had diffused all the way to the center of the section.

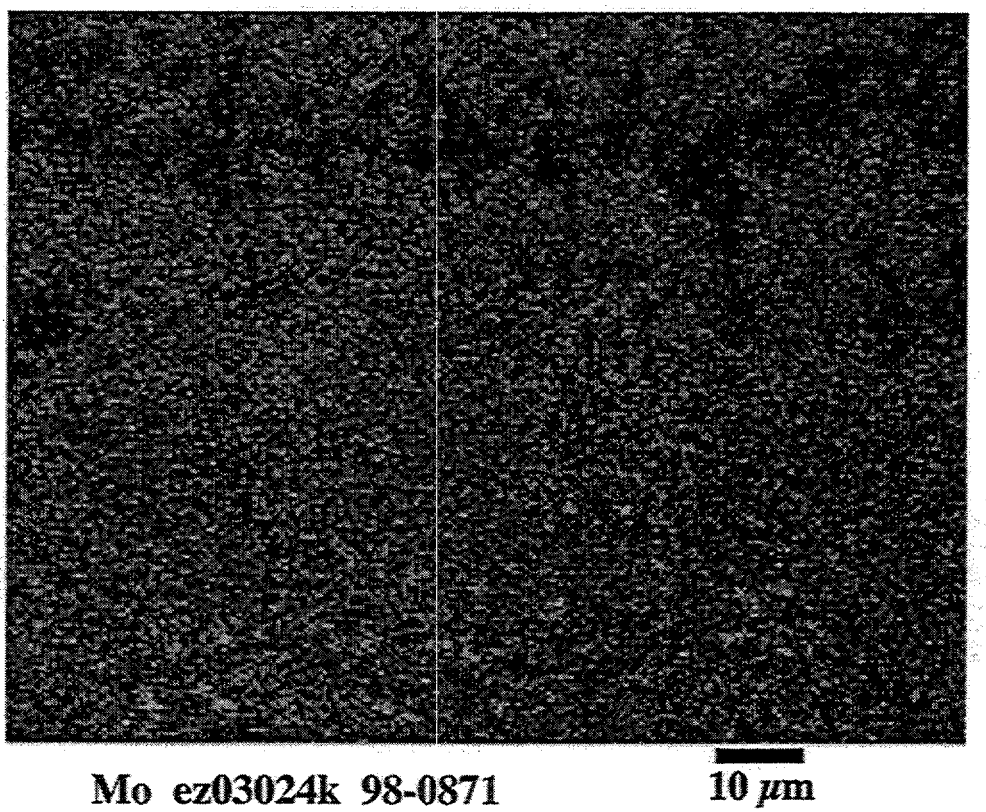

Fig. 80. Molybdenum elemental map of region shown in Fig. 73.

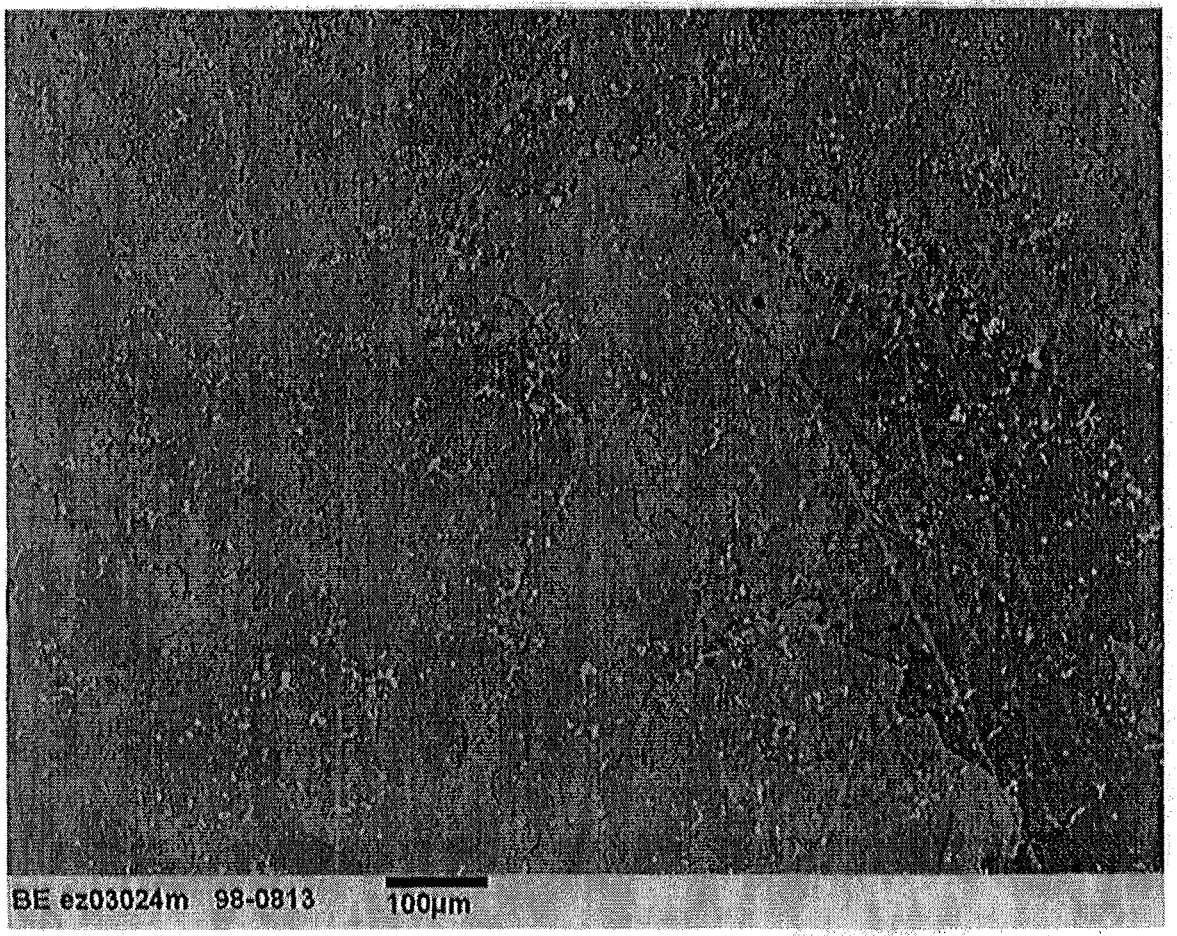

Fig. 81. Backscattered electron image of the matrix section of the IC-221M fixture removed from pusher carburizing furnace at Delphi Saginaw after 14 months of service. Low magnification.

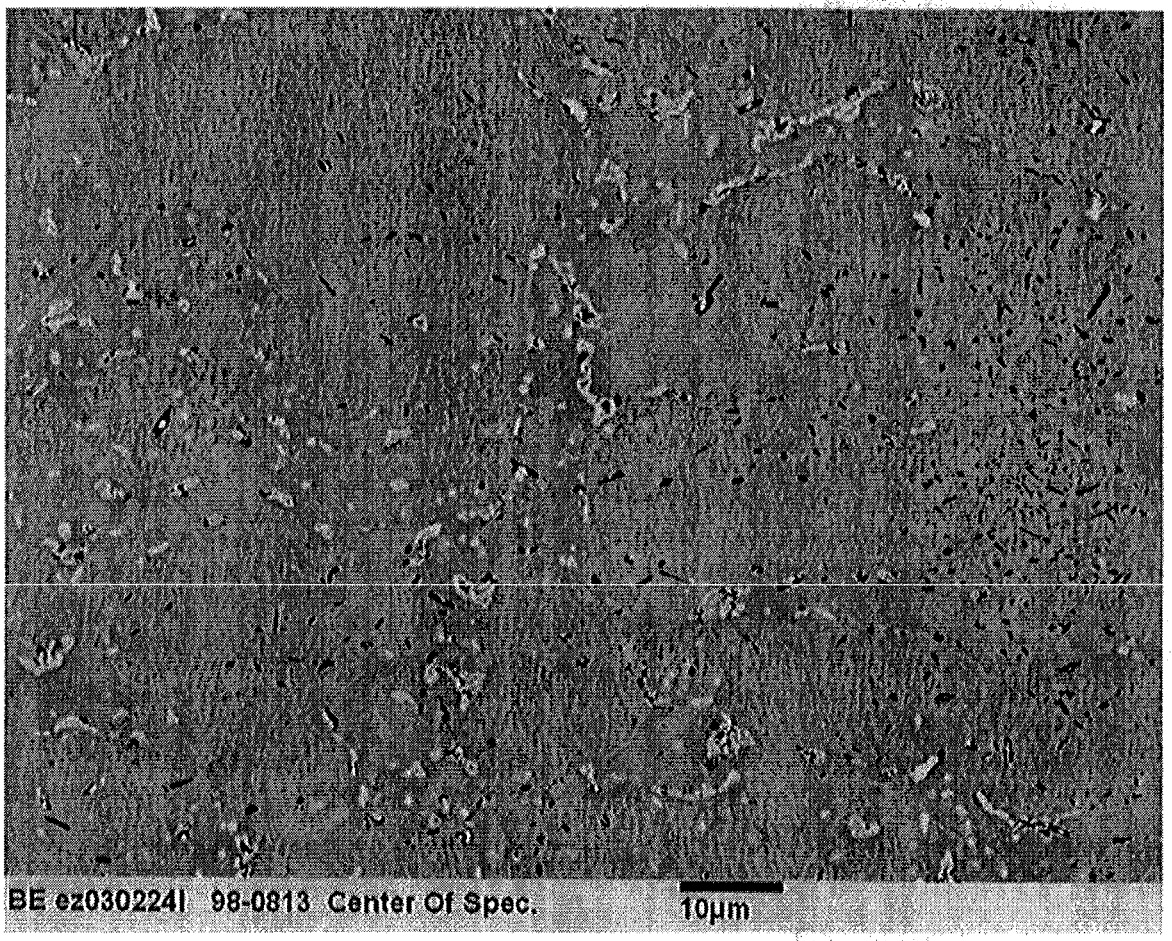

Fig. 82. Backscattered electron image of the matrix section of the IC-221M fixture removed from pusher carburizing furnace at Delphi Saginaw after 14 months of service. High magnification.

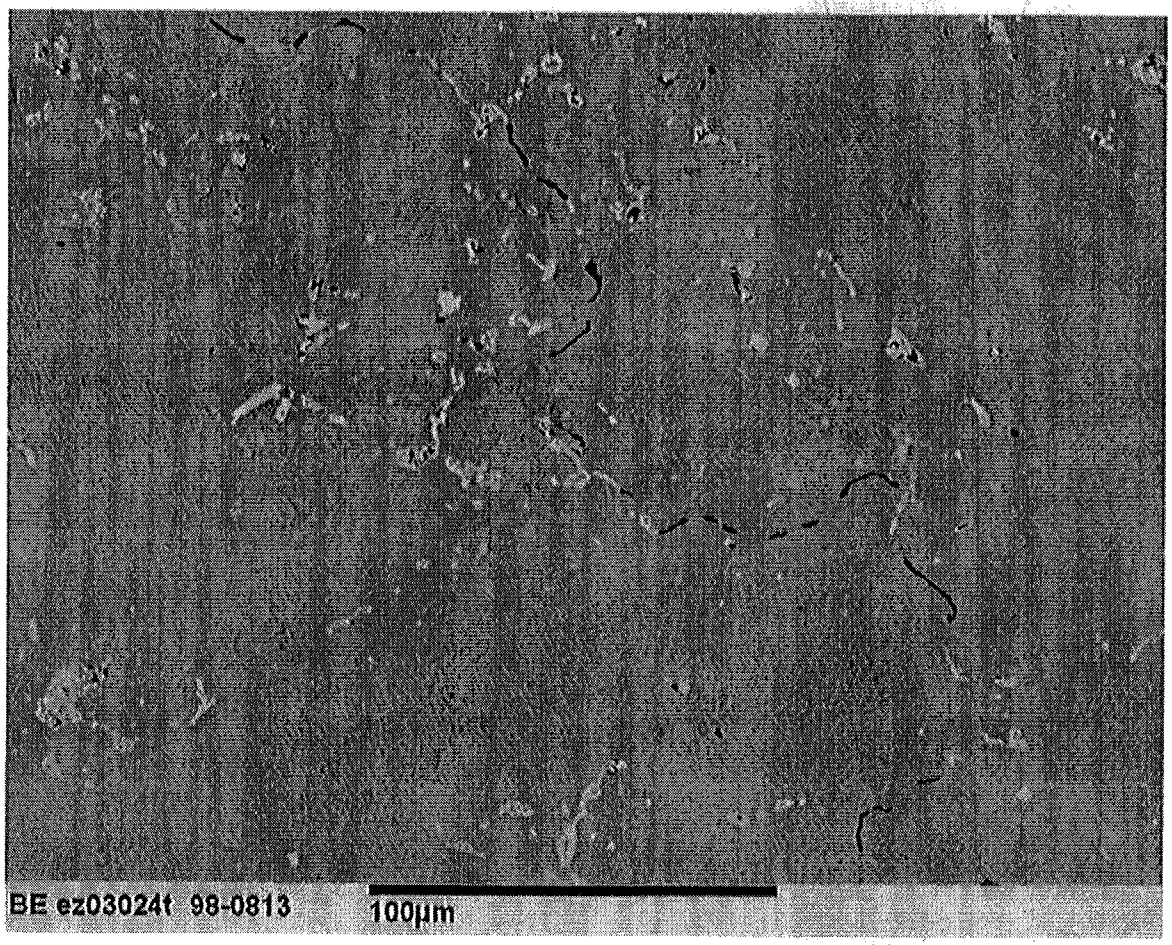

Fig. 83. Backscattered electron image of the matrix section of the IC-221M fixture removed from pusher carburizing furnace at Delphi Saginaw after 14 months of service. Highest magnification.

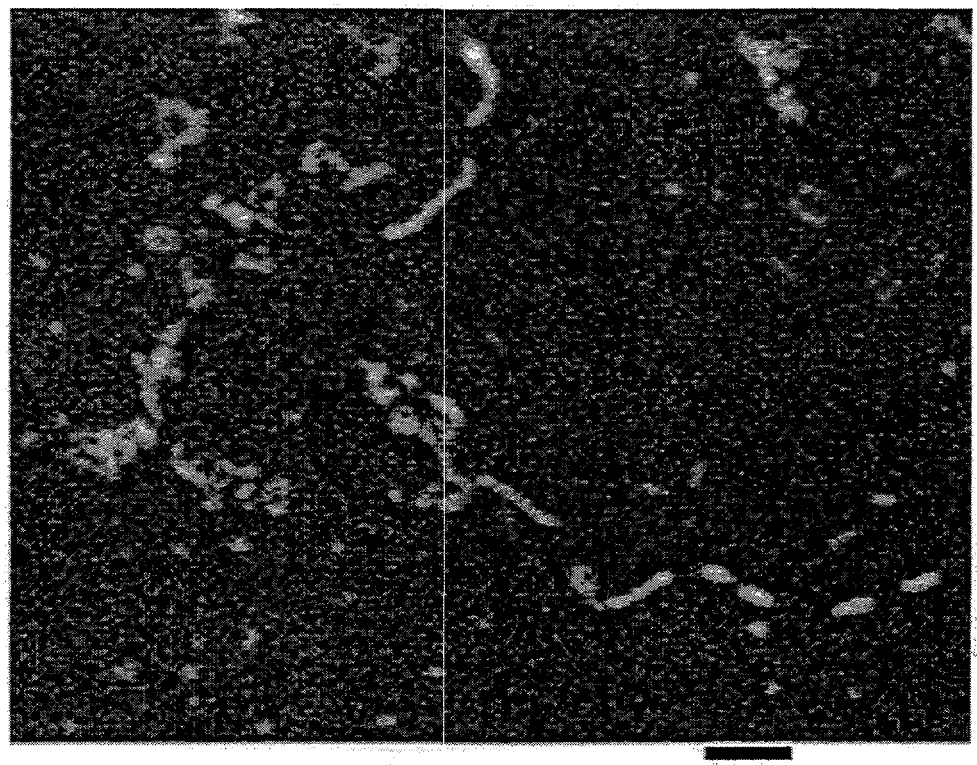

Fig. 84. Carbon elemental map of backscattered electron image of the matrix section in Fig. 83.

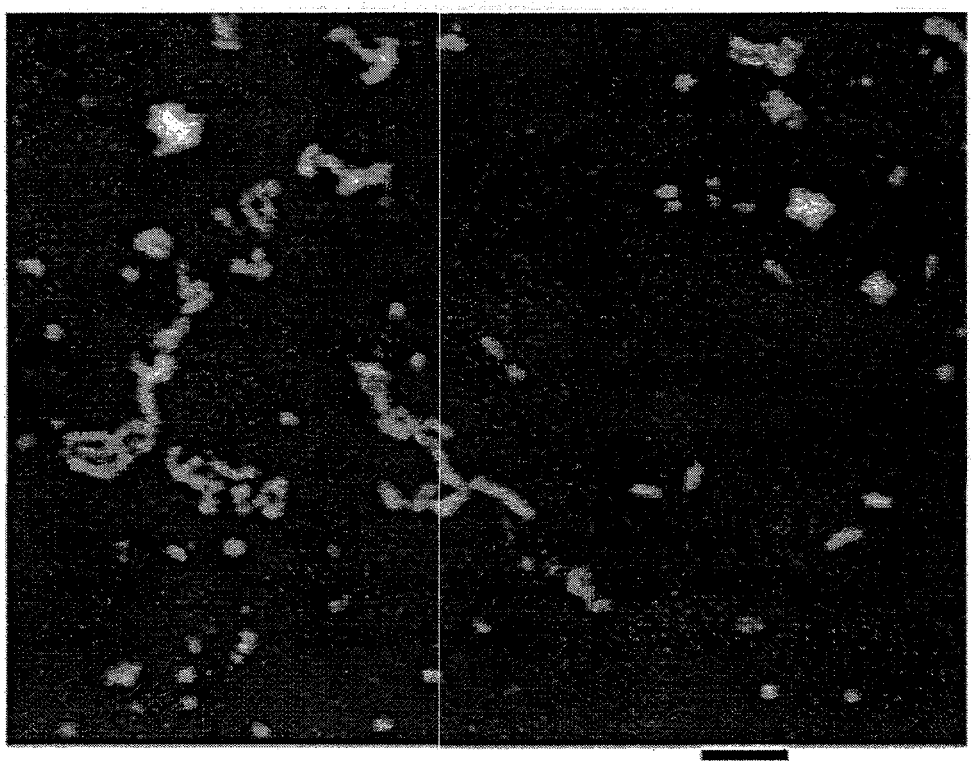

Fig. 85. Zirconium elemental map of backscattered electron image of the matrix section in Fig. 83.

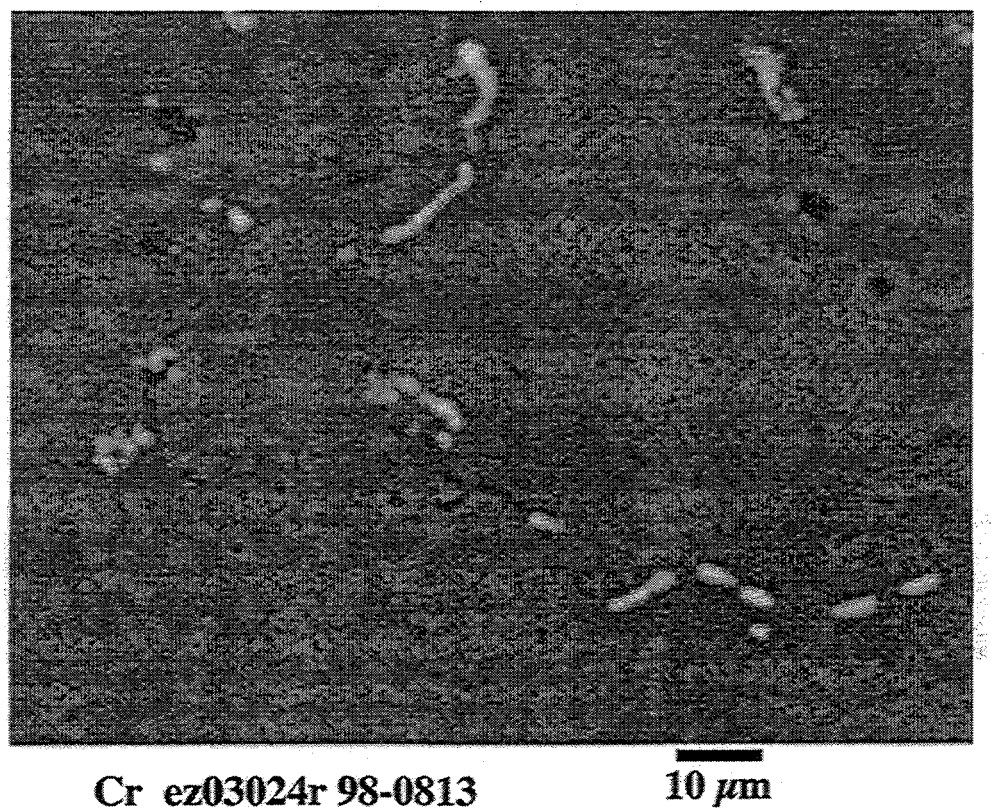

Fig. 86. Chromium elemental map of backscattered electron image of the matrix section in Fig. 83.

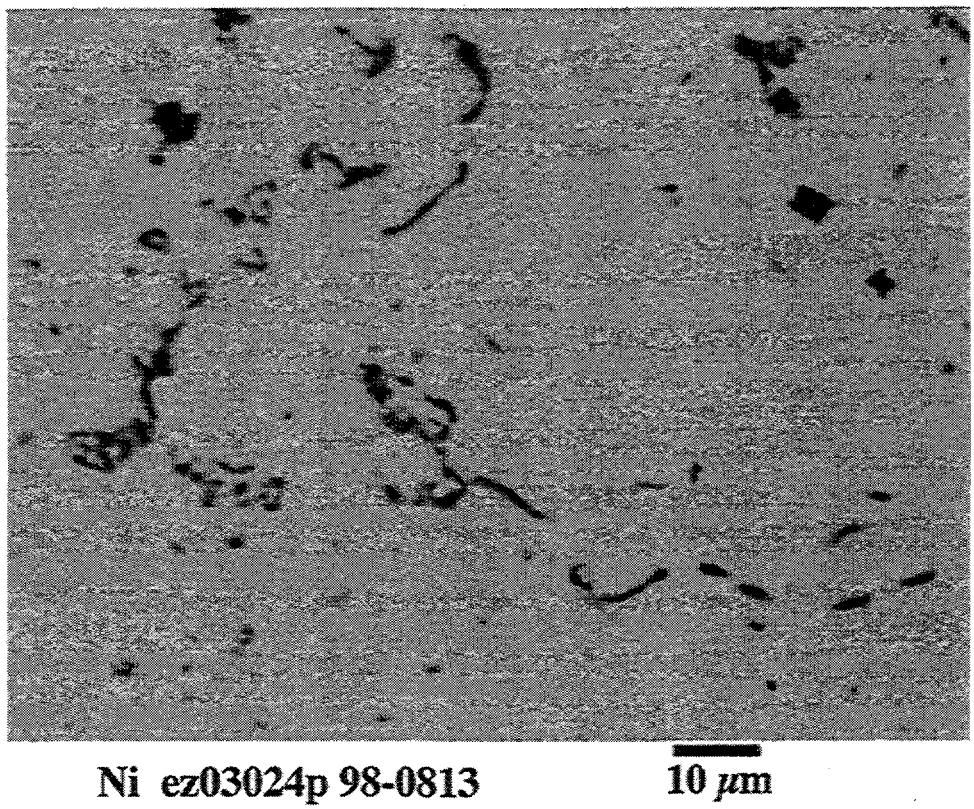

Fig. 87. Nickel elemental map of backscattered electron image of the matrix section in Fig. 83.

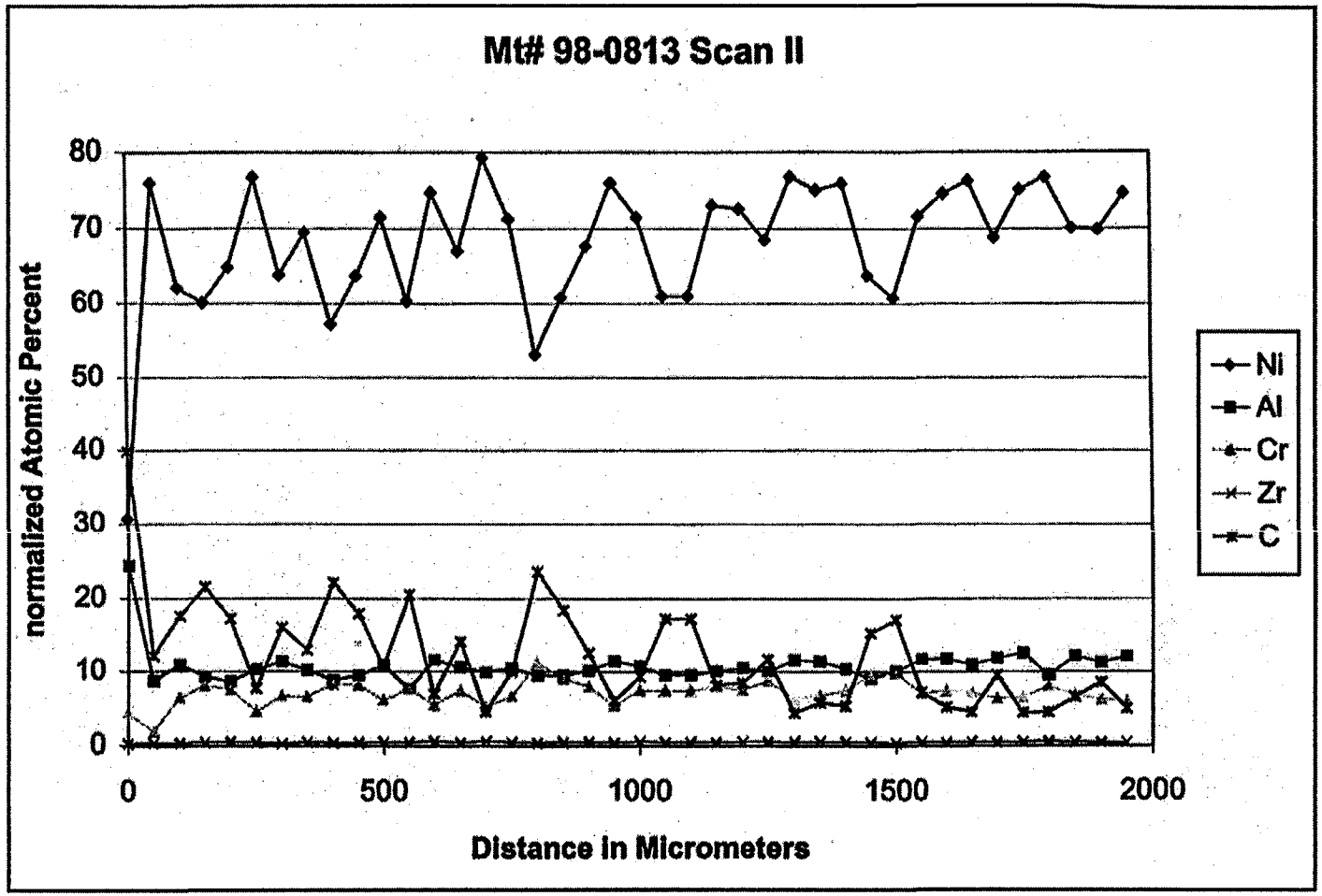

Fig. 88. Microprobe scan of carbon, aluminum, zirconium, chromium, and nickel from the surface to the matrix for the IC-221M fixture removed from the pusher carburizing furnace at Delphi Saginaw after 14 months of service.

Table 15. Elemental microprobe analysis as a function of distance for HU tray after 18 months exposure in a batch carburizing furnace at Delphi Saginaw

Distance in micrometers	Element (at. % normalized)							Total
	Mn	Ni	Cr	Fe	Si	C	Mo	
0	0.20	8.47	6.11	8.50	1.30	75.40	0.02	100
50	0.07	6.38	12.98	6.34	0.83	73.40	0.00	100
100	0.85	21.26	7.20	19.85	1.41	49.38	0.04	100
150	1.18	4.95	16.00	5.13	2.70	70.04	0.00	100
200	0.28	4.31	3.70	4.31	0.43	86.96	0.01	100
250	0.41	12.38	19.31	12.15	2.14	53.59	0.03	100
300	0.95	9.11	24.35	8.99	2.04	54.55	0.01	100
350	0.16	30.17	9.35	28.80	1.28	30.20	0.04	100
400	0.50	35.92	10.47	29.43	2.29	21.34	0.04	100
450	0.58	18.45	20.61	21.92	1.22	37.16	0.07	100
500	0.74	41.52	7.90	31.03	3.21	15.57	0.03	100
550	0.65	30.68	12.10	26.10	2.33	28.10	0.04	100
600	0.95	19.60	17.73	21.63	4.50	35.55	0.04	100
650	0.64	25.79	15.38	24.61	1.86	31.69	0.04	100
700	0.66	31.29	13.70	26.03	2.20	28.20	0.04	100
750	0.66	31.29	11.45	26.27	2.35	27.94	0.04	100
800	0.63	26.50	14.34	25.10	1.93	31.46	0.04	100
850	0.58	7.19	31.14	17.57	0.71	42.78	0.03	100
900	0.70	33.12	10.85	28.12	2.55	24.63	0.04	100
950	0.57	13.76	25.51	20.14	0.90	39.09	0.03	100
1000	0.70	31.15	12.13	27.38	2.46	26.15	0.04	100
1050	0.59	17.53	21.61	21.86	1.16	37.22	0.03	100
1150	0.72	32.90	12.40	29.01	2.55	22.38	0.04	100
1200	0.79	41.02	6.83	33.03	3.25	15.05	0.05	100
1250	0.66	27.93	14.93	26.18	1.99	28.28	0.04	100
1300	0.72	34.35	12.01	29.97	2.71	20.20	0.04	100
1350	0.66	27.79	14.55	25.88	2.05	29.04	0.04	100
1400	0.63	26.83	16.82	25.30	2.04	28.34	0.04	100
1450	0.72	31.57	13.16	28.89	2.41	23.20	0.04	100
1500	0.71	32.41	12.02	29.26	2.41	23.14	0.04	100
1550	0.61	24.51	17.39	24.53	1.74	31.19	0.04	100
1600	0.73	34.31	11.53	30.50	2.51	20.39	0.04	100
1650	0.64	25.43	18.43	24.51	1.83	29.13	0.04	100
1700	0.70	32.69	11.74	30.07	2.33	22.42	0.04	100
1750	0.61	24.07	16.02	23.72	1.69	33.85	0.03	100
1800	0.56	20.42	22.07	21.56	1.43	33.93	0.03	100
1850	0.64	24.70	20.02	24.85	1.87	27.89	0.04	100
1900	0.72	32.10	12.64	29.43	2.26	22.80	0.04	100
1950	0.78	35.22	13.32	28.84	4.52	17.28	0.04	100
2000	0.61	24.86	18.25	24.22	1.81	30.20	0.04	100
2050	0.61	22.75	20.38	23.07	1.59	31.56	0.04	100
2100	0.67	26.79	16.43	26.43	1.84	27.80	0.04	100
2150	0.71	31.79	13.85	29.13	3.16	21.31	0.04	100
2500	0.55	19.56	24.05	20.39	1.40	34.02	0.03	100
2700	0.74	30.74	15.40	29.48	2.24	21.36	0.04	100

Table 16. Elemental microprobe analysis as a function of distance for IC-221M fixture after 14 months exposure in a pusyer carburizing furnace at Delphi Saginaw

Distance in micrometers	Element (at. % normalized)							Total
	Ni	Al	Cr	Zr	Si	Fe	C	
0	30.65	24.41	4.22	0.24	0.36	0.29	39.83	100
50	75.68	8.70	1.87	0.36	0.82	0.07	12.19	100
100	62.07	10.99	6.37	0.39	2.27	0.27	17.64	100
150	60.09	9.25	8.07	0.42	0.43	0.20	21.54	100
200	64.85	8.62	7.53	0.52	1.04	0.21	17.24	100
250	76.73	10.28	4.54	0.40	0.08	0.27	7.70	100
300	63.85	11.35	6.58	0.32	1.62	0.21	16.07	100
350	69.48	10.21	6.50	0.48	0.09	0.26	12.97	100
400	57.26	8.86	8.30	0.38	2.87	0.17	22.16	100
450	63.70	9.48	8.14	0.36	0.13	0.24	17.95	100
500	71.50	10.94	6.10	0.46	0.10	0.22	10.69	100
550	60.30	7.63	7.62	0.48	3.32	0.13	20.52	100
600	74.73	11.60	5.42	0.60	0.41	0.26	6.98	100
650	67.01	10.64	7.39	0.45	0.15	0.21	14.15	100
700	79.32	9.98	5.21	0.60	0.07	0.27	4.54	100
750	71.28	10.55	6.61	0.52	0.74	0.24	10.06	100
800	53.16	9.52	11.24	0.37	1.96	0.14	23.62	100
850	60.76	9.50	9.05	0.46	1.58	0.20	18.45	100
900	67.71	10.19	7.99	0.49	0.81	0.18	12.63	100
950	75.99	11.50	5.43	0.40	0.40	0.24	6.05	100
1000	71.51	10.79	7.43	0.57	0.11	0.22	9.36	100
1050	60.94	9.58	7.40	0.46	4.16	0.21	17.25	100
1100	60.94	9.58	7.40	0.46	4.16	0.21	17.25	100
1150	73.07	10.09	7.91	0.40	0.17	0.20	8.16	100
1200	72.59	10.53	7.50	0.52	0.16	0.19	8.50	100
1250	68.50	10.09	8.76	0.53	0.20	0.19	11.73	100
1300	76.78	11.65	6.29	0.46	0.28	0.23	4.32	100
1350	75.09	11.44	6.72	0.49	0.23	0.25	5.77	100
1400	75.91	10.42	7.40	0.49	0.30	0.17	5.30	100
1450	63.76	9.00	9.65	0.45	1.64	0.19	15.32	100
1500	60.75	10.14	9.83	0.35	1.64	0.20	17.09	100
1550	71.70	11.74	7.02	0.50	1.56	0.29	7.19	100
1600	74.64	11.81	7.45	0.42	0.29	0.26	5.14	100
1650	76.29	10.97	7.09	0.51	0.42	0.24	4.48	100
1700	68.86	11.90	6.36	0.44	2.61	0.24	9.57	100
1750	75.20	12.59	6.48	0.51	0.59	0.27	4.37	100
1800	76.77	9.60	7.98	0.56	0.37	0.27	4.45	100
1850	70.12	12.18	6.88	0.45	3.62	0.23	6.52	100
1900	69.90	11.30	6.16	0.39	3.42	0.26	8.56	100
1950	74.60	12.11	6.01	0.39	1.67	0.27	4.96	100

Table 17. Qualitative estimation of free carbon for HU and IC-221M after exposure in carburizing furnace by assuming that all carbide-forming elements combine with carbon to form stable carbides and excess being left as free carbon

Distance from edge	Amount of carbon tied up as carbides										
	HU					IC-221M					
	$Cr_{23}C_6$	Fe_3C	SiC	Amount measured	Net-free carbon (at. %)	$Cr_{23}C_6$	ZrC	SiC	Fe_3C	Amount measured	Net-free carbon (at. %)
0	1.59	2.83	1.30	75.4	69.68	1.10	0.24	0.36	0.10	39.83	38.03
100	--	--	--	--	--	1.66	0.39	2.27	0.09	17.64	13.23
200	0.97	1.44	0.43	86.96	84.12	1.96	0.52	1.04	0.07	17.24	13.65
300	6.35	3.00	2.04	54.55	11.39	--	--	--	--	--	--
500	2.06	10.34	3.21	15.57	--	1.59	0.46	0.10	0.07	10.69	8.47
1000	--	--	--	--	--	1.94	0.57	0.11	0.07	9.36	6.67
1500	--	--	--	--	--	2.56	0.35	1.64	0.07	17.09	12.47
1950	--	--	--	--	--	1.57	0.39	1.67	0.09	4.96	1.24
2000	4.36	8.07	1.81	30.20	15.56	--	--	--	--	--	--
2700	4.02	5.13	2.24	21.36	10.00	--	--	--	--	--	--

2. The IC-221M fixture taken from the pusher furnace was covered with black dust. The dust was found to be fairly loose and could be removed by a simple sand-blasting operation. This generated the original gray looking surface.

3. Bulk chemical analysis revealed that the carbon content of the HU tray had increased from 0.55 to 1.00 wt % during the 18 months exposure in the batch furnace. In contrast, the carbon content of IC-221M had increased from 0.02 to 0.17 wt % during the 14 months exposure in the pusher furnace. A small decrease in the aluminum content was also observed in IC-221M. None of the other elements showed any significant change.

4. The microprobe traverses of carbon in the exposed HU and IC-221M revealed that both exhibited carbon enrichment on the surface. However, there were differences. The amount of carbon at the surface for IC-221M was 60% lower and peak value near the surface was approximately 30% lower than HU. The depth of carbon penetration with high values was half for IC-221M compared to HU.

5. The microhardness traverses were carried out for exposed specimens of both the HU and IC-221M. The comparative data showed the increased hardness value for the high carbon regions in both alloys. However, past the enriched carbon surface, the microhardness values for IC-221M either remained unchanged or slightly decreased as compared to the initial hardness. The microhardness values of the HU material showed significant increase at the surface throughout the tray section as compared to the initial hardness. The differences in the changes of bulk hardness of HU and IC-221M suggest that a surface crack in HU is more likely to propagate because of its high bulk hardness as opposed to IC-221M, where bulk hardness either remains the same or decreases as compared to the initial hardness.

6. Optical metallography revealed carbon reaction at the surface and multiple cracks initiated at the surface and penetrating through the bulk material underneath the reacted layer in the exposed HU tray. The cracks also facilitate easier path for carbon and air penetration into the bulk. The IC-221M showed the surface-reacted layer with very limited crack initiated at the surface. There was some preferential attack of grooving action for IC-221M. The grooving action appears to occur at the grain boundaries.

7. The visible surface corrosion layer was essentially the same (approximately 200 μm) for both HU and IC-221M. The IC-221M had a distinct depleted layer of 40 μm. Cracks in HU propagated to a depth of 1800 μm or 71 mils. A crack in IC-221M had a length of 820 μm or 32 mils.

8. The backscattered electron images revealed the presence of many transverse cracks in the corrosion layer of the HU layer. These transverse cracks are in addition to the penetrating long cracks observed in the optical metallography. The transverse cracks are primarily present in the fully reacted regions, which are chromium oxide as seen during elemental mapping. The corrosion layer for the IC-221M is layered (parallel to base metal) as opposed to penetrating (normal to the base metal) in HU.

9. The highly cracked regions in the corrosion layer of HU were associated with chromium and oxygen. It is interesting to note that the overall carbon content of the near-surface layer is high but the cracked regions are oxides. All of the chromium beneath the corroded surface layer is associated with carbon (assumed to be $Cr_{23}C_6$).

10. The corrosion layers on the surface of IC-221M were a combination of chromium and aluminum oxides. The feathery structure was chromium oxide (most likely Cr_2O_3) and the penetrating structure was aluminum oxide (most likely Al_2O_3). A distinct depleted layer was observed in the matrix underneath the corrosion layer. The depleted layer was found to be low in aluminum and chromium but contained zirconium. All of the chromium in the matrix of IC-221M was found to be associated with carbon.

11. Comparison of detailed microstructures of HU and IC-221M revealed that the corrosion layers are oxide in both cases and that the matrices are carbides. The oxide in HU is Cr_2O_3, whereas in IC-221M, it is Cr_2O_3 and Al_2O_3. The carbides in HU are primarily chromium as compared to chromium and zirconium in IC-221M.

12. The qualitative analysis of the carbides in HU and IC-221M, based on the microprobe analysis, indicate that HU has significantly more unreacted carbon than IC-221M. It is this low unreacted carbon along with the high yield strength of IC-221M that resist the crack propagation into the matrix.

Recommendations for Future Work

1. A detailed surface and matrix analyses of new HU and IC-221M trays and fixtures are needed to arrive at a better understanding of the sequence of events that happen during carburizing.

2. Comparable trays and fixtures of the HU and IC-221M from the same furnace should be examined rather than one from the batch and the other from the pusher as was investigated in the present report.

Acknowledgments

The authors gratefully acknowledge the contributions of the following individuals:

ORNL: Peter Angelini and Phil Sklad for their active participation during the casting trials, planning sessions, and visits to Delphi Saginaw for review meetings and examination of the operating trays and fixtures.

Joe Vought for melting trial melts and the development of the Exo-Melt™ process.

Randy Howell for compiling data on the test specimens.

Jeff McNabb for weld repair and welding of the tray assemblies.

Millie Atchley for typing the report.

Delphi Saginaw: Steve Avery, Jerry Jablonski, Randy Bal, and James Farago for their participation in the casting trials and assistance in the testing of the coupons and components.

Alloy Engineering & Casting Company: Jim Lytle and David Robinson for their company's significant cost share and for their willingness to accommodate the casting trials in their busy schedules, and Peter Swenson for his assistance in identifying tray and fixture drawings and for following up on their operating experience.

Report of Inventions

No inventions resulted from this CRADA.

Commercialization Possibilities

A significant commercialization possibility has resulted from the coupon and heat-treating fixture testing at Delphi Saginaw. The commercialization possibilities occurred through: (1) trial use of heat-treating fixtures by several other commercial heat treaters, and (2) two commercial casting sources were developed to a point of taking license to manufacture heat-treating fixtures. For the Delphi Saginaw CRADA, ORNL was actively involved in the casting trials. However, the commercialization has now reached a point to where the users are directly able to purchase the heat-treating fixtures from the commercial casting foundries.

Plans for Future Collaboration

Informal collaborations with Delphi Saginaw will continue to determine the life expectancy for nickel aluminide trays and fixtures as compared to the currently used HU fixtures. No additional CRADA is expected in the near future.

Conclusions

This CRADA dealt with the development of the nickel aluminide alloy for improved longer life heat-resistant assemblies for both batch and continuous pusher carburizing furnaces. The nickel aluminide development was compared with the currently used Fe-Ni-Cr heat-resisting alloy known as HU. The specific goals of the CRADA were: (1) casting process development, (2) characterization and possible modification of the alloy composition to optimize its manufacturing ability and performance under typical furnace operating conditions, and (3) testing and evaluation of specimens and prototype parts.

In support of the CRADA objectives, coupons of nickel aluminide and the HU alloy were installed in both the batch and pusher furnaces. Following the successful testing of the coupons, the trays and fixtures of nickel aluminide were installed in the batch and pusher furnaces at Delphi Saginaw. The following conclusions are drawn from the completion of this CRADA:

1. The Ni_3Al-based alloy IC-221M can be melted using the Exo-Melt ™ process along with the normal foundry practice. The molten metal from the Exo-Melt™ process can be sand cast into trays, fixtures, and posts using practices similar to those used for HU. The solidification modeling has helped guide the foundry with more details of actual mold pouring for Ni_3Al-based alloy.

2. The weld repair capability of trays and fixtures was demonstrated. The IC-221LA wire appears acceptable for all situations.

3. The coupon testing has been conducted in both batch and pusher furnaces. The longest exposure time reached has been 336 days for IC-221M in a batch furnace.

4. The IC-221M showed a surface corrosion layer. However, the penetration was limited to shallower depth distances, as compared to the HU coupons which showed deep penetrations after short exposure times. The preoxidized coupon appears to show even less carburization penetration than the as-cast coupon.

5. The testing of the HU and IC-221M trays in the batch furnace at Delphi Saginaw has confirmed the results from the coupon study in that the HU trays have cracked and the Ni_3Al-based alloy tray is relatively unaffected.

6. Initial installation of one batch furnace tray at Delphi Saginaw was extended to two pusher furnace fixtures during January 1996.

7. A commercial production run of 63 pusher furnace fixture assemblies was completed. This production run used a total of 94 heats, 26 of which were from virgin stock and 68 were made up of 50% virgin and 50% revert stocks.

8. The 63 pusher furnace fixtures from the production run have been operating at Delphi Saginaw since March 1997 and is still operating without any noticeable change.

9. Six batch furnace trays of nickel aluminide, bolted to HU trays, have been operating at Delphi Saginaw in the six-batch furnace since March 1997.

10. The results of this CRADA have shown that the nickel aluminide alloy, IC-221M, can be cast into trays and fixtures under production conditions. Furthermore, these trays and fixtures are continuing to operate, and there is no indication of failure mode.

APPENDIX

Delphi Steering Divisional Materials Laboratory
Materials Engineering Report No. D-1359

MATERIALS ENGINEERING REPORT

DELPHI
Saginaw Steering Systems

REPORT ANALYSIS TO: M. CHATTERJEE LAB. NO. D1359

ENGINEERING ORDER: _____ DATE 4/9/98

PART NAME & NO. Ni_3Al Experimental tray MATERIAL SPEC. _____

SUBJECT Evaluate surface scale & condition of casting just below the surface.

CHEMISTRY

SAMPLE	C	Mn	P	S	Si	Ni	Cr	Mo	V	Cu	Al	Pb

SEE ATTACHED ANALYSIS.

MICROSTRUCTURE

HARDNESS

SAMPLE	SURFACE	CORE	CASE DEPTH

GRAIN SIZE:	MACRO-ETCH	MAGNAGLOW:

CONCLUSIONS:

SIGNED:

DELPHI
Automotive Systems

REPORT NO. D-1359

DELPHI STEERING DIVISIONAL MATERIALS LABORATORY

Lead Technician / Author: Kalkman/Pitz **Date Completed:** June 19, 1998

PURPOSE:

Evaluate surface scale and condition of casting just below the surface.

TEST RESULTS:

SAMPLE DESCRIPTION

Sample is a section of an alloy furnace tray.

CHEMISTRY

As-Tested: **STANDARDLESS SEM/EDX** Analysis

Ni	79.322 wt.%
Al	7.943 wt.%
Cr	9.001 wt.%
P	1.373 wt.%
S	1.816 wt.%
Fe	0.546 wt.%

DISCUSSION:

The surface of the piece of tray is black, and appears to be heavily oxidized. A section of the tray was mounted and polished to examine the surface further. There is varying amounts of oxidation on all surfaces to a depth of 0.38 mm. SEM/EDX analysis of the tray material confirms it is a nickel base alloy containing aluminum, chromium and iron. The oxidation may be due to inadequate or nonexistent coating on the surface of the tray.

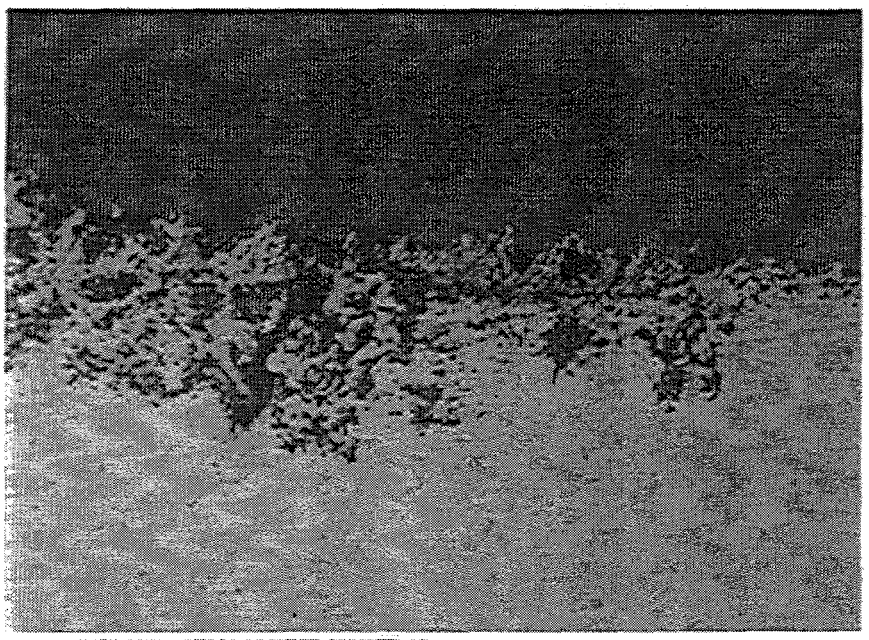

DELPHI AUTOMOTIVE SYSTEMS

Fig. A1. Photograph of a section of a furnace tray showing oxidation on the surface.

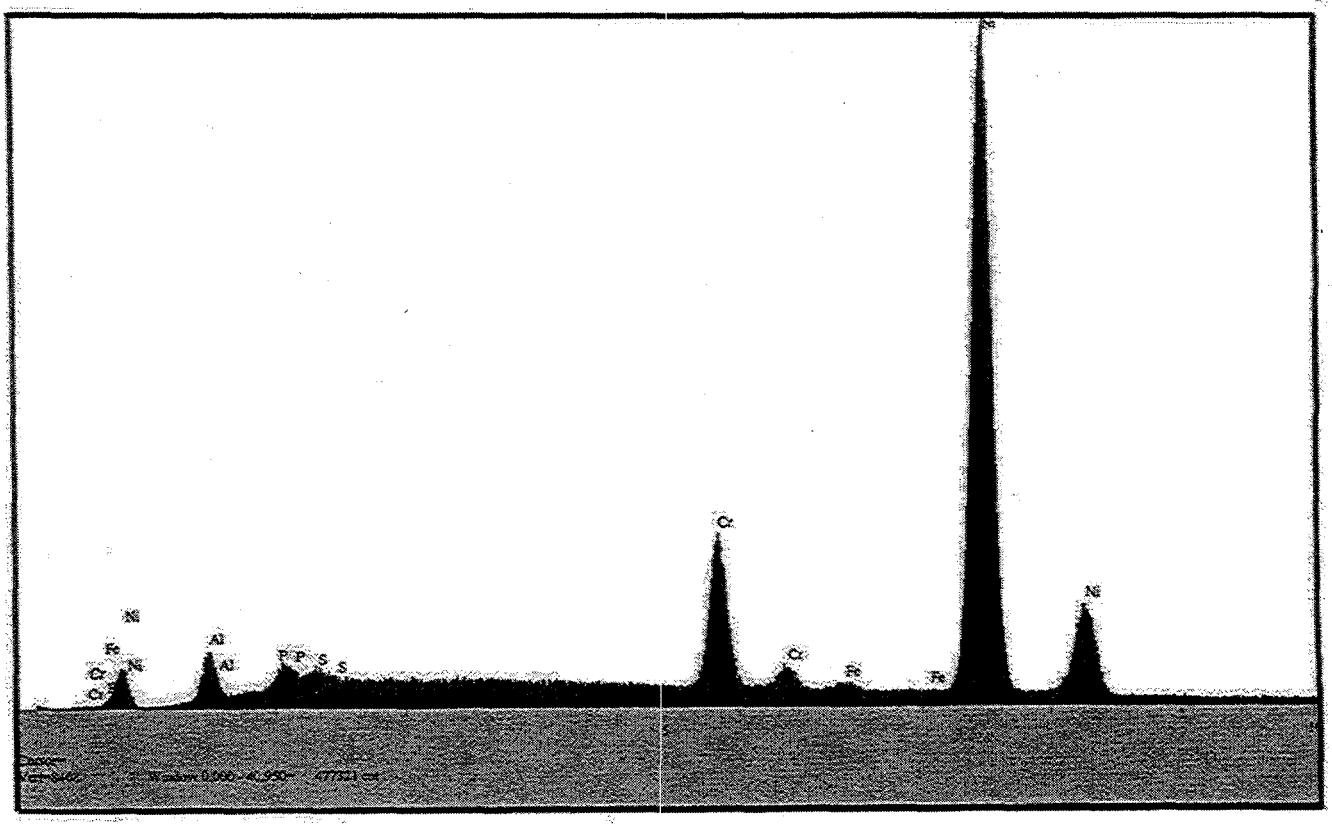

Fig. A2. Spectrum: D1359 Ni_3Al furnace tray.

D1359 Ni_3Al furnace tray report
June 19, 1998

Component	Type	Conc.
Al	Calc	7.943 wt %
P	Calc	1.373 wt %
S	Calc	1.816 wt %
Cr	Calc	9.001 wt %
Fe	Calc	0.546 wt %
Ni	Calc	79.322 wt %

STANDARDLESS
SEM/EDX Analysis

INTERNAL DISTRIBUTION

1. D. J. Alexander
2. P. Angelini
3. P. J. Blau
4. E. E. Bloom
5. C. A. Blue
6. R. A. Bradley
7. D. F. Craig
8. S. A. David
9. R. H. Ford
10. L. M. Dickens
11. J. R. DiStefano
12. L. B. Dunlap
13. G. M. Goodwin
14. P. L. Gorman

15-16. D. R. Hamrin

17. H. W. Hayden, Jr.
18. L. L. Horton
19. R. R. Judkins
20. M. A. Karnitz
21. C. T. Liu
22. H. F. Longmire
23. Gail M. Ludtka
24. Gerald M. Ludtka
25. A. J. Luffman
26. A. E. Pasto
27. T. M. Rosseel
28. M. L. Santella
29. J. H. Schneibel
30. J. W. Shepherd

31-32. V. K. Sikka

33. P. S. Sklad
34. R. W. Swindeman
35. C. A. Valentine
36. S. Viswanathan
37. L. R. Walker
38. Central Research Library
39. Document Reference Section
40. Laboratory Records - RC
41. ORNL Patent Section
42. Y-12 Central Files

EXTERNAL DISTRIBUTION

43-44. General Motors Corporation, Saginaw Division, 3900 Holland Road, Saginaw, MI 48601-9494

M. S. Chatterjee

45. U.S. DOE, EE-232, 1000 Independence Avenue, SW, Washington, DC 20585

C. A. Sorrell

46-47. U.S. DOE, OFFICE OF SCIENTIFIC AND TECHNICAL INFORMATION, P.O. Box 62, Oak Ridge, TN 37831

48. DOE, Oak Ridge Operations, P.O. Box 2001, Oak Ridge, TN 37831-6269

49. DOE Work For Others Office, P.O. Box 2001, Room G209, Oak Ridge, TN 37831